PNAS
www.pnas.org

Supplementary Information for

Interrogating dense ligand chemical space with a forward-synthetic library

Florent Chevillard, Silvia Stotani, Anna Karawajczyk , Stanimira Hristeva , Els Pardon , Jan Steyaert , Dimitrios Tzalis and Peter Kolb

Dimitrios Tzalis and Peter Kolb
Email: dtzalis@taros.de, peter.kolb@uni-marburg.de

This PDF file includes:

www.pnas.org/cgi/doi/10.1073/pnas.1818718116

Results

Binding site partitioning

We split the binding cavity of the β_2 AR into the three regions OP, SBP, and TBP. Each region is defined by a few key residues that constitute interaction possibilities for the ligands. These key residues are: OP; Asp113$^{3.32}$, Phe193^{ECL2} , Ser203$^{5.42}$, Ser204$^{5.43}$, Ser205$^{5.46}$, Asn293$^{6.55}$, and Asn312$^{7.39}$; SBP; Trp109$^{3.28}$ and Asp192^{ECL2} ; TBP; Thr195^{ECL2} , and Ala200$^{5.39}$ (numbers in superscript are Ballesteros-Weinstein numbers).

Structure-Activity Relationship of the amide pool.

The main goal of the amide pool was to investigate whether the hydroxyl motif known to interact with Asn312$^{7.39}$ and present in many β2AR ligands can be replaced with a carbonyl group acting as an H-bond acceptor. For the **bb.A**'s, these results suggest that the amine predicted to interact with Asp113$^{3.32}$ and the carbonyl moiety oxygen should be separated by two carbons, which is consistent with the canonical pharmacophore of adrenoceptor ligands. Three carbon atoms separation yielded only non-binding products (derivative products of BBs **A08** and **A09**. Moreover, we can deduce that nitrogen-containing rings of six or seven atoms seem to be too big to be accommodated at the entrance of the OP. In contrast, rings of five atoms can be placed favorably, with a methyl providing a hydrophobic contact to Phe193^{ECL2}. For the **bb.B**, six-atom rings fused with six- or five-atom aromatic rings with one substituent yield ligands. In the case of six-membered aromatic rings, the chlorine at position 5 for **amd_A10B49** seems to be important for binding. When not present **amd_A10B52**, the resulting product did not show activity. Furthermore, the hydroxy moiety at position 7 **amd_A10B37** is predicted to interact with Ser207$^{5.46}$. For the five-atom aromatic rings, donor moieties at position 3 and acceptors at position 2 influence binding (cf. **amd_A10B29**, because no activity was observed when acceptor moieties are present in position 3 (cf. **amd_A10B33**. Larger (usually with twelve or more heavy atoms) **bb.B** aimed at exploring the TBP did not show affinity for the β2AR.

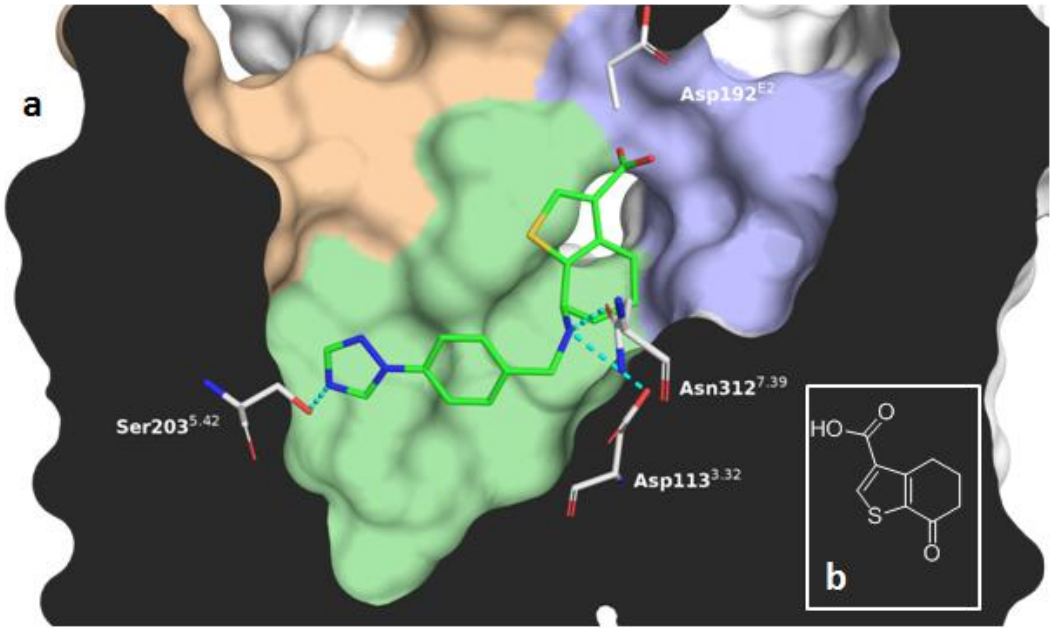

Fig. S1. (a) Illustration of compound 1 (green carbon) identified through docking. The bb.A binding mode prediction shows nearly optimal polar interactions with the SBP (green surface), while the bb.B makes unfavorable interactions in the SBP (blue background). Polar interactions are represented with cyan dots. For clarity's sake, the backbone atoms of Asp192 are not represented. **(b)** 2D depiction of BB **B53**.

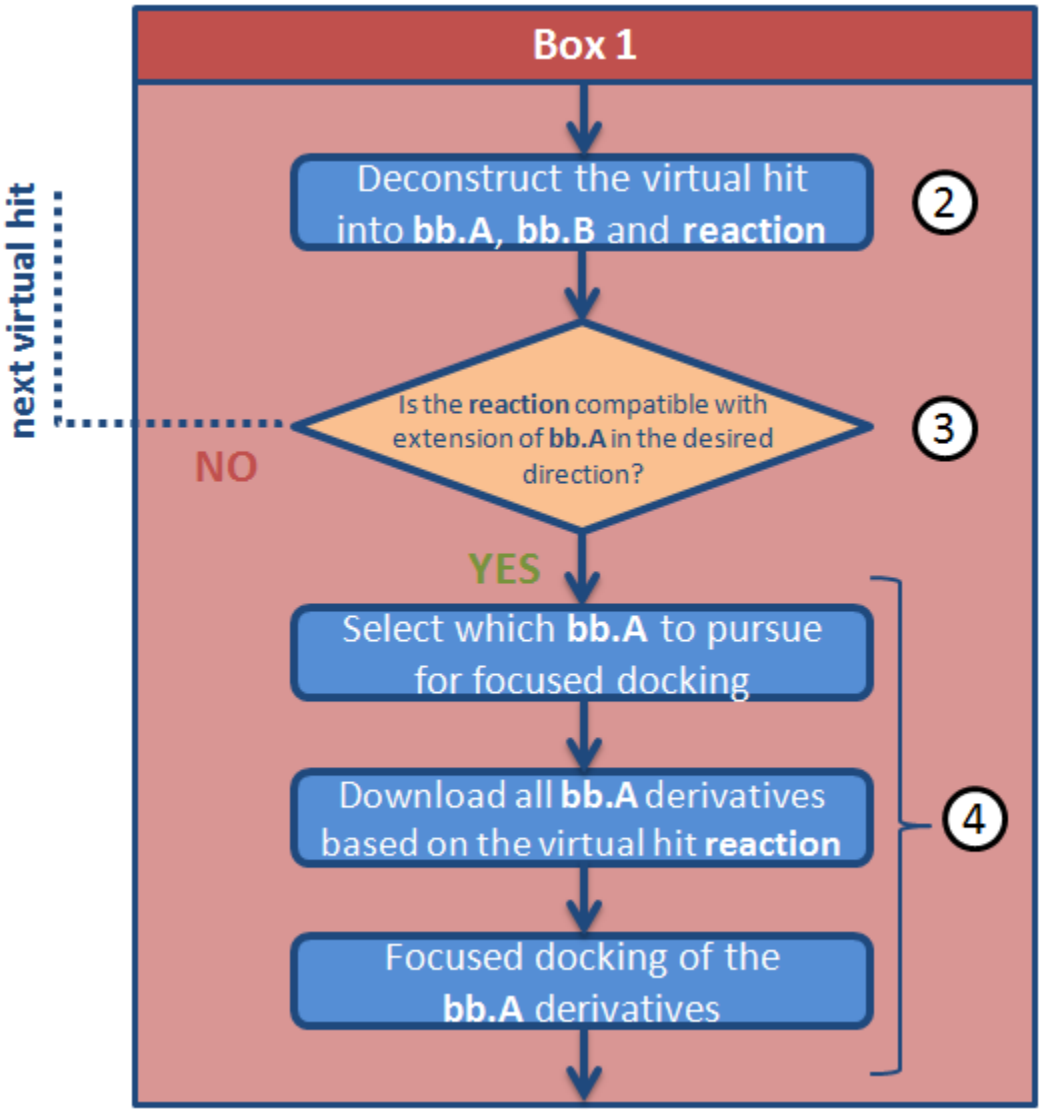

Fig. S2. Box1 of the schematic flowchart illustrated in Figure 2.

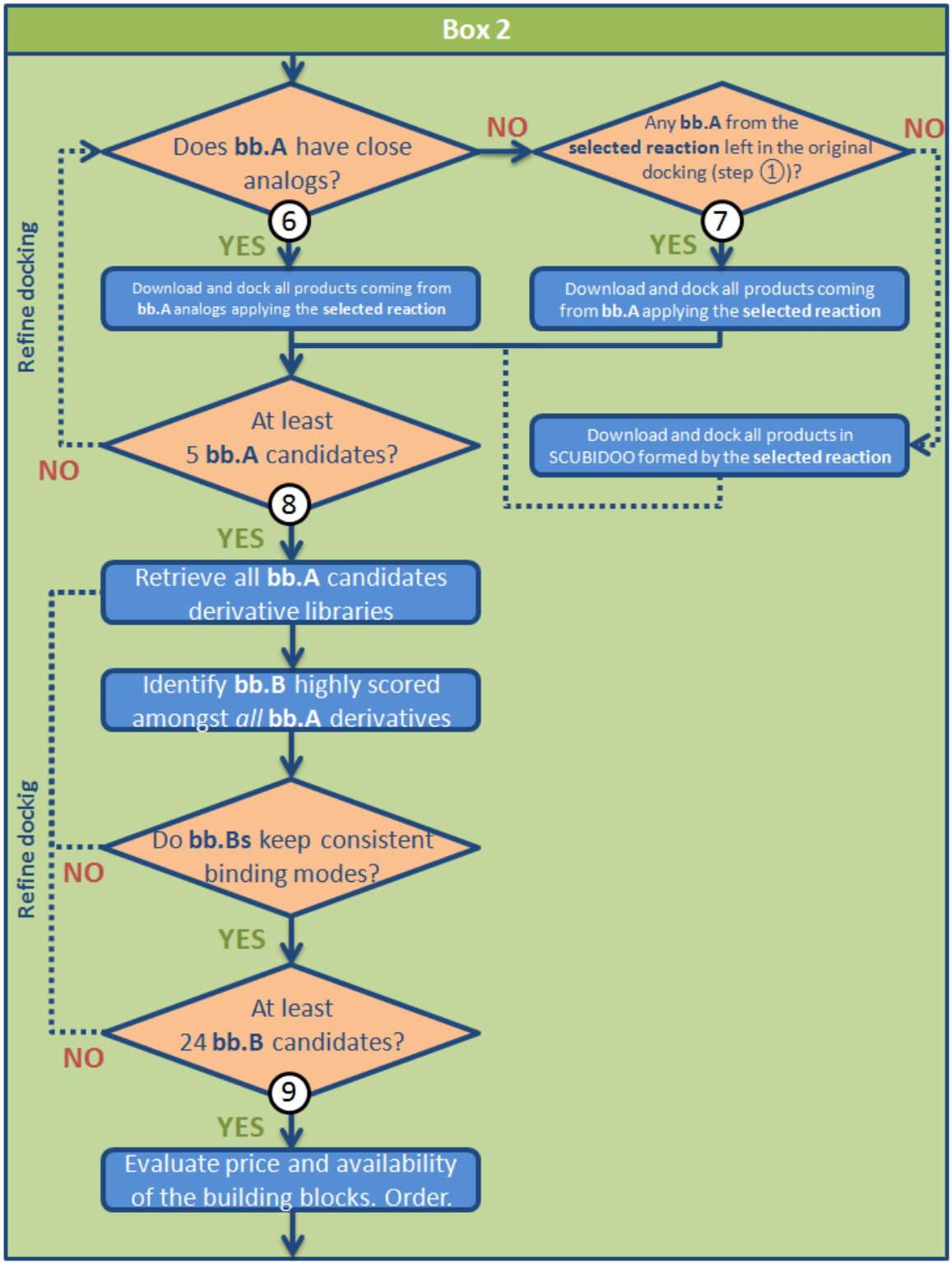

Fig. S3. Box2 of the schematic flowchart illustrated in Figure 2.

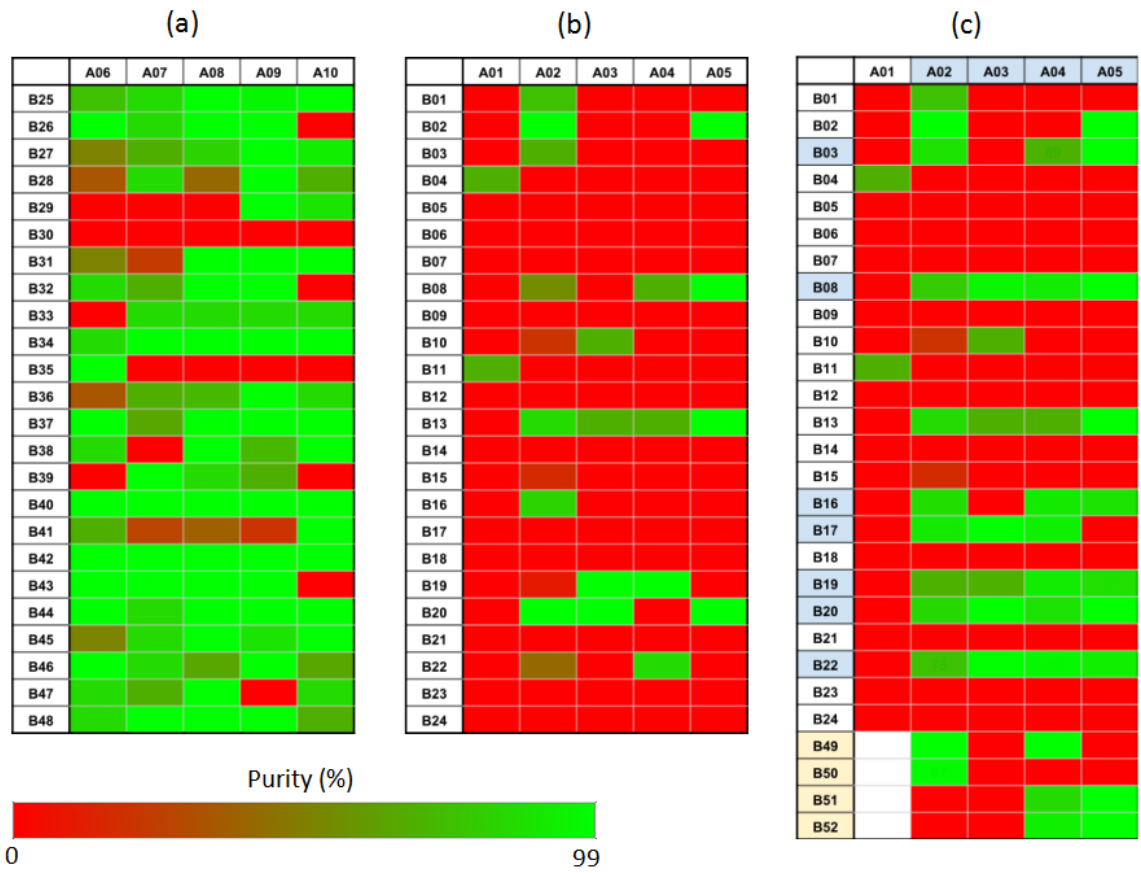

Fig. S4. Synthesis results of the (a) amide pool, (b) amination pool and the (c) amination pool in the second round. Each column represents one **bb.A** and each row represents one **bb.B**. Thus, each cell represents a candidate product for synthesis. Red cells indicate failed synthesis. Green cells indicate a successful synthesis and the brighter the green, the higher the purity (up to 99%, cf. color scale). White cells indicate product that were not considered for synthesis. Blue-grey cells contain the **bb.B** that were considered for yield and affinity optimization (i.e. second round of synthesis).

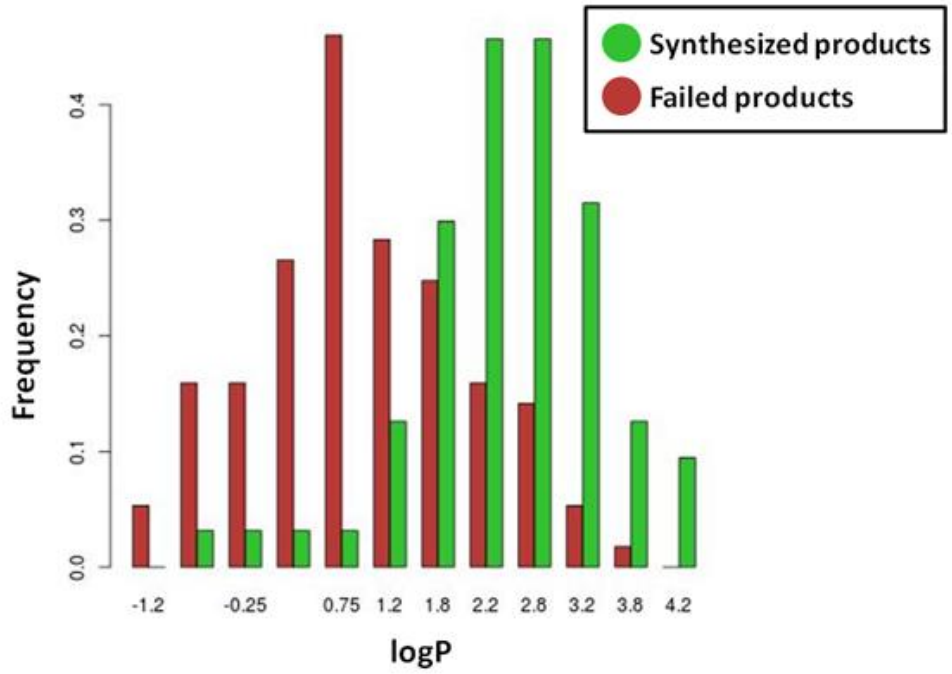

Fig. S5. Distribution of the logP values for the synthesized products (green) and the failed products (red). The failed products show a higher lipophilic signature.

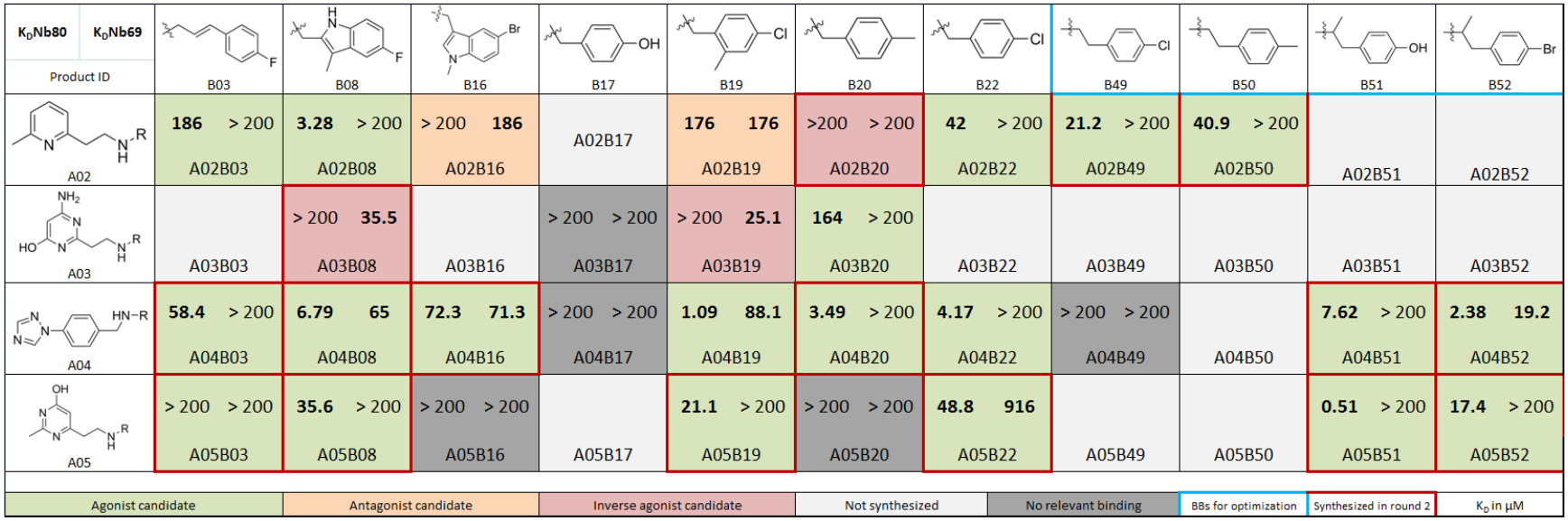

Fig. S6. Assay results of the compounds in the amination pool in both rounds. The first column contains four bb.A and the first row depicts eleven bb.B. Each cell represents the product formed by the combination of the respective bb.A and bb.A. Green cells correspond to an AC product, red cells to an IAC product, and orange cells to an antagonist candidate (AntC) product. Dark grey cells indicate products with very low binding and light grey cells contain products which were not obtained. Each product cell contains up to three values. Top row: average of two measurements against the br-Nb80 (left) and br-Nb69 (right) in uM. Bottom row: product ID. Red-border cells are products from the second round. Blue-border cells contain the bb.B used for affinity optimization. Full experimental results for all compounds are listed in SI_01.

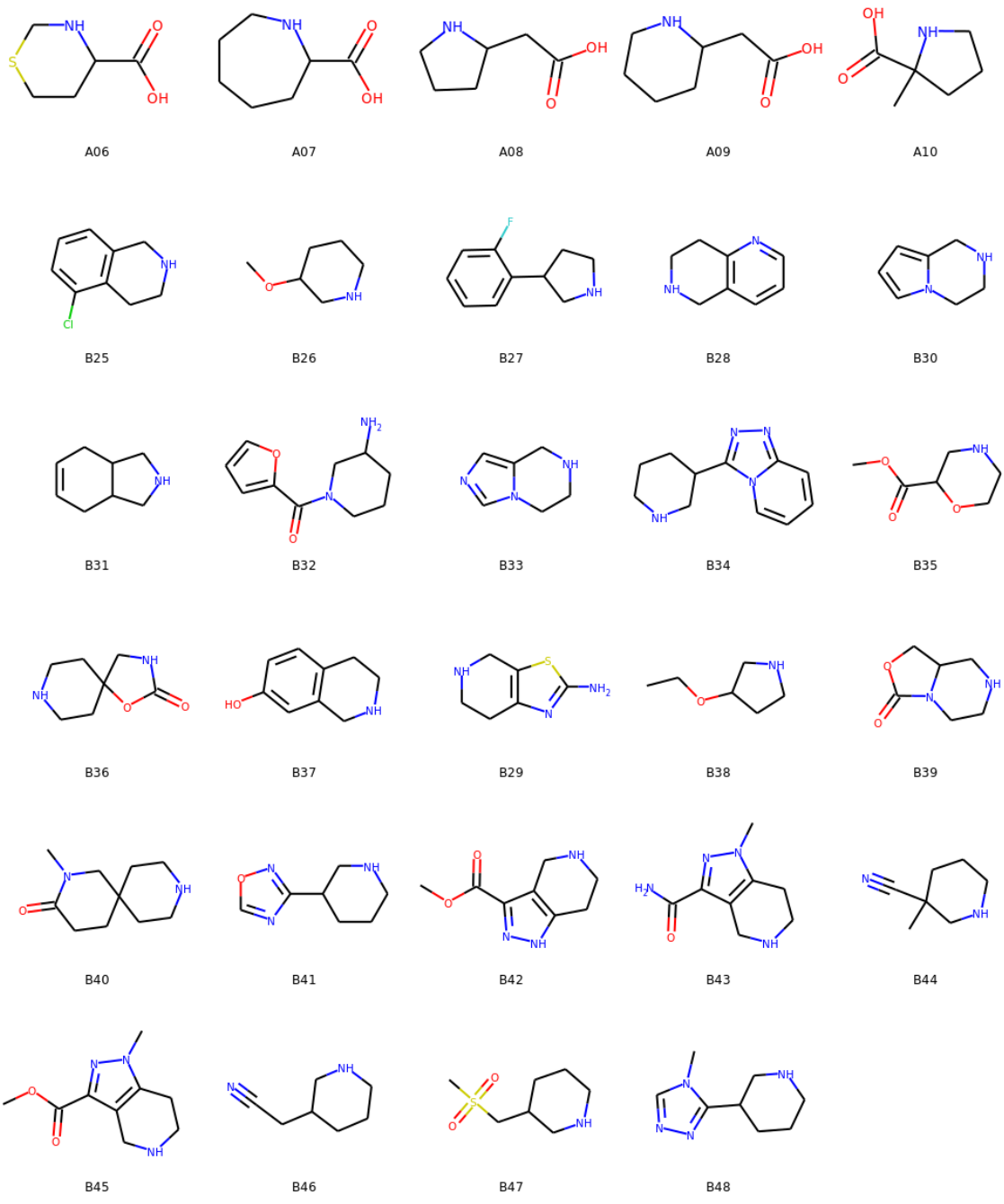

Scheme. S1.2D depiction of all BB used to create the amide pool.

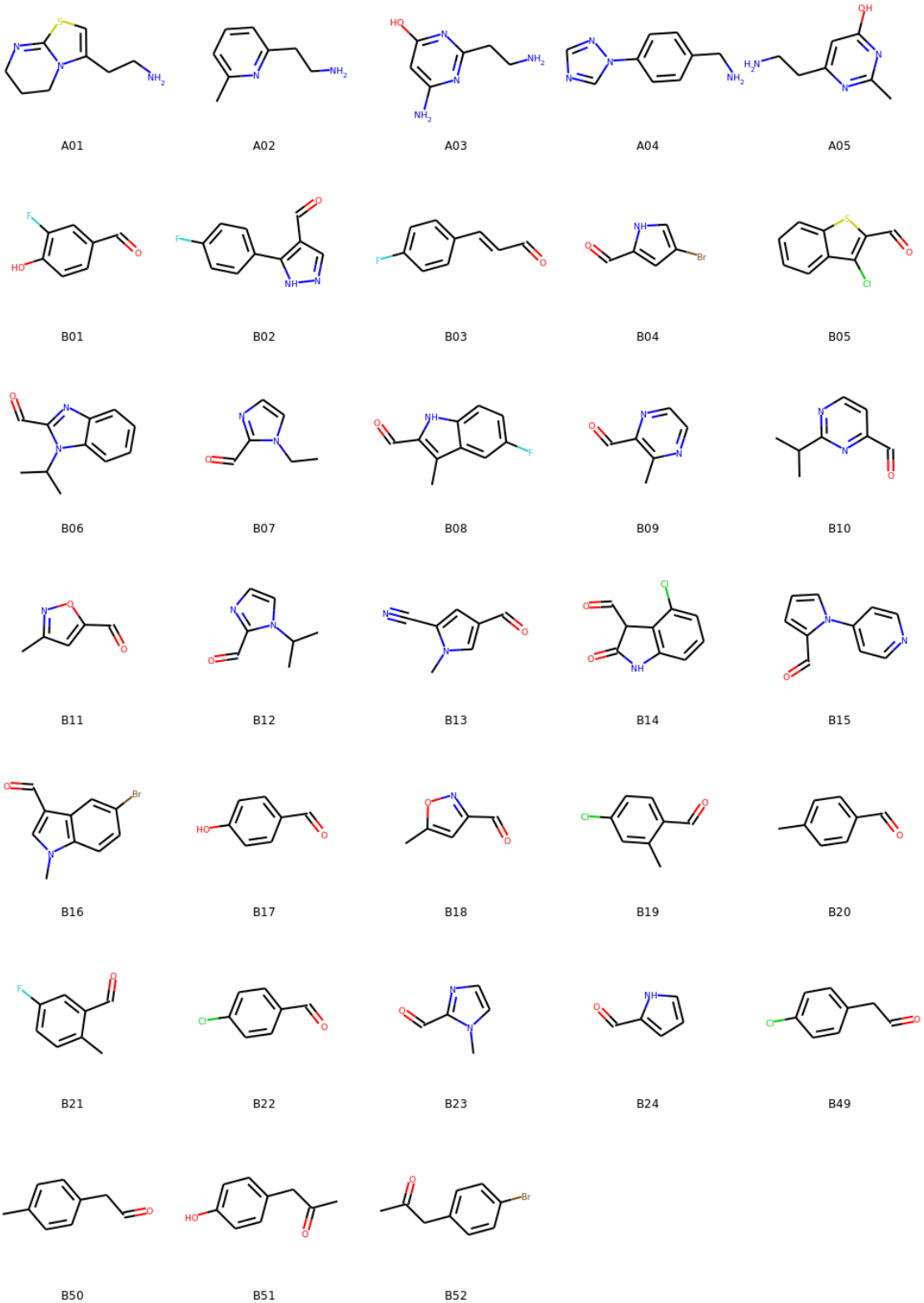

Scheme. S2.2D depiction of all BB used to create the amination pool.

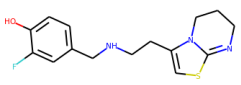

red_A01B01

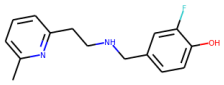

red_A02B01

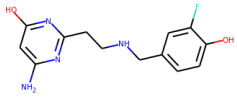

red_A03B01

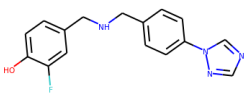

red_A04B01

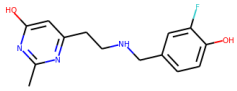

red_A05B01

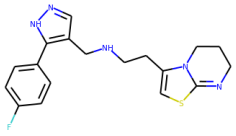

red_A01B02

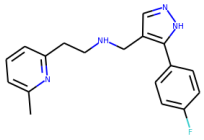

red_A02B02

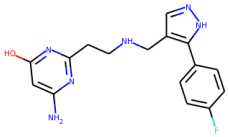

red_A03B02

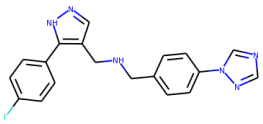

red_A04B02

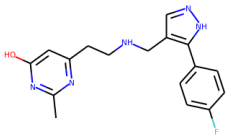

red_A05B02

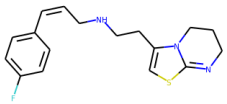

red_A01B03

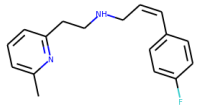

red_A02B03

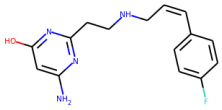

red_A03B03

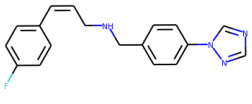

red_A04B03

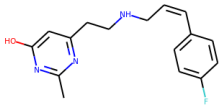

red_A05B03

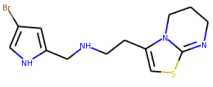

red_A01B04

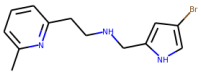

red_A02B04

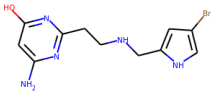

red_A03B04

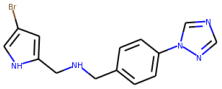

red_A04B04

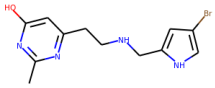

red_A05B04

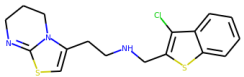

red_A01B05

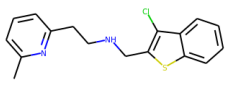

red_A02B05

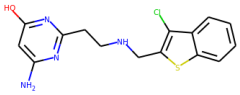

red_A03B05

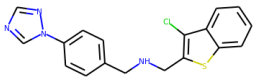

red_A04B05

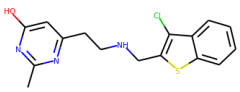

red_A05B05

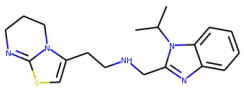

red_A01B06

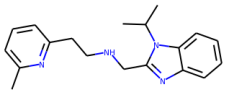

red_A02B06

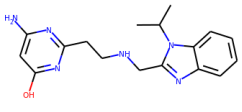

red_A03B06

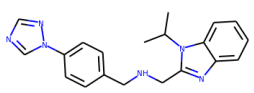

red_A04B06

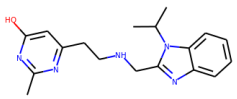

red_A05B06

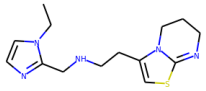

red_A01B07

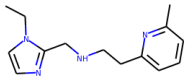

red_A02B07

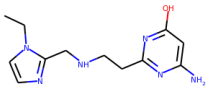

red_A03B07

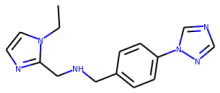

red_A04B07

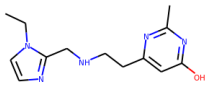

red_A05B07

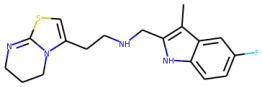

red_A01B08

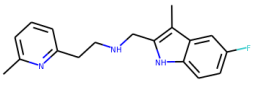

red_A02B08

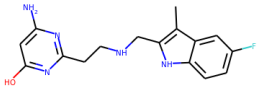

red_A03B08

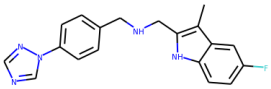

red_A04B08

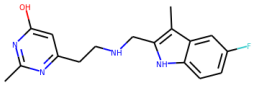

red_A05B08

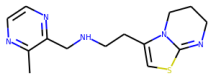

red_A01B09

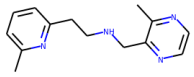

red_A02B09

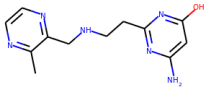

red_A03B09

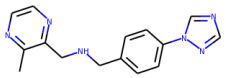

red_A04B09

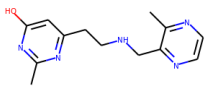

red_A05B09

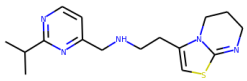

red_A01B10

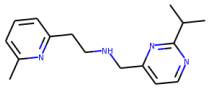

red_A02B10

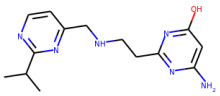

red_A03B10

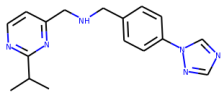

red_A04B10

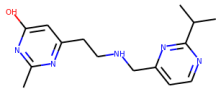

red_A05B10

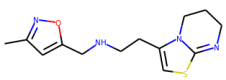

red_A01B11

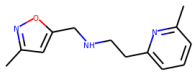

red_A02B11

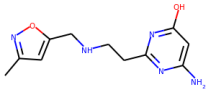

red_A03B11

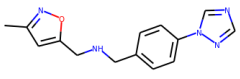

red_A04B11

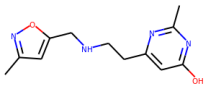

red_A05B11

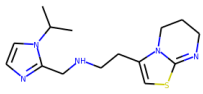

red_A01B12

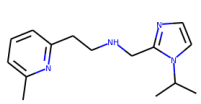

red_A02B12

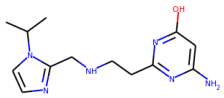

red_A03B12

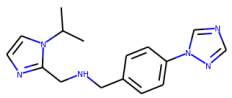

red_A04B12

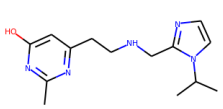

red_A05B12

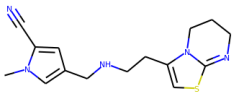

red_A01B13

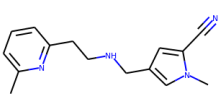

red_A02B13

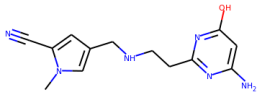

red_A03B13

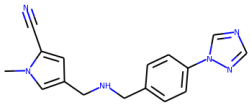

red_A04B13

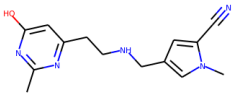

red_A05B13

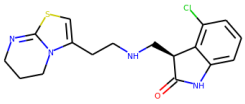

red_A01B14

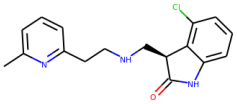

red_A02B14

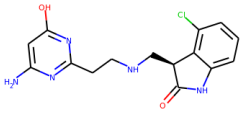

red_A03B14

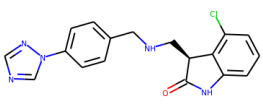

red_A04B14

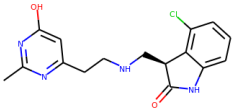

red_A05B14

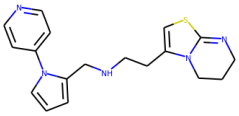

red_A01B15

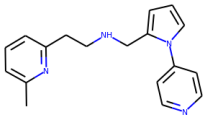

red_A02B15

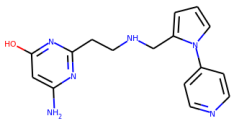

red_A03B15

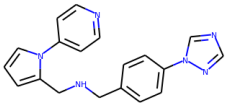

red_A04B15

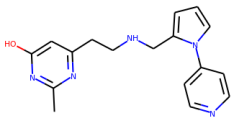

red_A05B15

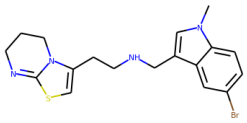

red_A01B16

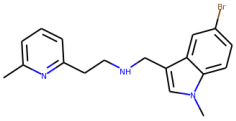

red_A02B16

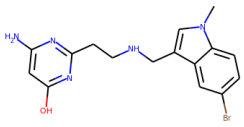

red_A03B16

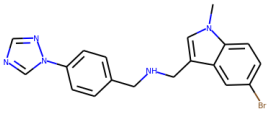

red_A04B16

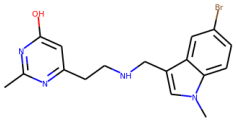

red_A05B16

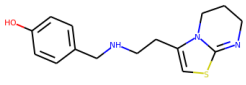

red_A01B17

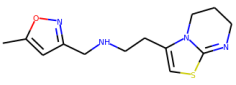

red_A01B18

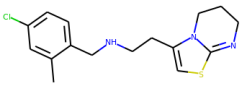

red_A01B19

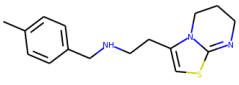

red_A01B20

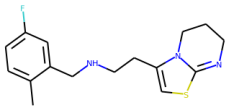

red_A01B21

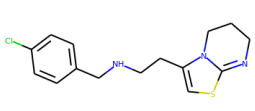

red_A01B22

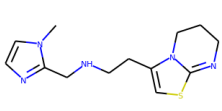

red_A01B23

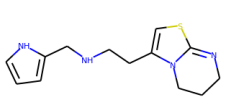

red_A01B24

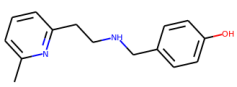

red_A02B17

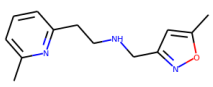

red_A02B18

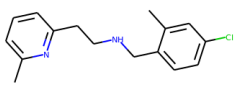

red_A02B19

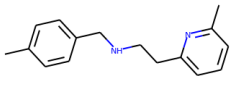

red_A02B20

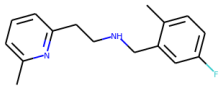

red_A02B21

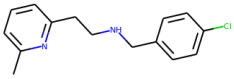

red_A02B22

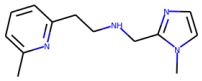

red_A02B23

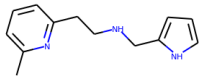

red_A02B24

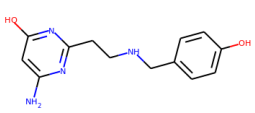

red_A03B17

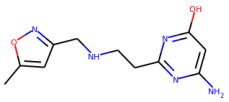

red_A03B18

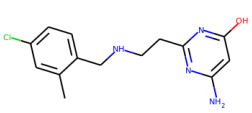

red_A03B19

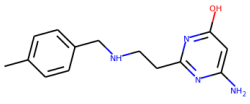

red_A03B20

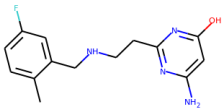

red_A03B21

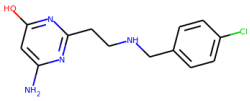

red_A03B22

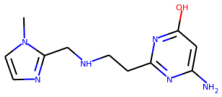

red_A03B23

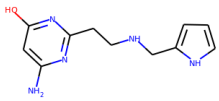

red_A03B24

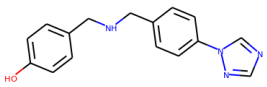

red_A04B17

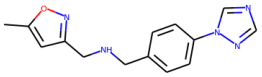

red_A04B18

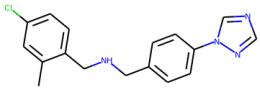

red_A04B19

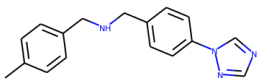

red_A04B20

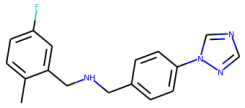

red_A04B21

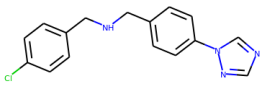

red_A04B22

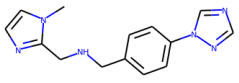

red_A04B23

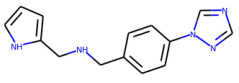

red_A04B24

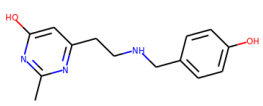

red_A05B17

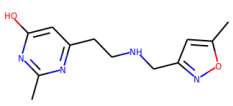

red_A05B18

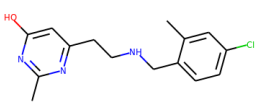

red_A05B19

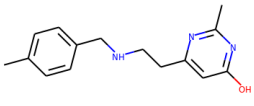

red_A05B20

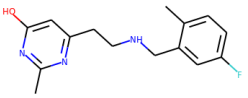

red_A05B21

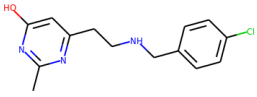

red_A05B22

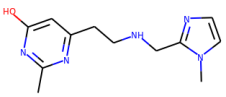

red_A05B23

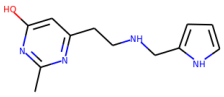

red_A05B24

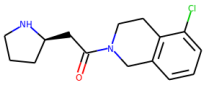

amd_A08B25

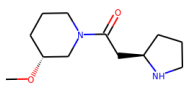

amd_A08B26

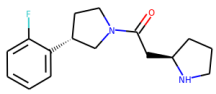

amd_A08B27

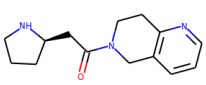

amd_A08B28

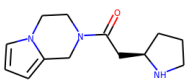

amd_A08B30

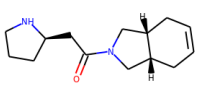

amd_A08B31

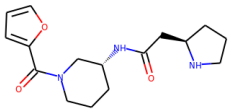

amd_A08B32

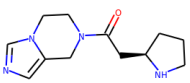

amd_A08B33

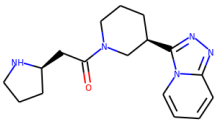

amd_A08B34

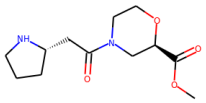

amd_A08B35

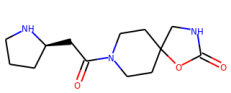

amd_A08B36

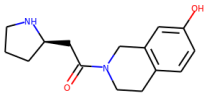

amd_A08B37

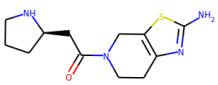

amd_A08B29

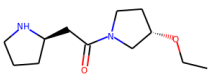

amd_A08B38

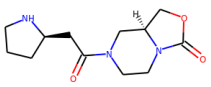

amd_A08B39

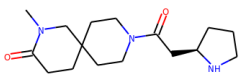

amd_A08B40

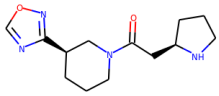

amd_A08B41

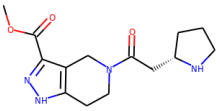

amd_A08B42

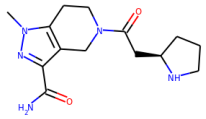

amd_A08B43

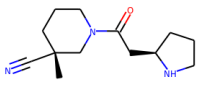

amd_A08B44

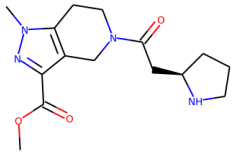

amd_A08B45

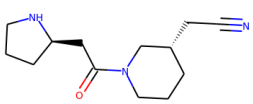

amd_A08B46

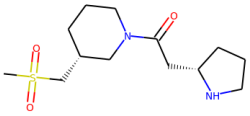

amd_A08B47

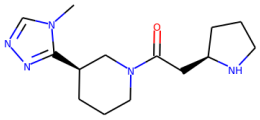

amd_A08B48

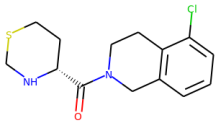

amd_A06B25

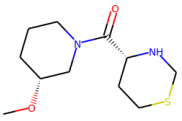

amd_A06B26

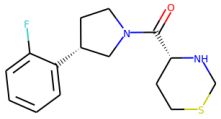

amd_A06B27

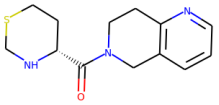

amd_A06B28

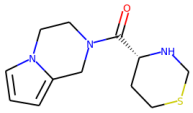

amd_A06B30

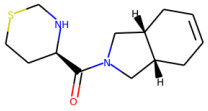

amd_A06B31

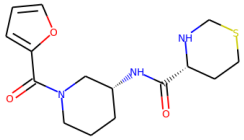

amd_A06B32

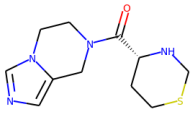

amd_A06B33

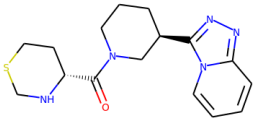

amd_A06B34

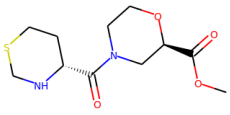

amd_A06B35

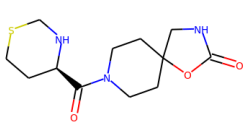

amd_A06B36

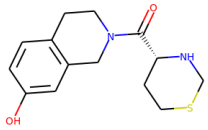

amd_A06B37

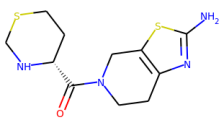

amd_A06B29

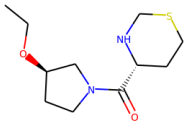

amd_A06B38

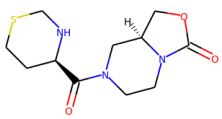

amd_A06B39

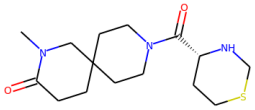

amd_A06B40

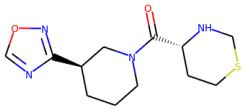

amd_A06B41

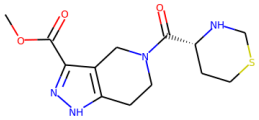

amd_A06B42

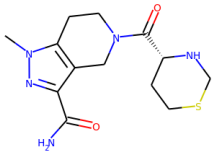

amd_A06B43

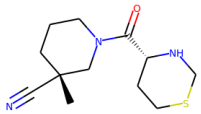

amd_A06B44

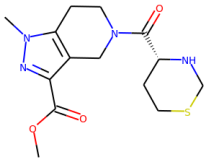

amd_A06B45

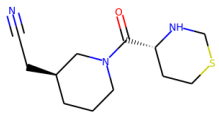

amd_A06B46

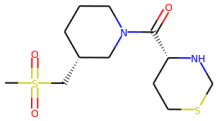

amd_A06B47

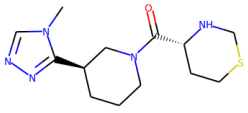

amd_A06B48

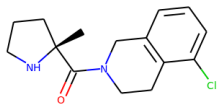

amd_A10B25

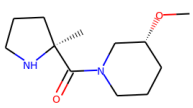

amd_A10B26

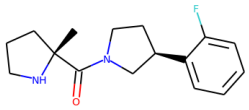

amd_A10B27

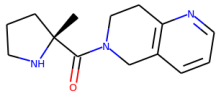

amd_A10B28

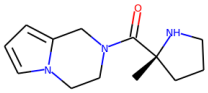

amd_A10B30

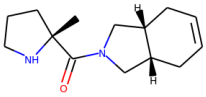

amd_A10B31

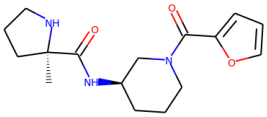

amd_A10B32

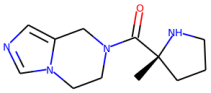

amd_A10B33

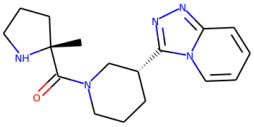

amd_A10B34

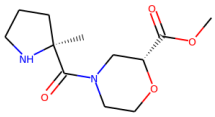

amd_A10B35

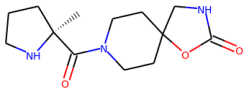

amd_A10B36

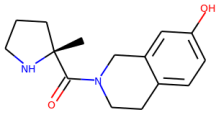

amd_A10B37

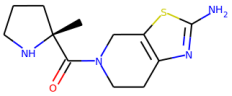

amd_A10B29

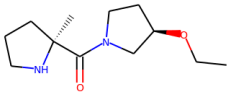

amd_A10B38

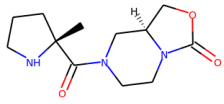

amd_A10B39

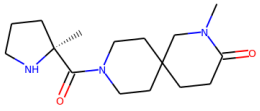

amd_A10B40

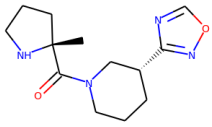

amd_A10B41

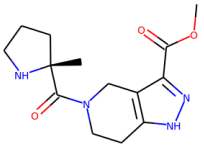

amd_A10B42

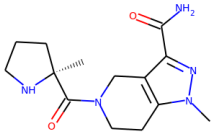

amd_A10B43

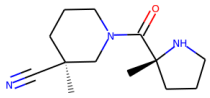

amd_A10B44

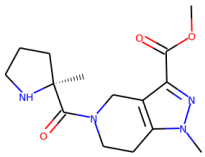

amd_A10B45

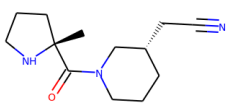

amd_A10B46

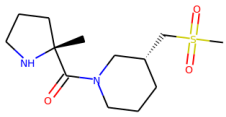

amd_A10B47

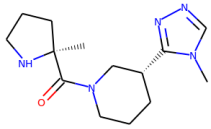

amd_A10B48

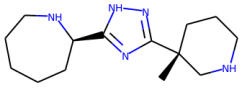

amd_A07B44

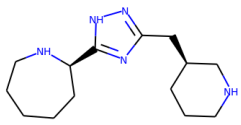

amd_A07B46

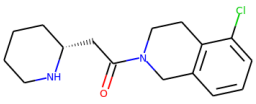

amd_A09B25

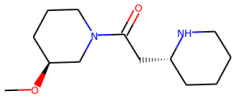

amd_A09B26

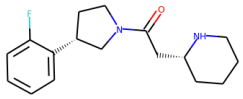

amd_A09B27

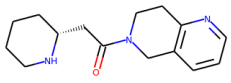

amd_A09B28

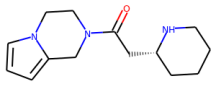

amd_A09B30

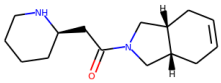

amd_A09B31

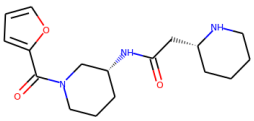

amd_A09B32

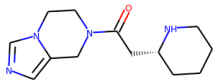

amd_A09B33

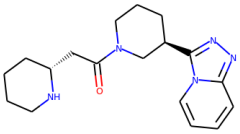

amd_A09B34

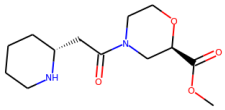

amd_A09B35

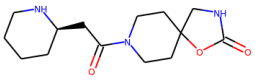

amd_A09B36

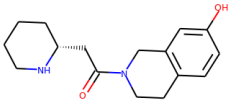

amd_A09B37

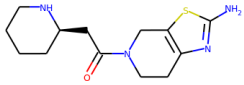

amd_A09B29

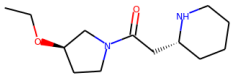

amd_A09B38

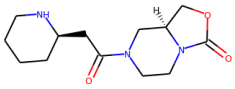

amd_A09B39

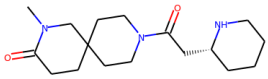

amd_A09B40

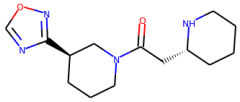

amd_A09B41

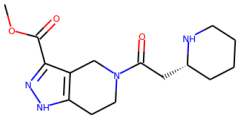

amd_A09B42

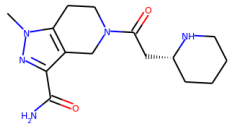

amd_A09B43

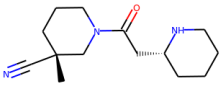

amd_A09B44

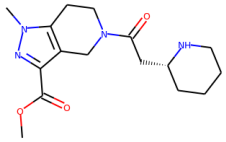

amd_A09B45

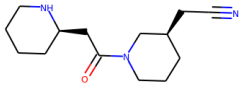

amd_A09B46

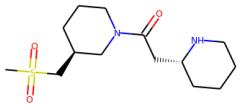

amd_A09B47

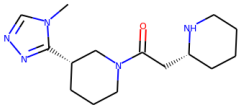

amd_A09B48

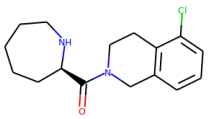

amd_A07B25

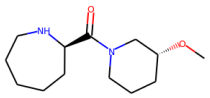

amd_A07B26

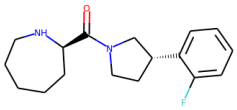

amd_A07B27

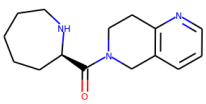

amd_A07B28

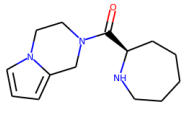

amd_A07B30

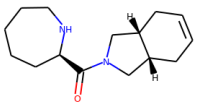

amd_A07B31

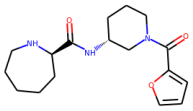

amd_A07B32

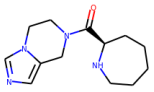

amd_A07B33

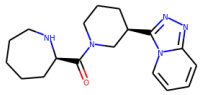

amd_A07B34

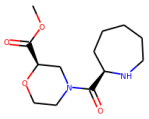

amd_A07B35

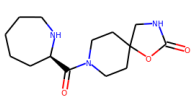

amd_A07B36

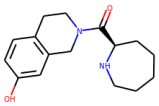

amd_A07B37

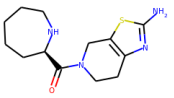

amd_A07B29

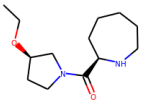

amd_A07B38

amd_A07B39

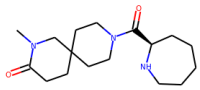

amd_A07B40

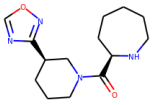

amd_A07B41

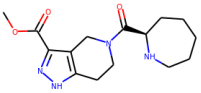

amd_A07B42

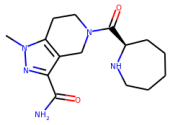

amd_A07B43

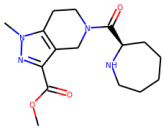

amd_A07B45

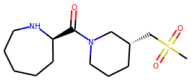

amd_A07B47

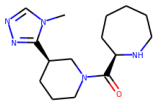

amd_A07B48

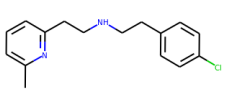

red_A02B49

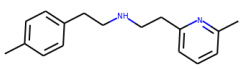

red_A02B50

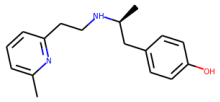

red_A02B51

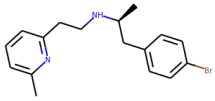

red_A02B52

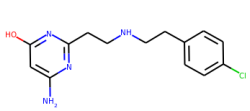

red_A03B49

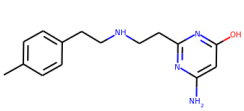

red_A03B50

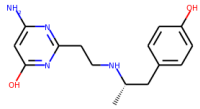

red_A03B51

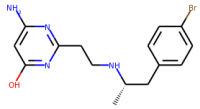

red_A03B52

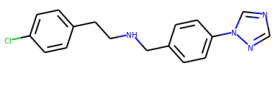

red_A04B49

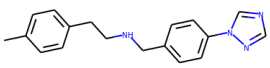

red_A04B50

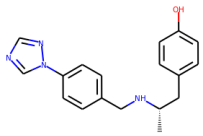

red_A04B51

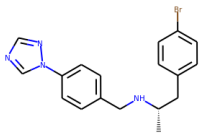

red_A04B52

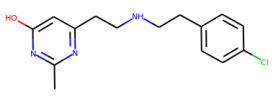

red_A05B49

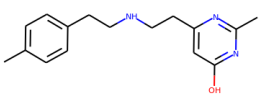

red_A05B50

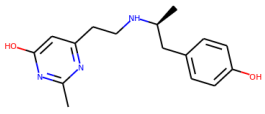

red_A05B51

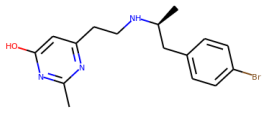

red_A05B52

Scheme. S3. 2D depictions of the 256 products generated in our study. Every compound is named after the ID of its bb.A and bb.B combination with a prefix for the reaction. For instance, compound red_**A05B51** is built from the assembly of BB **A05** and **B51** using reductive-amination.

Methods

Computational Methods.

Docking calculations were performed with the basal conformation of the β_2AR in complex with carazolol (PDB: 2RH1) (1-2) and an active conformation in complex with the ligand BI167107 (PDB: 4LDE)(3) using FRED(4–7). All ligands, solvent, lipid molecules as well as the T4-lysozyme insertion were removed. The hydrogens were placed and minimized using the HBUILD module in CHARMM (8). CHARMm22(9) atom types and MPEOE (10, 11) partial charges were assigned using the program Witnotp [Novartis Pharma AG, available at http://www.biochem-caflisch.uzh.ch/download]. All products to be docked were subject to conformer generation using OMEGA(12), with an RMSD of 0.1 Å and up to 500 conformers. The protonation states were defined using QUACPAC(13). The antagonist and agonist datasets were downloaded from the GDD/GLL project(14). The active set, used for similarity comparison, was created by merging the antagonist and agonist datasets together. Similarity comparison were performed using a python script written using the RDKit library(15). The tanimoto score based on the ECFP4 fingerprints(16) were employed.

Radioligand displacement Assay

For each compound to be tested, a comparative assay was performed. A first assay with a β_2AR-Nanobody fusion locked in an active state by a G protein-mimicking Nanobody called β_2AR-Nb80. A second experiment was conducted using the same receptor fused to an irrelevant Nanobody called β_2AR-Nb69, thus in its basal state. Thereby, we were able to classify the candidate efficacy of each hit (i.e. agonist (AC), antagonist (AntC) or inverse-agonist candidates (IAC)). We use the term "candidate" here to clearly distinguish the assigned efficacy from one that was determined in a cellular assay. As has been shown in an earlier publication (8), however, candidate efficacy and cellular efficacy are highly congruent. An AC molecule is defined as displaying a shift in affinity between the β_2AR-Nb69 and the β_2AR-Nb80 higher than 1.1 (i.e. the compound is more selective towards the β_2AR-Nb80). An IAC molecule is defined by a shift in affinity between the β_2AR-Nb69 and the β_2AR-Nb80 below 0.9. An AntC molecule does not display any obvious selectivity shift between the two receptor fusions (shift = 1 ± 0.1).

Compounds were examined for their ability to inhibit the binding of [^{3}H]-dihydroalprenolol ([^{3}H]-DHA; 2 nM final concentration) to membranes of Sf9 cells expressing the β_2AR. Five µg of total protein were mixed with each compound in concentrations ranging from 10^{-10} M to 10^{-3} M. The reaction mixtures were incubated for 2h at RT and free radioligand was removed by filtrating over a Whatman GF/C filter. Filters were washed six times, then dried, and 40 µl of scintillation fluid (MicroScintTM-O, Perkin Elmer) was added. Radioactivity (counts per minutes [cpm]) retained on the filters was determined in a Wallac MicroBeta TriLux scintillation counter. The half-maximal inhibitory concentrations (IC_{50}) for these compounds were calculated from normalized dose-response curves obtained using a one-site competition binding model (nonlinear regression analysis) of the GraphPad Prism software (17). Each assay was performed in triplicates. IC_{50} values were transformed to K_D using the Cheng-Prusoff equation (18).

Experimental procedure for synthesis

General Informations

Chemicals and solvents were obtained from commercial suppliers and were used without further purification. All dry reactions were performed under nitrogen atmosphere using commercial dry solvents. Thin layer chromatography was performed on Macherey Nagel precoated TLC aluminum sheets with silica gel 60 UV254 (5 – 17 µm). TLC visualization was accomplished by irradiation with a UV lamp (254 nm) and/or staining with $KMnO_4$ solution. ^{1}H NMR spectra were recorded on a JEOL ECX400 spectrometer operated at 400 MHz. Chemical shifts are given in ppm (δ) from tetramethylsilane as an internal standard or residual solvent peak. Significant ^{1}H NMR data are tabulated in the following order: multiplicity (s, singlet; d, doublet; t, triplet; q, quartet; m, multiplet; dd, doublet of doublets; dt, doublet of triplets; td, triplet of doublets; br, broad), coupling constant(s) in hertz, number of protons. Proton decoupled ^{13}C NMR data were acquired at 100 MHz. ^{13}C chemical shifts are reported in parts per million (δ, ppm). All NMR data were collected at room temperature (25 °C). Analytical preparative HPLC and Electron Spray Ionization (ESI) mass spectra were performed on an Agilent uHPLC (1290 Infinity) and an Agilent Prep-HPLC (1260 Infinity) both equipped with a Diode Array Detector and a Quadrupole MS using mixture gradients of formic acid/water/acetonitrile as system solvent. High-resolution electrospray ionization mass spectra (ESI-FTMS) were recorded on a LTQ-FT Ultra (high-resolution mass spectrometer from Thermo Fisher Scientific) coupled to an Agilent 1100 HPLC.

General procedure for the Boc-protection

In a three necked round bottomed flask the appropriate aminoacid (1.5 g, 1.0 eq) was diluted with 20 mL of MeOH. To the reaction mixture was added Et_3N (1.1 eq) and Boc-anhydride (2.0 eq) dissolved in 5 mL of MeOH was added dropwise over 5 minutes. The reaction was stirred at room temperature for 2 – 3 hours (starting material consumption was monitored by TLC). The reaction mixture was evaporated to dryness. The crude material was re-dissolved in EtOAC and washed twice with $NaHCO_3$. The aqueous layer was acidified with 10% HCl until pH = 2 and extracted three times with EtOAC. The combined organic layers were dried over $MgSO_4$, filtered and concentrated in vacuo to yield the corresponding Boc-protected aminoacids with moderate to excellent yields (38% – 92%).

General procedure for the amide formation

Reactions were performed in parallel in 15 ml reaction tubes in a 24 position Mettler-Toledo Miniblock® equipped with a heat transfer block and inert gas manifold.

Each reaction tube was loaded with a previously prepared solution of 40 mg of the corresponding Boc-protected aminoacid (1.0 eq) in 2 mL of DMF, DIPEA (5.0 eq), HOBt (1.5 eq), EDC*HCl (2.0 eq). Then the corresponding amine was added (1.0 eq). The reaction mixtures were stirred at room temperature overnight. Reaction conversion was confirmed through UHPLC check of some representative samples.

The mixtures were evaporated until dryness. The crudes were re-dissolved in 1.0 mL of ACN, filtered and purified with preparative HPLC (gradient, Acetonitrile: water with 0.1% Formic acid, 2 – 98%). Fractions containing pure product were combined and evaporated to dryness in Mettler Vials.

General procedure for the de-Boc

Reactions were performed in parallel in 15 ml reaction tubes in a 24 position Mettler-Toledo Miniblock® equipped with a heat transfer block and inert gas manifold.

Into each reaction tube containing the Boc-protected amidification product was added 0.5 mL of 1,4-dioxane and 0.5 mL of 4N HCl in dioxane. The mixtures were stirred at room temperature overnight. Reaction conversion was confirmed through UHPLC check of some representative samples.

The mixtures were evaporated until dryness. The crudes were re-dissolved in 1.0 mL of ACN, filtered and purified with preparative HPLC (gradient, Acetonitrile: water with 0.1% Formic acid, 2 – 98%). Fractions containing pure product were analysed by UHPLC. ^{1}H NMR, ^{13}C NMR and HRMS were measured for some representative samples.

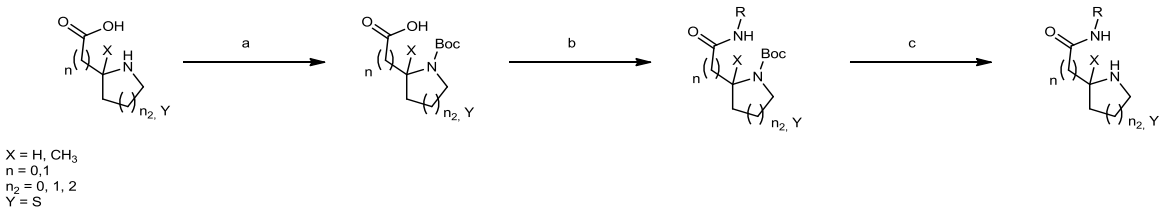

Scheme S4: Synthesis of the amide pool. Reagents and conditions: (a) Et_3N (1.1 eq), Boc_2O (2.0 eq), MeOH, rt, 2 – 5 h; (b) DIPEA (5.0 eq), HOBt (1.5 eq), EDC*HCl (2.0 eq), DMF, amine (1.0 eq), rt, overnight; (c) 4M HCl in dioxane, 1,4-dioxane, rt, overnight.

Analytical section of some representative amidification products

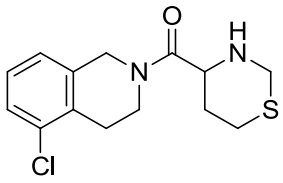

5-chloro-2-(1,3-thiazinane-4-carbonyl)-1,2,3,4-tetrahydroisoquinoline (amd_A06B25), colorless oil, 42%, UHPLC-ESI-MS: R_t= 1.89, *m*/*z* = 297.2 $[M + H]^+$. ^{1}H NMR (300 MHz, DMSO-d_6) δ 8.55 – 8.51 (m, 1H), 8.43 – 8.36 (m, 2H), 5.23 – 5.09 (m, 1H), 4.39 – 4.35 (m, 1H), 4.32 – 4.29 (m, 1H), 4.18 – 3.99 (m, 2H), 3.49 (s, 4H), 3.26 – 3.23 (m, 1H), 2.96 – 2.77 (m, 3H) ppm; ^{13}C NMR (100 MHz, DMSO-d_6) δ 203.3, 160.2, 156.3, 155.0, 149.3, 148.5, 146.8, 58.7, 50.5, 44.4, 42.3, 25.6, 24.0, 23.3 ppm; HRMS (ESI-MS) calcd. for $C_{14}H_{17}ClN_2OS$ $[M + H]^+$ = 297.0750. Found: 297.0823.

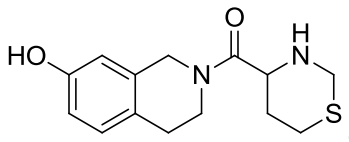

2-(1,3-thiazinane-4-carbonyl)-1,2,3,4-tetrahydroisoquinolin-7-ol (amd_A06B37), colorless oil, 60%, UHPLC-ESI-MS: R_t = 1.43 min., *m*/*z* = 279.2 $[M + H]^+$. ^{1}H NMR (400 MHz, DMSO-d_6) δ 9.55 (s, 0.5 H), 8.05 (dd, *J* = 5.9 Hz, *J* = 10.1 Hz, 1H), 7.61 – 7.56 (m, 2H), 5.22 – 4.92 (m, 2H), 4.64 (d, *J* = 16.3 Hz, 1H), 4.36 (dd, *J* = 2.7 Hz, *J* = 16.3 Hz, 1H), 4.02 – 3.95 (m, 2H), 3.29 – 3.22 (m, 1H), 2.87 – 2.74 (m, 2H), 2.65 (t, *J* = 7.4 Hz, 1H), 1.59 – 1.49 (m, 1H), 1.32 – 1.19 (m, 1H) ppm; ^{13}C NMR (100 MHz, DMSO-d_6) δ 203.6, 193.9, 184.5, 157.7, 151.6, 132.4, 130.8, 58.9, 50.5, 44.9, 43.5, 25.8, 25.3, 23.4 ppm; HRMS (ESI-MS) calcd. for $C_{14}H_{18}N_2O_2S$ $[M + H]^+$ = 279.1089. Found: 279.1162.

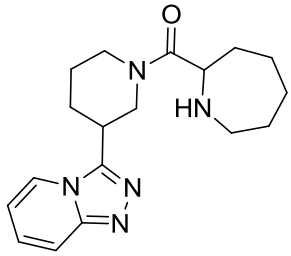

2-(3-{[1,2,4]triazolo[4,3-a]pyridin-3-yl}piperidine-1-carbonyl)azepane (amd_A07B34), yellowish oil, 73%, UHPLC-ESI-MS: R_t = 1.40 min., *m*/*z* = 328.2 $[M + H]^+$. ^{1}H NMR (400 MHz, DMSO-d_6) δ 10.11 (d, *J* = 8.7 Hz, 0.3H), 10.04 (d, *J* = 7.2 Hz, 0.2 H), 9.95 (dd, *J* = 8.5 Hz, *J* = 19.6 Hz, 0.4 H), 9.72 (s, 1H), 9.04 (dd, *J* = 5.4 Hz, *J* = 10.9 Hz, 1 H), 8.57 (t, *J* = 6.3 Hz, 1 H), 8.11 (t, *J* = 8.4 Hz, 1H), 4.83 – 4.74 (m, 1H), 4.54 – 4.24 (m, 2H), 3.15 – 3.08 (m, 2H), 2.93 – 2.87 (m, 2H), 2.10 – 2.07 (m, 1H), 1.74 – 1.65 (m, 3H), 1.53 – 1.25 (m, 9H) ppm; ^{13}C NMR (100 MHz, DMSO-d_6) δ 195.3, 176.3, 174.4, 149.3, 144.7, 134.1, 131.6, 60.2, 50.2, 46.6, 42.5, 30.5, 29.5, 28.9, 26.1, 23.4, 21.0, 20.1 ppm; HRMS (ESI-MS) calcd. for $C_{18}H_{25}N_5O$ $[M + H]^+$ = 328.2059. Found: 328.2143.

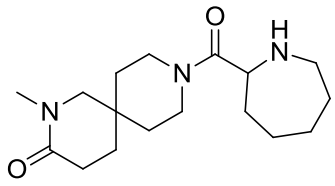

9-(azepane-2-carbonyl)-2-methyl-2,9-diazaspiro[5.5]undecan-3-one (amd_A07B40), colorless oil, 40%, UHPLC-ESI-MS: R_t = 1.39, *m*/*z* = 308.4 $[M + H]^+$. ^{1}H NMR (400 MHz, DMSO-d_6) δ 9.71 (s, 1H), 4.31 (dd, *J* = 5.1 Hz, *J* = 10.8 Hz, 1H), 3.68 – 3.62 (m, 4H), 3.30 (d, *J* = 23.8 Hz, 2H), 3.16 – 3.10 (m, 1H), 2.88 (s, 3H), 2.86 – 2.81 (m, 1H), 2.14 (t, *J* = 8.8 Hz, 2H), 1.68 – 1.62 (m, 1H), 1.50 – 1.41 (m, 6H), 1.34 – 1.30 (m, 3H), 1.22 – 1.20 (m, 2H), 1.11 – 1.05 (m, 2H) ppm; ^{13}C NMR (100 MHz, DMSO-d_6) δ 209.8, 204.8, 69.9, 56.5, 46.4, 42.6, 41.4, 40.6, 38.7, 38.4, 37.6, 35.7, 34.4, 32.9, 30.7 ppm; HRMS (ESI-MS) calcd. for $C_{17}H_{29}N_3O_2$ $[M + H]^+$ = 308.2260. Found: 308.2333.

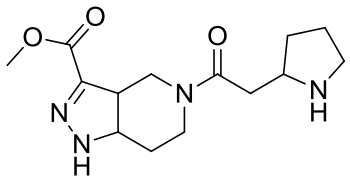

Methyl 5-[2-(pyrrolidin-2-yl)acetyl]-1*H*,4*H*,5*H*,6*H*,7*H*-pyrazolo[4,3-c]pyridine-3-carboxylate (amd_A08B42), yellowish oil, 49%, UHPLC-ESI-MS: R_t= 1.33, *m*/*z* = 293.2 $[M + H]^+$. ^{1}H NMR (300 MHz, DMSO-d_6) δ 5.19 – 5.11 (m, 2H), 4.14 (s, 3H), 4.10 – 4.07 (m, 1H), 3.98 (dd, *J* = 7.0 Hz, *J* = 13.6 Hz, 1H), 3.84 – 3.77 (m, 2H), 3.15 – 3.02 (m, 2H), 2.86 – 2.83 (m, 2H), 2.71 (t, *J* = 7.1 Hz, 1H), 1.88 – 1.80 (m, 1H), 1.65 – 1.60 (m, 1H),

1.55 – 1.49 (m, 1H), 1.25 – 1.17 (m, 1H) ppm; ^{13}C NMR (100 MHz, DMSO-d_6) δ 202.0, 196.1, 134.9, 120.6, 116.1, 59.3, 54.4, 46.1, 42.6, 38.5, 36.5, 36.1, 27.9, 19.7 ppm; HRMS (ESI-MS) calcd. for $C_{14}H_{20}N_4O_3$ [M + H] $^+$ = 293.1535. Found: 293.1619.

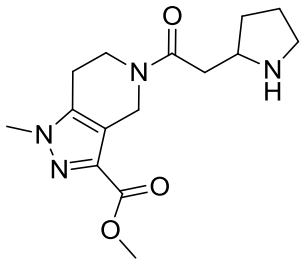

methyl 1-methyl-5-[2-(pyrrolidin-2-yl)acetyl]-1*H*,4*H*,5*H*,6*H*,7*H*-pyrazolo[4,3-c]pyridine-3-carboxylate(amd_A08B45), colorless oil, 38%, UHPLC-ESI-MS: R_t = 1.25 min., *m*/*z* = 307.2 [M + H] $^+$. ^{1}H NMR (300 MHz, DMSO-d_6) δ 10.61 (s br, 1H), 10.20 (s, 1H), 5.23 – 5.06 (m, 2H), 4.12 (s, 3H), 4.09 (s, 3H), 4.04 – 3.93 (m, 4H), 3.28 – 3.23 (m, 2H), 3.17 – 3.12 (m, 0.4H), 3.08 – 2.94 (m, 1H), 2.90 – 2.86 (m, 1H), 2.81 – 2.74 (m, 0.4H), 2.04 – 1.96 (m, 1H), 1.80 – 1.77 (m, 1H), 1.74 – 1.61 (m, 1H), 1.44 – 1.34 (m, 1H) ppm; ^{13}C NMR (100 MHz, DMSO-d_6) δ 201.3, 193.0, 163.4, 160.7, 135.7, 60.0, 54.4, 46.0, 42.1, 37.7, 35.6, 34.1, 27.3, 19.0, 17.0 ppm; HRMS (ESI-MS) calcd. for $C_{15}H_{22}N_4O_3$ [M + H] $^+$ = 307.1692. Found: 307.1765.

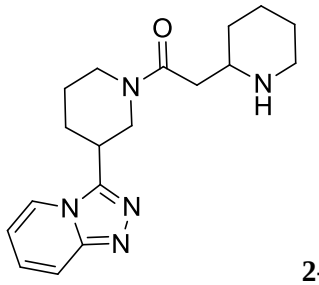

2-(piperidin-2-yl)-1-(3-{[1,2,4]triazolo[4,3-a]pyridin-3-yl}piperidin-1-yl)ethan-1-one (amd_A09B34), colorless oil, 69%, UHPLC-ESI-MS: R_t = 1.26 min., *m*/*z* = 328.2 [M + H] $^+$. ^{1}H NMR (400 MHz, DMSO-d_6) δ 10.10 (dd, *J* = 8.4 Hz, *J* = 29.4 Hz, 0.5H), 9.94 (t, *J* = 7.2 Hz, 0.5H), 9.79 (s, 1H), 9.04 (d, *J* = 11.5 Hz, 1H), 8.57 (dd, *J* = 8.5 Hz, *J* = 11.1 Hz, 1H), 8.11 (dd, *J* = 8.3 Hz, *J* = 16.6 Hz, 1H), 3.22 (s, 3H), 3.12 – 2.87 (m, 2H), 2.78 – 2.67 (m, 2H), 2.61 (d, *J* = 6.9 Hz, 1H), 2.08 (s, 1H), 1.80 – 1.58 (m, 2H), 1.49 – 1.27 (m, 5H), 1.20 – 0.96 (m, 4H) ppm; ^{13}C NMR (100 MHz, DMSO-d_6) δ 205.6. 185.9, 158.9, 154.4, 153.9, 143.8 (d, *J* = 19.2 Hz), 141.2 (d, *J* = 19.5 Hz), 66.1, 59.9, 56.7, 54.9, 51.4, 39.9, 39.2, 37.0, 30.6, 29.2, 28.2 ppm; HRMS (ESI-MS) calcd. for $C_{18}H_{25}N_5O$ [M + H] $^+$ = 328.2059. Found: 328.2131.

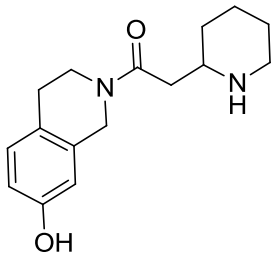

1-(7-hydroxy-1,2,3,4-tetrahydroisoquinolin-2-yl)-2-(piperidin-2-yl)ethan-1-one (amd_A09B37), colorless oil, 65%, UHPLC-ESI-MS: R_t = 1.53 min., *m*/*z* = 275.2 $[M + H]^+$. ^{1}H NMR (400 MHz, DMSO-d_6) δ 9.72 (s, 0.3H), 8.07 (dd, *J* = 6.2 Hz, *J* = 10.1 Hz, 1H), 7.65 – 7.58 (m, 2H), 5.06 – 5.03 (m, 2H), 3.36 (d, *J* = 15.4 Hz, 3H), 2.92 (t, *J* = 15.5 Hz, 2H), 2.81 (q, *J* = 7.3 Hz, 3H), 2.69 (t, *J* = 7.4 Hz, 1H), 1.62 – 1.46 (m, 3H), 1.32 – 1.16 (m, 3H) ppm; ^{13}C NMR (100 MHz, DMSO-d_6) δ 200.4, 184.6, 157.7, 151.5, 145.5, 132.4, 130.7, 56.3, 45.3, 44.6, 43.9, 34.9, 24.7, 23.9, 18.0, 17.4 ppm; HRMS (ESI-MS) calcd. for $C_{16}H_{22}N_2O_2$ $[M + H]^+$ = 275.1681. Found: 275.1765.

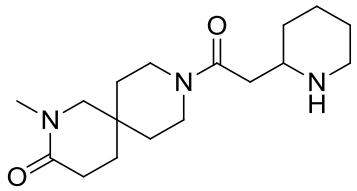

2-methyl-9-[2-(piperidin-2-yl)acetyl]-2,9-diazaspiro[5.5]undecan-3-one (amd_A09B40), colorless oil, 43%, UHPLC-ESI-MS: R_t= 1.34, *m*/*z* = 308.4 $[M + H]^+$. ^{1}H NMR (300 MHz, DMSO-d_6) δ 3.66 – 3.63 (m, 4H), 3.29 (d, *J* = 2.8 Hz, 2H), 3.22 – 3.16 (m, 2H), 2.88 (s, 3H), 2.73 (dt, *J* = 3.6 Hz, *J* = 14.9 Hz, 1H), 2.55 – 2.53 (m, 2H), 2.14 (t, *J* = 8.8 Hz, 2H), 1.52 – 1.44 (m, 4H), 1.38 – 1.35 (m, 1H), 1.18 – 1.08 (m, 7H) ppm; ^{13}C NMR (100 MHz, DMSO-d_6) δ 200.2, 195.7, 62.3, 56.5, 46.2, 41.1, 36.5, 36.2, 32.9, 31.9, 31.0, 28.6, 24.7, 19.7, 18.7 ppm; HRMS (ESI-MS) calcd. for $C_{17}H_{29}N_3O_2$ $[M + H]^+$ = 308.2260. Found: 308.2344.

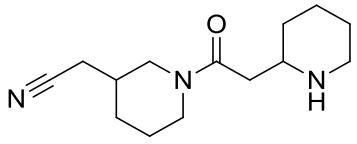

2-{1-[2-(piperidin-2-yl)acetyl]piperidin-3-yl}acetonitrile (amd_A09B46),yellowish oil, 34%, UHPLC-ESI-MS: R_t = 1.40 min., *m*/*z* = 250.2 $[M + H]^+$. ^{1}H NMR (300 MHz, DMSO-d_6) δ 9.80 (s, 1H), 4.72 – 4.67 (m, 1H), 4.59 (d, *J* = 15.9 Hz, 1H), 4.10 (d, *J* = 11.1 Hz, 1H), 4.00 – 3.97 (m, 2H), 3.28 – 3.25 (m, 2H), 2.82 – 2.77 (m, 1H), 2.61 – 2.59 (m, 2H), 2.55 (s, 1H), 1.69 – 1.65 (m, 1H), 1.50 – 1.40 (m, 5H), 1.21 – 1.10 (m, 2H), 1.08 – 0.98 (m, 3H) ppm; ^{13}C NMR (100 MHz, DMSO-d_6) δ 206.0, 148.6, 62.2, 61.4, 56.5, 55.7, 45.4, 40.2,

36.5, 30.3, 29.5, 28.7, 27.9, 24.7 ppm; HRMS (ESI-MS) calcd. for $C_{14}H_{23}N_3O$ $[M + H]^+$ = 250.1841. Found: 250.1914.

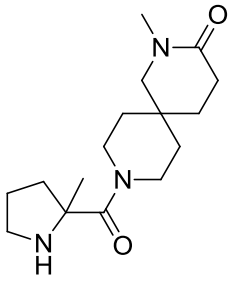

2-methyl-9-(2-methylpyrrolidine-2-carbonyl)-2,9-diazaspiro[5.5]undecan-3-one (amd_A10B40),colorless oil, 53%, UHPLC-ESI-MS: R_t = 1.24 min., m/z = 294.2 $[M + H]^+$. ^{1}H NMR (300 MHz, DMSO-d_6) δ 9.70 (s, 1H), 3.30 (s, 2H), 3.06 – 3.00 (m, 1H), 2.88 (s, 3H), 2.86 – 2.81 (m, 1H), 2.55 (s, 1H), 2.14 (t, J = 8.8 Hz, 2H), 2.09 – 2.05 (m, 1H), 1.62 – 1.58 (m, 2H), 1.47 (t, J = 8.7 Hz, 3H), 1.16 (s, 4H), 1.06 (s, 3H) ppm; ^{13}C NMR (100 MHz, DMSO-d_6) δ 210.0, 204.6, 83.0, 72.0, 56.2, 50.2, 44.7, 42.6, 41.2, 38.4, 37.1, 34.4, 31.1, 30.9 ppm; HRMS (ESI-MS) calcd. for $C_{16}H_{27}N_3O_2$ $[M + H]^+$ = 294.2103. Found: 294.2187.

General procedure for reductive amination (first round)

Reactions were performed in parallel in 15 ml reaction tubes in a 24 position Mettler-Toledo Miniblock® equipped with a heat transfer block and inert gas manifold.

Each tube was loaded with the appropriate amine (30 mg, 1.0 eq) and diluted with 2 mL of dry DCE. To this solution was added the appropriate aldehyde (0.9 eq) and CH_3COOH (1.5 eq). The reactions were stirred at room temperature for 20 minutes and then $NaBH(OAc)_3$ (1.5 eq) was added. The mixtures were stirred at room temperature overnight. Reaction conversion was confirmed through UHPLC check of some representative samples.

The reaction mixtures were washed with 1 mL of water and the organic layers were evaporated to dryness. The crudes were re-dissolved in 1.0 mL of ACN, filtered and purified with preparative HPLC (gradient, Acetonitrile: water with 0.1% Formic acid, 2-98%). Fractions containing pure product were analysed by UHPLC. ^1H NMR, ^{13}C NMR and HRMS were measured for some representative samples.

General procedure for reductive amination (second round)

Reactions were performed in parallel in 15 ml reaction tubes in a 24 position Mettler-Toledo Miniblock® equipped with a heat transfer block and inert gas manifold.

Each tube was loaded with the appropriate amine (50 mg, 1.0 eq) and diluted with 4 mL of dry DCE. To this solution was added the appropriate aldehyde (0.7 eq) and CH_3COOH (0.5 eq). The reactions were stirred at room temperature for 15 hours and then $NaBH(OAc)_3$ (1.5 eq) was added. The mixtures were stirred at room temperature for 5 hours. Reaction conversion was confirmed through UHPLC check of some representative samples.

The reaction mixtures were quenched with 1 mL of water, the water phase was further extracted with 4 mL of $CHCl_3$/*i*-PrOH (7:3) and the organic layer was evaporated to dryness.

The crudes were re-dissolved in 1.0 mL of ACN, filtered and purified with preparative HPLC (gradient, Acetonitrile: water with 0.1% Formic acid, 2-98%). Fractions containing pure product were analysed by UHPLC. ^1H NMR, ^{13}C NMR and HRMS were measured for some representative samples.

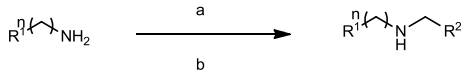

R^1 = Ar, HetAr
n = 1, 2

Scheme S5: Synthesis of the reductive amination pool. Reagents and conditions: (a) CH_3COOH (1.5 eq), aldehyde (0.9 eq), DCE, rt, 20 min.; (b) $NaBH(OAc)_3$ (1.5 eq), rt, overnight.

Analytical section of some representative reductive amination products

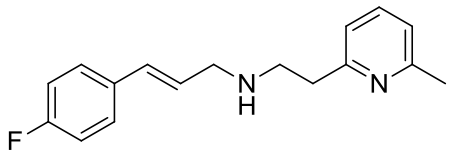

[(2*E*)-3-(4-fluorophenyl)prop-2-en-1-yl][2-(6-methylpyridin-2-yl)ethyl]amine (red_A02B03), colorless oil, 32%, UHPLC-ESI-MS: R_t = 1.62 min., *m*/*z* = 271.2 $[M + H]^+$. ^{1}H NMR (400 MHz, DMSO-d_6) δ 9.74 (s, 0.4H), 8.85 (t, *J* = 9.5 Hz, 1H), 8.71 – 8.68 (m, 2H), 8.32 (t, *J* = 11.0 Hz, 2H), 8.21 (d, *J* = 9.5 Hz, 2H), 7.59 (d, *J* = 19.9 Hz, 1H), 7.24 – 7.17 (m, 1H), 3.10 – 3.05 (m, 2H), 2.99 (t, *J* = 8.7 Hz, 2H), 2.40 (s, 3H) ppm; ^{13}C NMR (100 MHz, DMSO-d_6) δ 193.1, 188.4, 186.4, 160.9, 156.5, 152.9, 150.0 (d, *J* = 9.6 Hz), 148.7, 140.8, 140.0, 134.4 (d, *J* = 26.8 Hz), 52.7, 49.7, 35.9, 20.1 ppm; HRMS (ESI-MS) calcd. for $C_{17}H_{19}FN_2$ $[M + H]^+$ = 271.1532. Found: 271.1616.

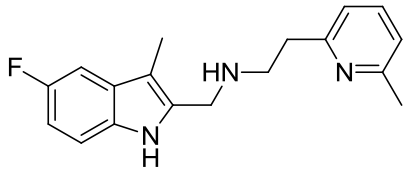

[(5-fluoro-3-methyl-1*H*-indol-2-yl)methyl][2-(6-methylpyridin-2-yl)ethyl]amine (red_A02B08), yellowish oil, 57%, UHPLC-ESI-MS: R_t = 1.79 min., *m*/*z* = 298.2 $[M + H]^+$. ^{1}H NMR (400 MHz, DMSO-d_6) δ 13.48 (s, 1H), 9.75 (s, 1H), 8.84 (t, *J* = 9.6 Hz, 1H), 8.48 (dd, *J* = 5.7 Hz, *J* = 10.9 Hz, 1H), 8.35 (dd, *J* = 3.2 Hz, *J* = 12.4 Hz, 1H), 8.19 (t, *J* = 10.0 Hz, 1H), 7.97 (td, *J* = 3.2 Hz, *J* = 11.1 Hz, *J* = 11.9 Hz, 1H), 4.42 (s, 2H), 3.16 (t, *J* = 8.9 Hz, 2H), 3.05 (t, *J* = 9.3 Hz, 2H), 2.39 (s, 3H), 2.13 (s, 3H) ppm; ^{13}C NMR (100 MHz, DMSO-d_6) δ 196.0, 187.7, 186.5, 184.6, 161.0, 156.1, 155.2, 150.6 (d, *J* = 12.0 Hz), 141.0, 140.0, 129.8 (d, *J* = 12.1 Hz), 126.3 (d, *J* = 32.9 Hz), 118.6 (d, *J* = 28.5 Hz), 49.1, 43.4, 34.7, 20.0, 0.4 ppm; HRMS (ESI-MS) calcd. for $C_{18}H_{20}FN_3$ $[M + H]^+$ = 298.1641. Found: 298.1714.

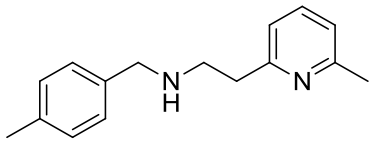

[(4-methylphenyl)methyl][2-(6-methylpyridin-2-yl)ethyl]amine (red_A02B20), colorless oil, 54%, UHPLC-ESI-MS: R_t = 1.49 min., *m*/*z* = 241.2 $[M + H]^+$. ^{1}H NMR (400 MHz, DMSO-d_6) δ 9.69 (d, *J* = 2.3 Hz, 1H), 8.84 (dt, *J* = 2.3 Hz, *J* = 9.5 Hz 1H), 8.43 (d, *J* = 9.9 Hz, 1H), 8.30 – 8.28 (m, 2H), 8.21 – 8.17 (m, 2H), 4.14 (s, 2H), 3.06 – 2.96 (m, 4H), 2.39 (s, 3H), 2.22 (s, 3H) ppm; ^{13}C NMR (100 MHz, DMSO-d_6) δ 195.0, 193.5,

188.2, 186.4, 160.9, 151.0, 150.5, 140.8, 140.0, 54.5, 49.5, 35.4, 20.0, 15.9 ppm; HRMS (ESI-MS) calcd. for $C_{16}H_{20}N_2$ $[M + H]^+$ = 241.1626. Found: 241.1710.

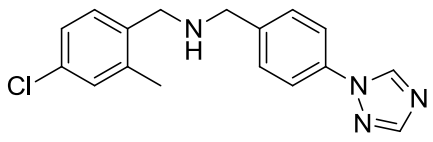

[(4-chloro-2-methylphenyl)methyl]({[4-(1*H*-1,2,4-triazol-1-yl)phenyl]methyl})amine (red_A04B19),yellowish oil, 25%, UHPLC-ESI-MS: R_t = 1.85 min., *m*/*z* = 313.2 $[M + H]^+$. ^{1}H NMR (400 MHz, DMSO-d_6) δ 10.95 (s, 1H), 9.65 (s, 1H), 9.54 (s, 1H), 9.16 (d, *J* = 10.6 Hz, 2H), 8.83 (d, *J* = 10.6 Hz, 2H), 8.60 (d, *J* = 10.1 Hz, 1H), 8.43 – 8.39 (m, 2H), 4.22 (s, 2H), 4.04 (s, 2H), 2.21 (s, 3H) ppm; ^{13}C NMR (100 MHz, DMSO-d_6) δ 193.7, 180.4, 174.1, 167.7, 163.6, 159.6, 154.1, 152.9, 152.0, 151.8, 146.8, 139.0, 54.4, 50.9, 13.0 ppm; HRMS (ESI-MS) calcd. for $C_{17}H_{17}ClN_4$ $[M + H]^+$ = 313.1142. Found: 313.1225.

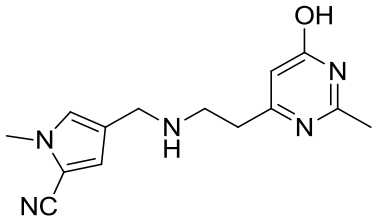

4-({[2-(6-hydroxy-2-methylpyrimidin-4-yl)ethyl]amino}methyl)-1-methyl-1*H*-pyrrole-2-carbonitrile (red_A05B13), colorless oil, 32%, UHPLC-ESI-MS: R_t = 1.30 min., *m*/*z* = 272.2 $[M + H]^+$. ^{1}H NMR (400 MHz, DMSO-d_6) δ 9.55 (s, 0.3H), 8.42 (s, 1H), 8.10 (s, 1H), 6.95 (s, 1H), 4.23 (s, 2H), 4.06 (s, 3H), 3.19 (t, *J* = 9.1 Hz, 2H), 2.75 (t, *J* = 9.1 Hz, 2H), 2.19 (s, 3H) ppm; ^{13}C NMR (100 MHz, DMSO-d_6) δ 198.5, 196.7, 188.9, 151.5, 140.6, 131.7, 127.9, 119.3, 117.9, 53.2, 45.7, 43.6, 33.9, 16.4 ppm; HRMS (ESI-MS) calcd. for $C_{14}H_{17}N_5O$ $[M + H]^+$ = 272.1433. Found: 272.1517.

^{1}H, ^{13}C NMR, HRMS of some representative reductive amination products

^{1}H NMR (400 MHz, DMSO-*d*6) 5-chloro-2-(1,3-thiazinane-4-carbonyl)-1,2,3,4-tetrahydroisoquinoline (amd_A06B25)

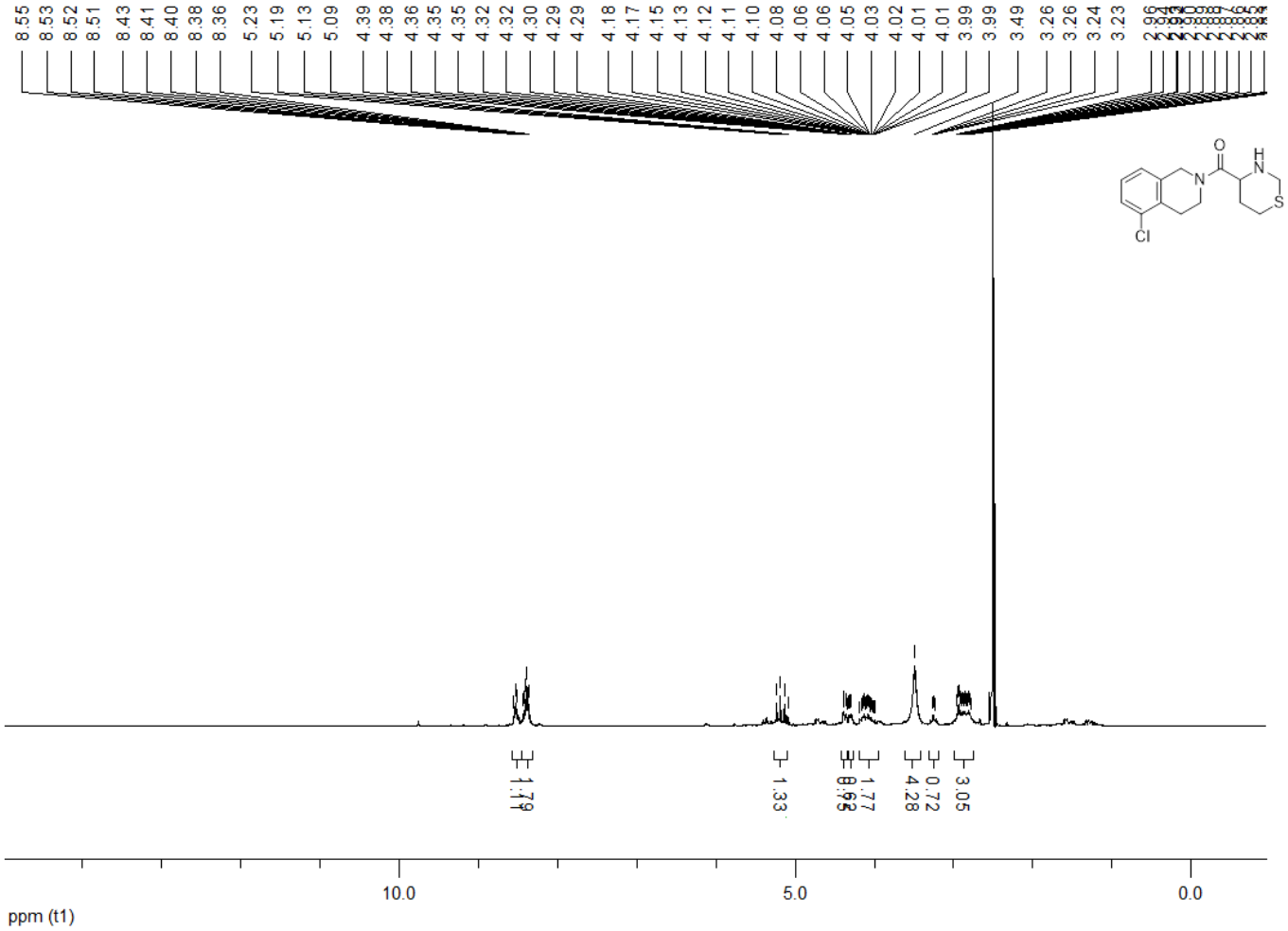

^{13}C NMR (100 MHz, DMSO-*d*$_6$)5-chloro-2-(1,3-thiazinane-4-carbonyl)-1,2,3,4-tetrahydroisoquinoline (amd_A06B25)

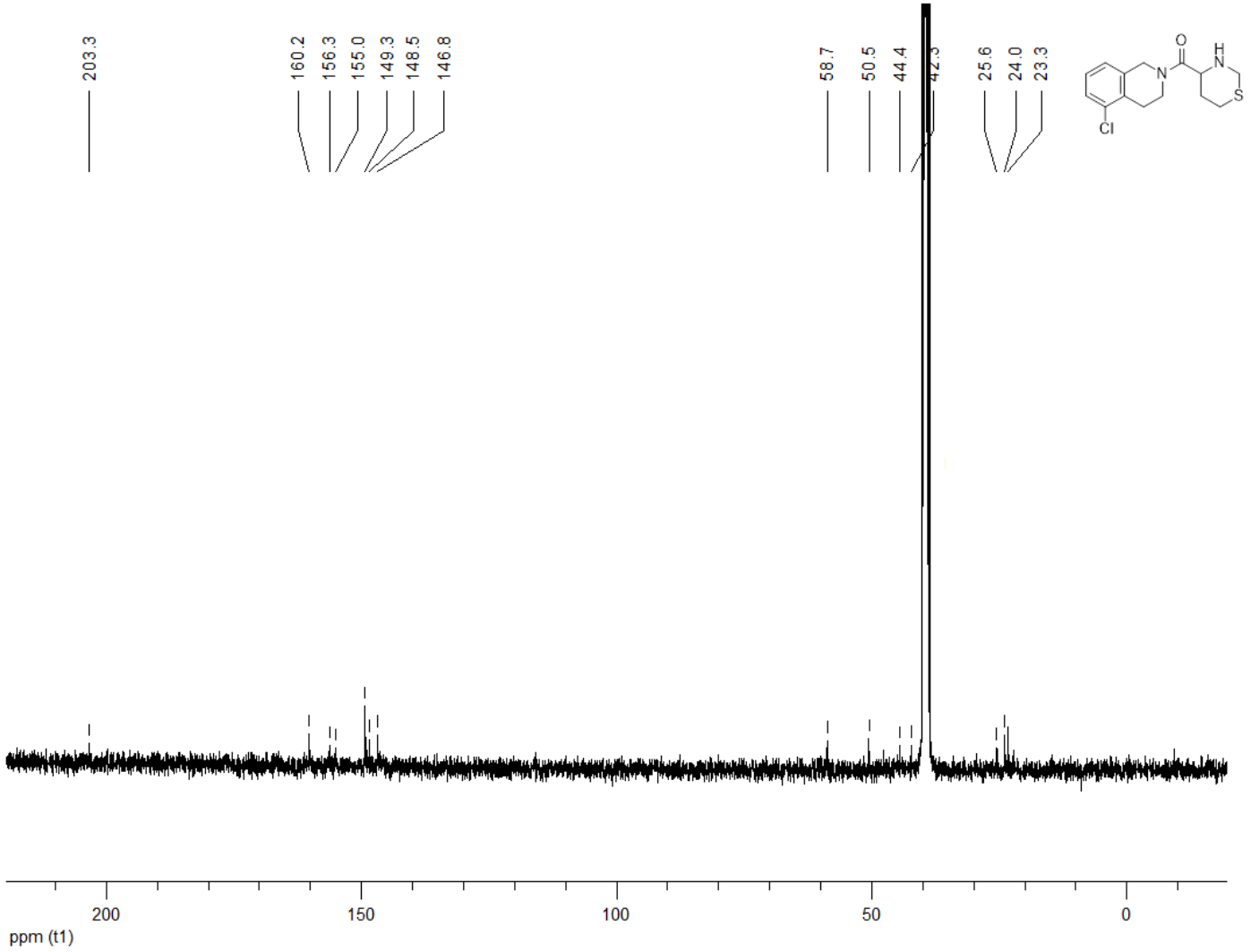

HRMS (ESI-MS)5-chloro-2-(1,3-thiazinane-4-carbonyl)-1,2,3,4-tetrahydroisoquinoline (amd_A06B25)

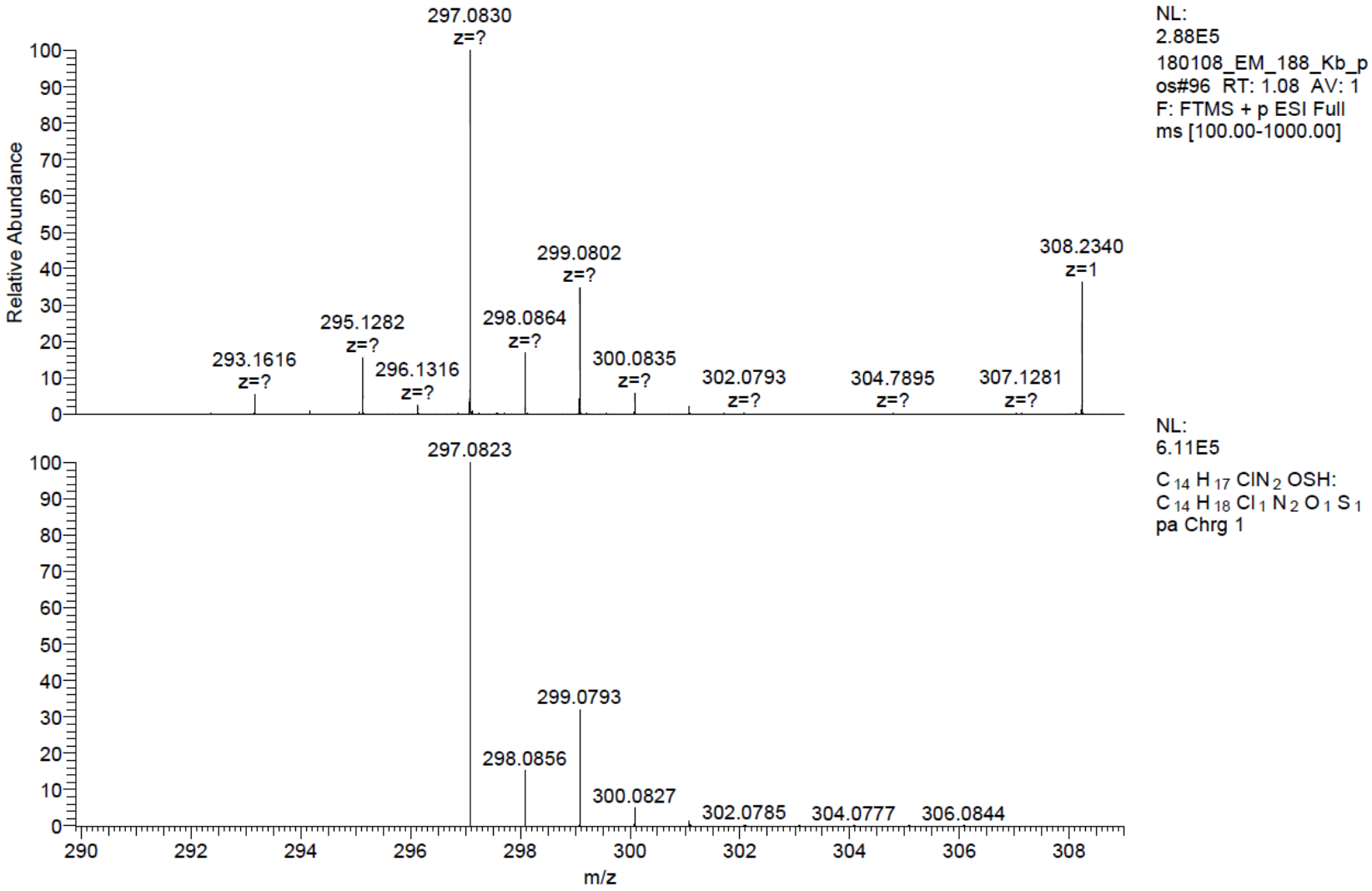

^{1}H NMR (400 MHz, DMSO-*d*$_6$)[(2*E*)-3-(4-fluorophenyl)prop-2-en-1-yl][2-(6-methylpyridin-2-yl)ethyl]amine (red_A02B03)

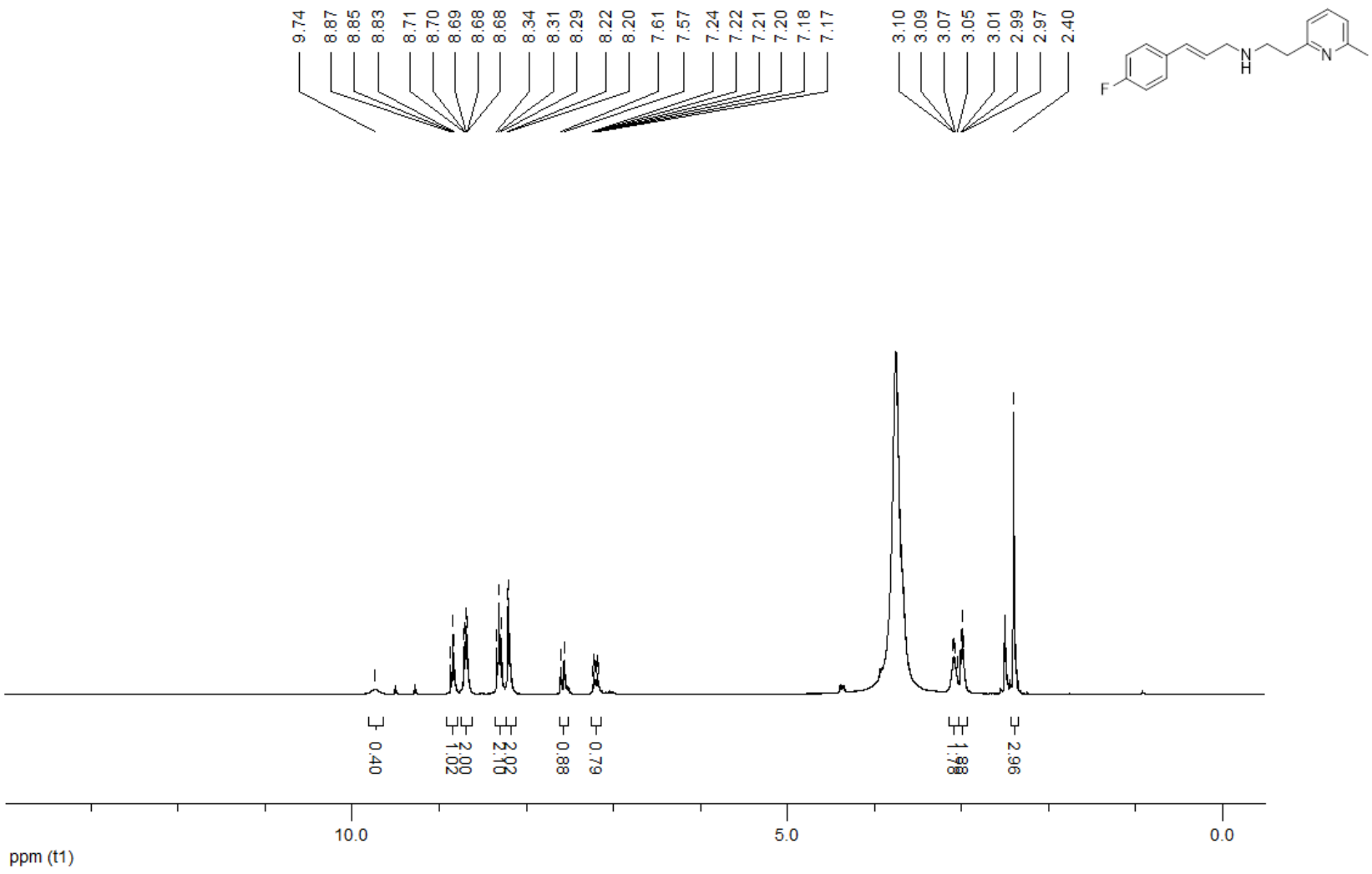

^{13}C NMR (100 MHz, DMSO-*d*$_6$)[(2*E*)-3-(4-fluorophenyl)prop-2-en-1-yl][2-(6-methylpyridin-2-yl)ethyl]amine (red_A02B03)

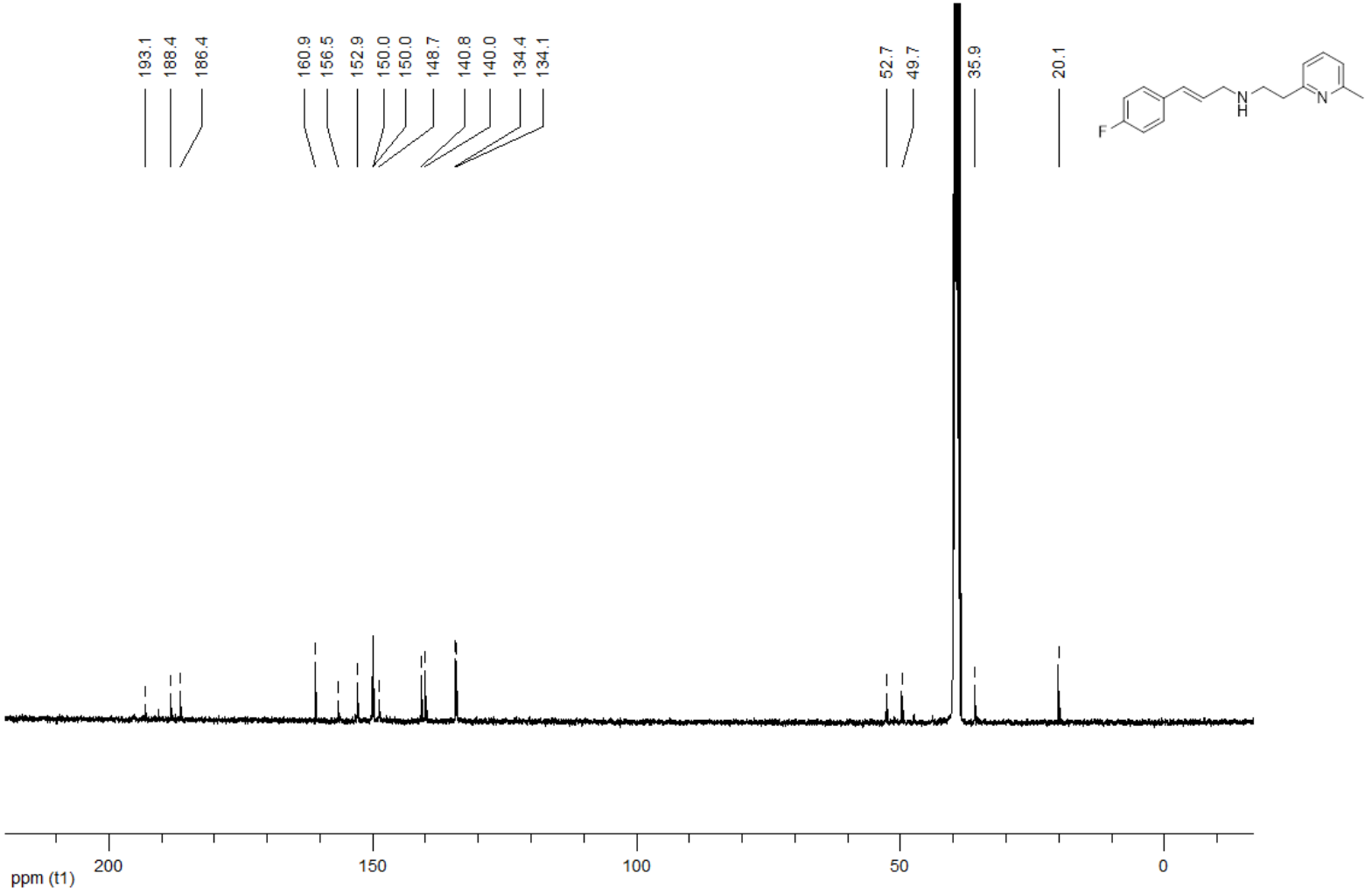

HRMS (ESI-MS)[(2*E*)-3-(4-fluorophenyl)prop-2-en-1-yl][2-(6-methylpyridin-2-yl)ethyl]amine (red_A02B03)

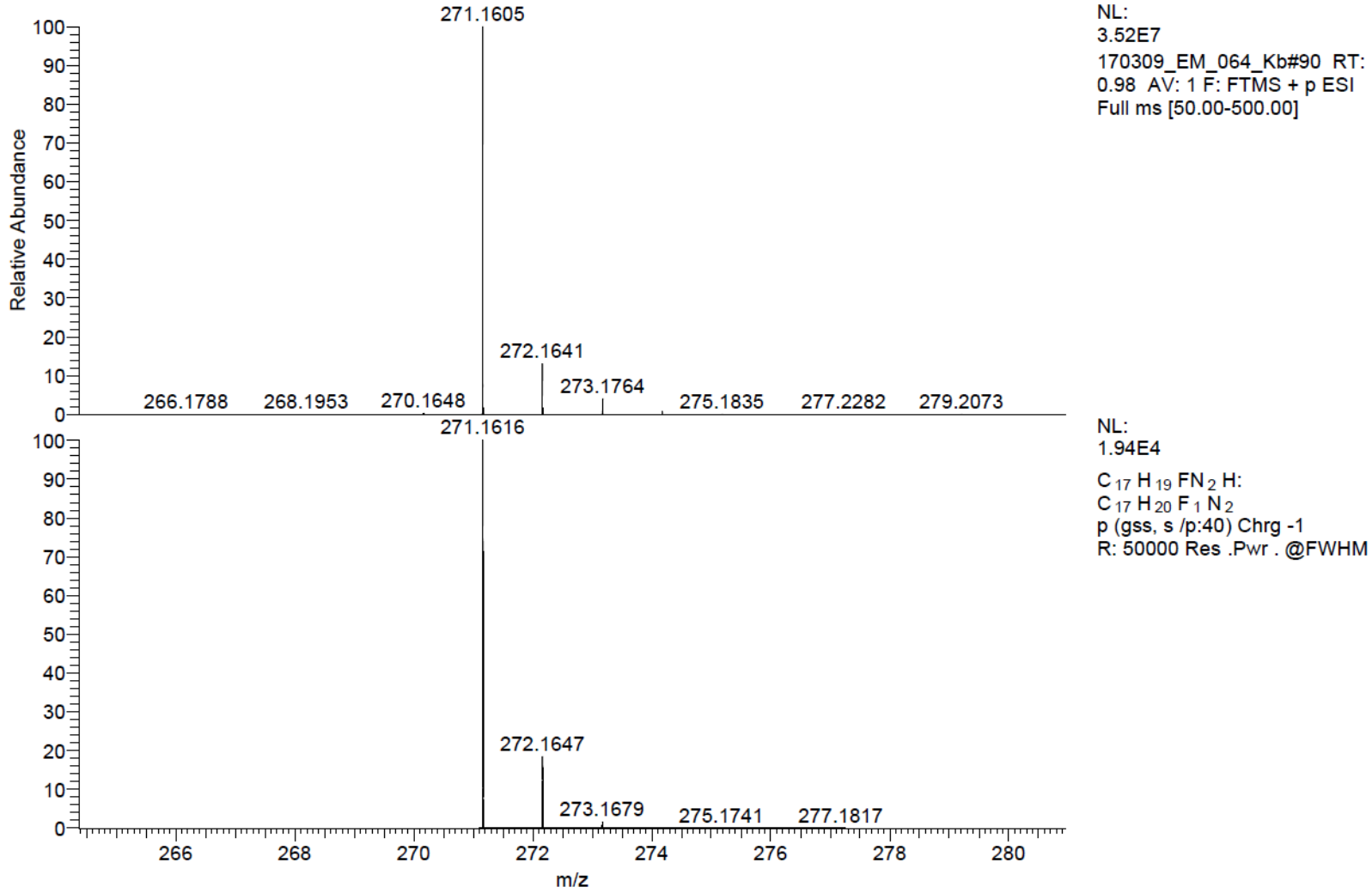

^{1}H NMR (400 MHz, DMSO-*d*$_6$)[(5-fluoro-3-methyl-1*H*-indol-2-yl)methyl][2-(6-methylpyridin-2-yl)ethyl]amine (red_A02B08)

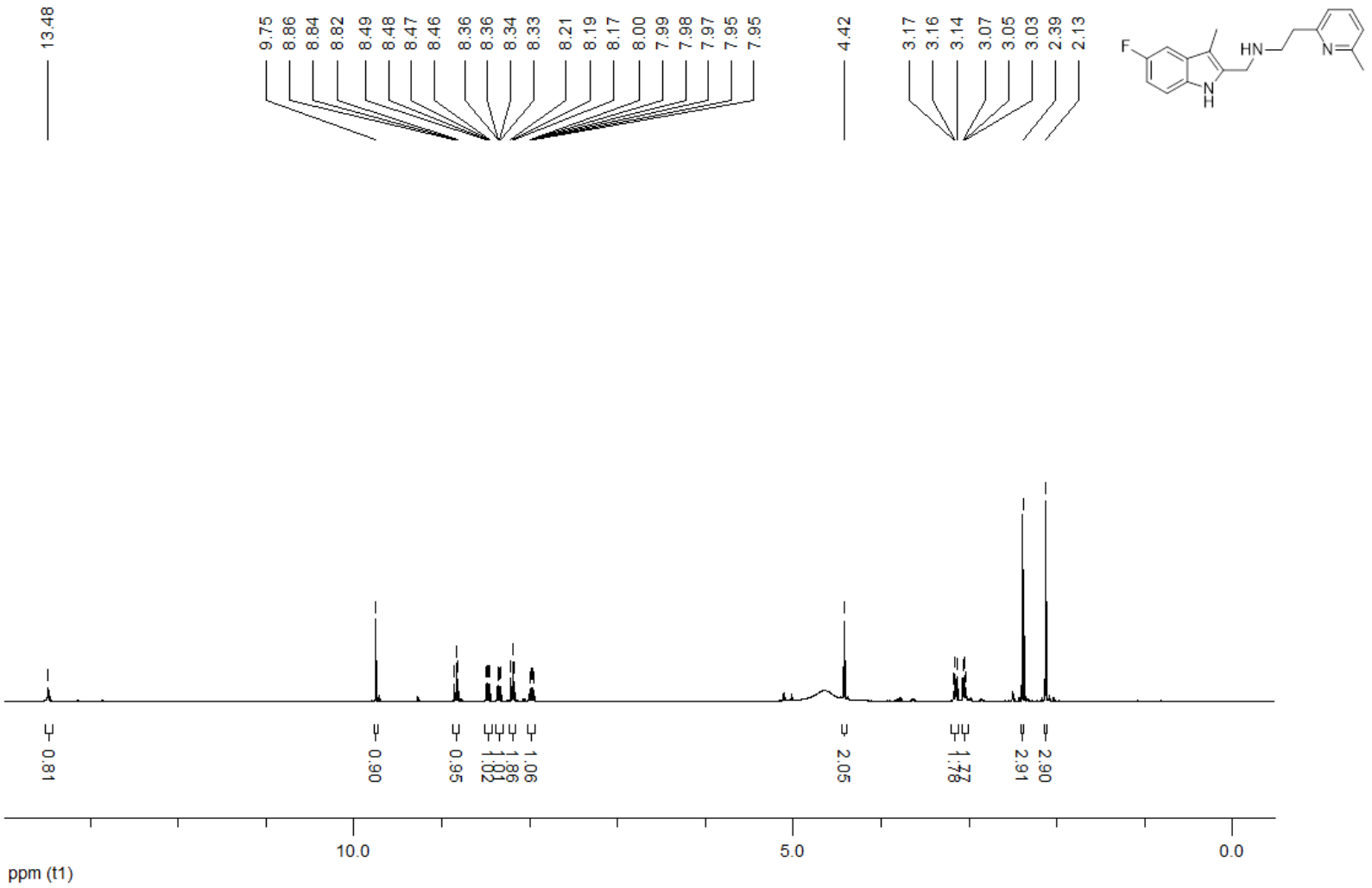

^{13}C NMR (100 MHz, DMSO-*d*$_6$)[(5-fluoro-3-methyl-1*H*-indol-2-yl)methyl][2-(6-methylpyridin-2-yl)ethyl]amine (red_A02B08)

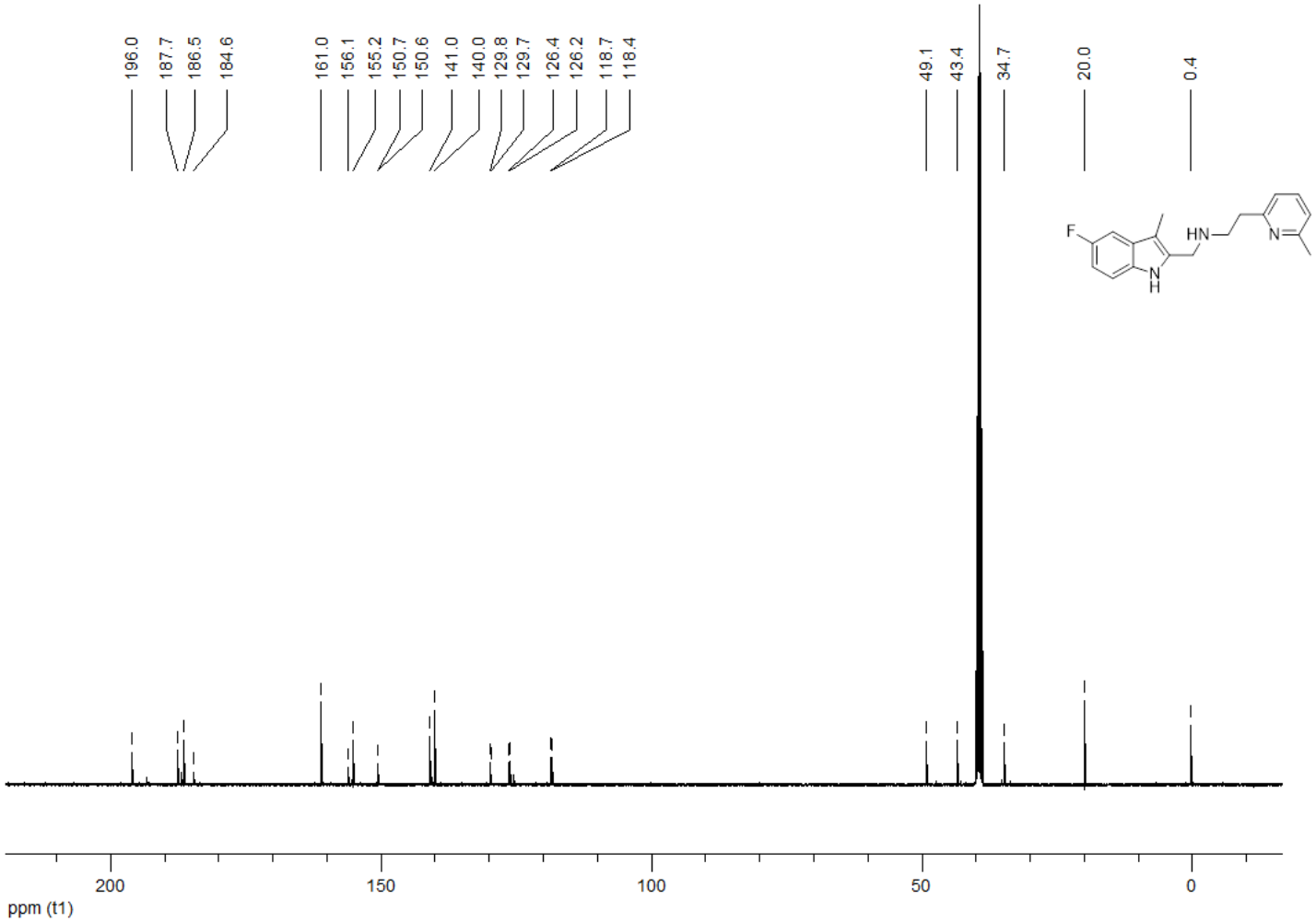

HRMS (ESI-MS)[(5-fluoro-3-methyl-1*H*-indol-2-yl)methyl][2-(6-methylpyridin-2-yl)ethyl]amine (red_A02B08)

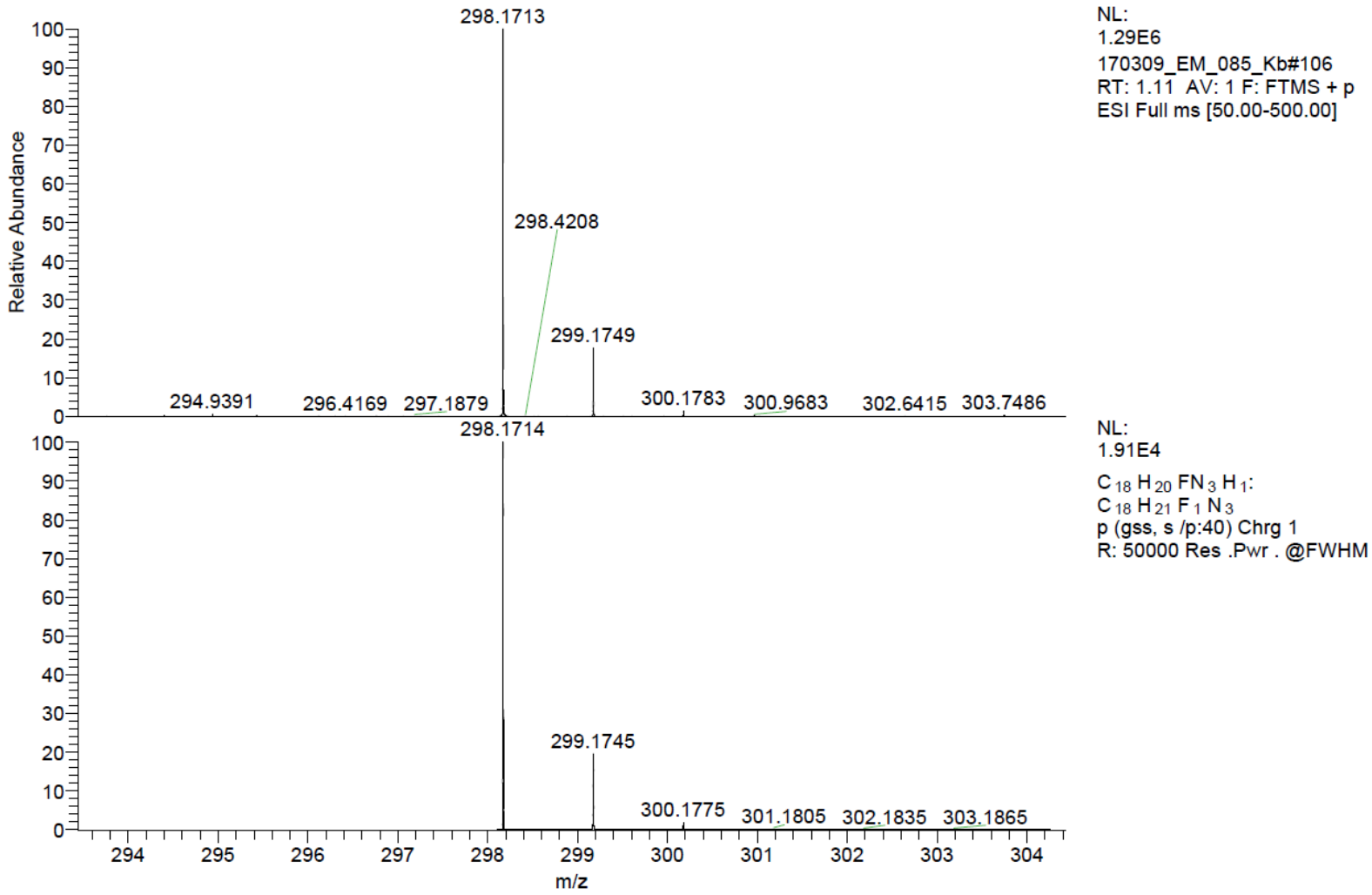

^{1}H NMR (400 MHz, DMSO-*d*$_6$)[(4-methylphenyl)methyl][2-(6-methylpyridin-2-yl)ethyl]amine (red_A02B20)

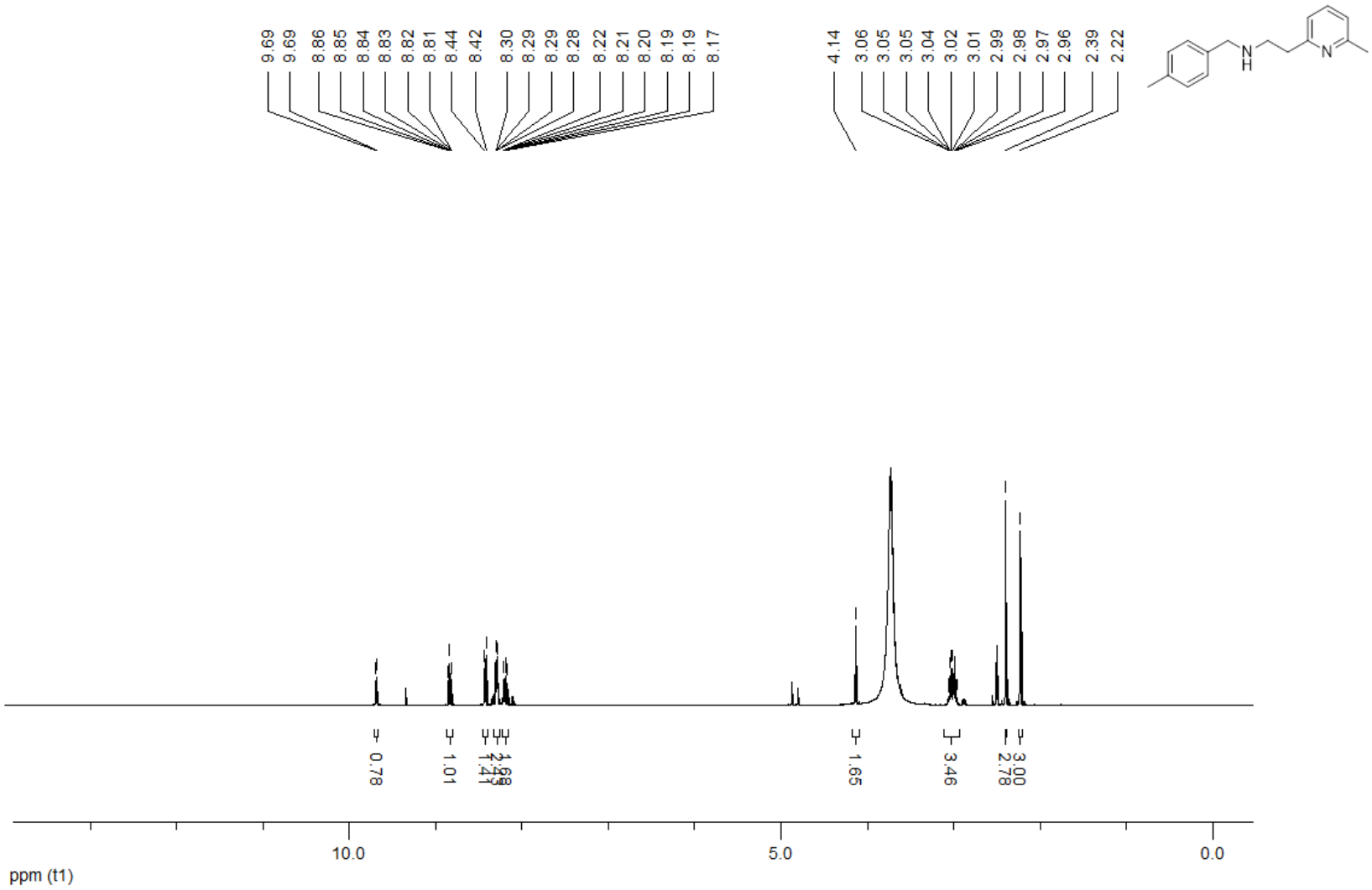

^{13}C NMR (100 MHz, DMSO-*d*$_6$)[(4-methylphenyl)methyl][2-(6-methylpyridin-2-yl)ethyl]amine (red_A02B20)

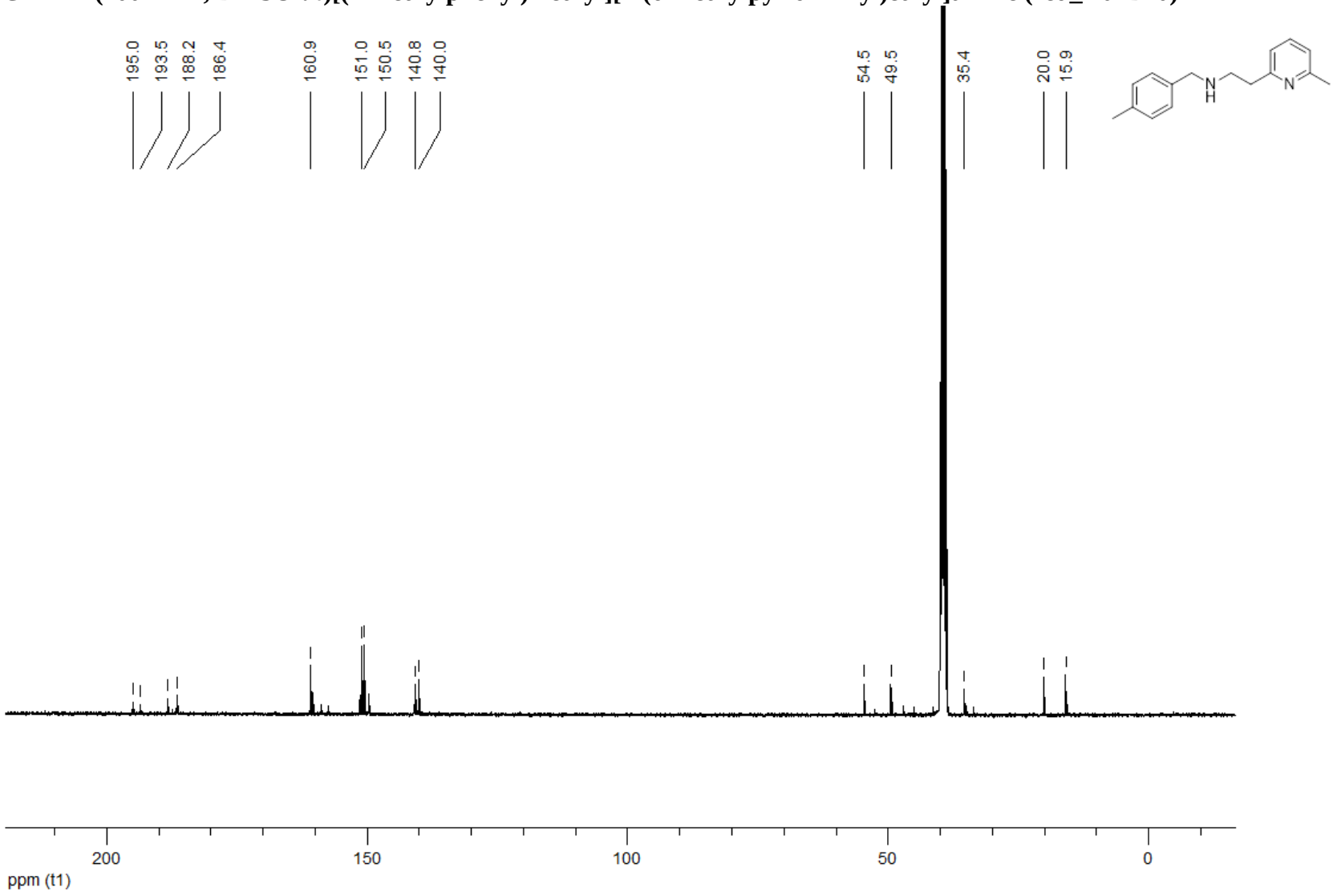

HRMS (ESI-MS)[(4-methylphenyl)methyl][2-(6-methylpyridin-2-yl)ethyl]amine (red_A02B20)

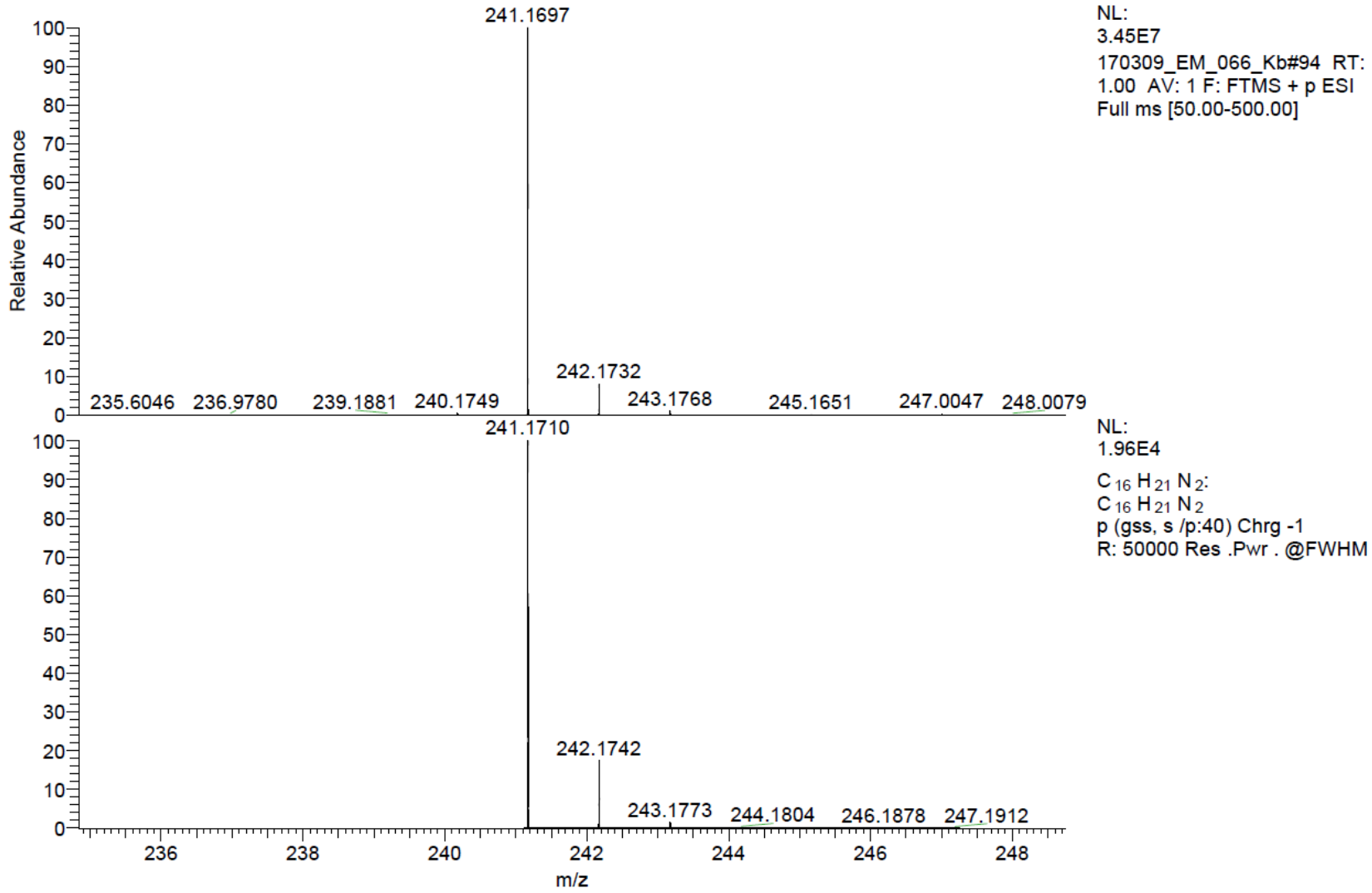

^{1}H NMR (400 MHz, DMSO-*d*$_6$)[(4-chloro-2-methylphenyl)methyl]({[4-(1*H*-1,2,4-triazol-1-yl)phenyl]methyl})amine (red_A04B19)

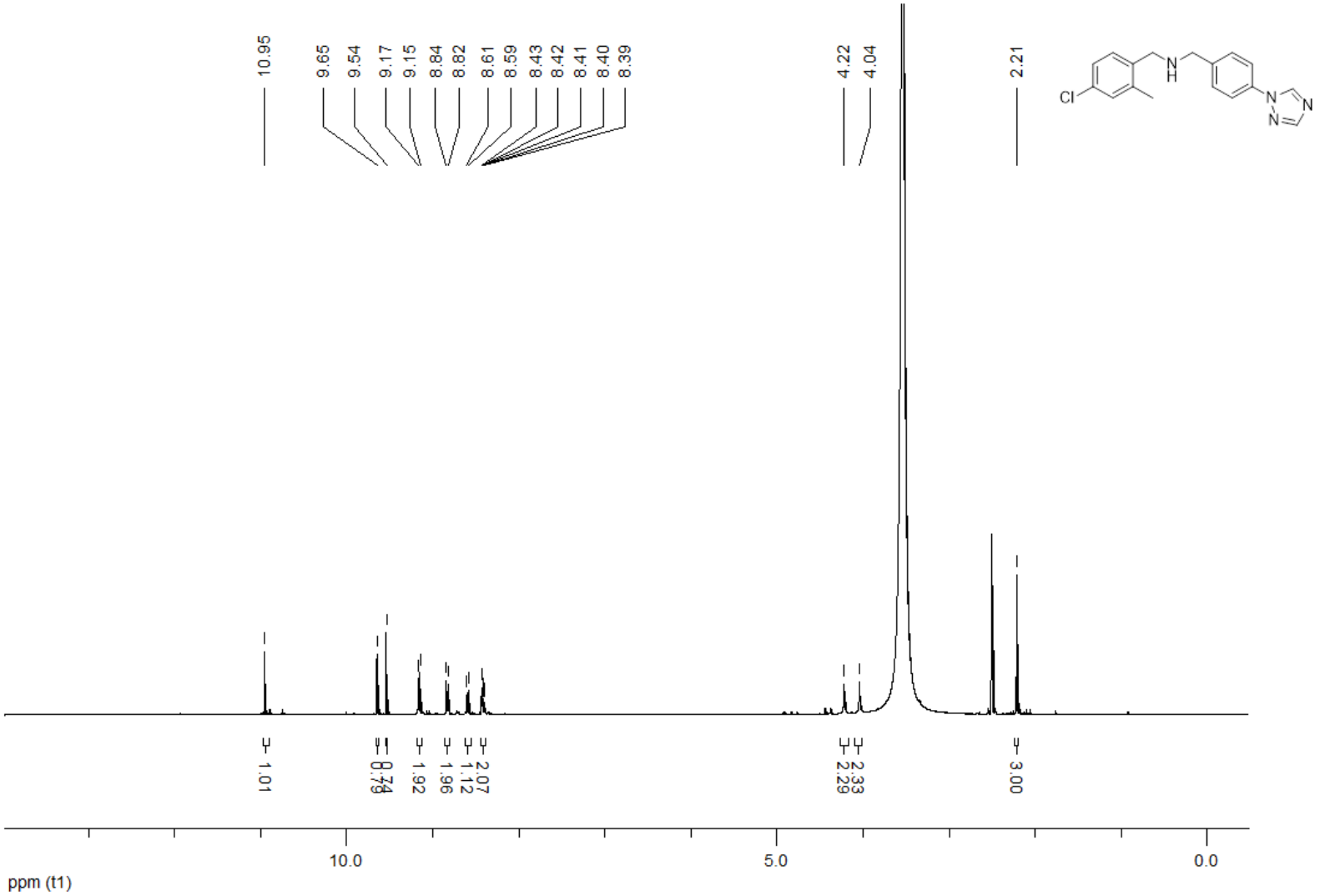

^{13}C NMR (100 MHz, DMSO-*d*$_6$)[(4-chloro-2-methylphenyl)methyl]({[4-(1*H*-1,2,4-triazol-1-yl)phenyl]methyl})amine (red_A04B19)

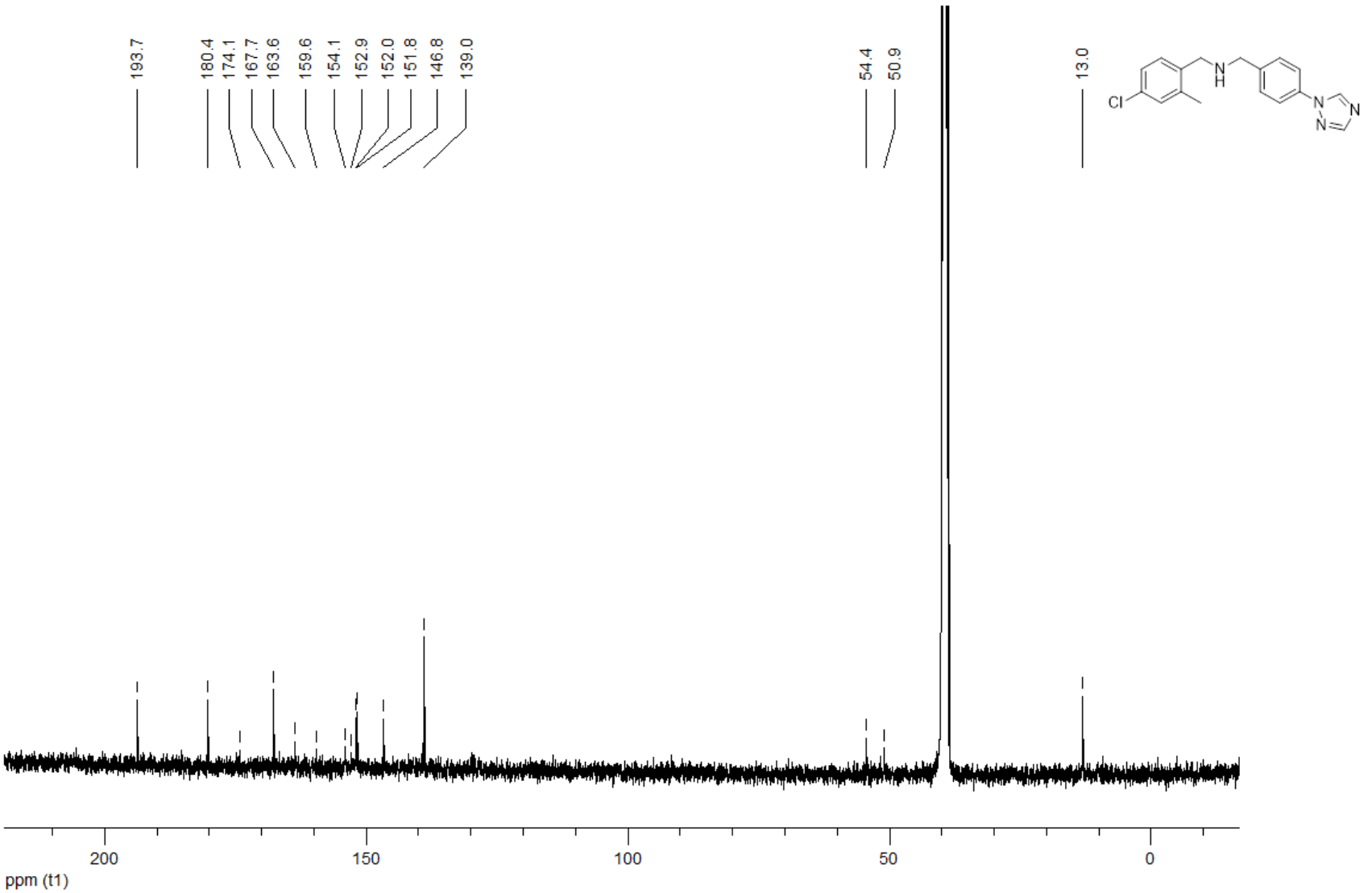
193.7
180.4
174.1
167.7
163.6
159.6
154.1
152.9
152.0
151.8
146.8
139.0
54.4
50.9
13.0
Cl
N
H
N
N
N
200
150
100
50
0
ppm (t1)

HRMS (ESI-MS)[(4-chloro-2-methylphenyl)methyl]({[4-(1*H*-1,2,4-triazol-1-yl)phenyl]methyl})amine (red_A04B19)

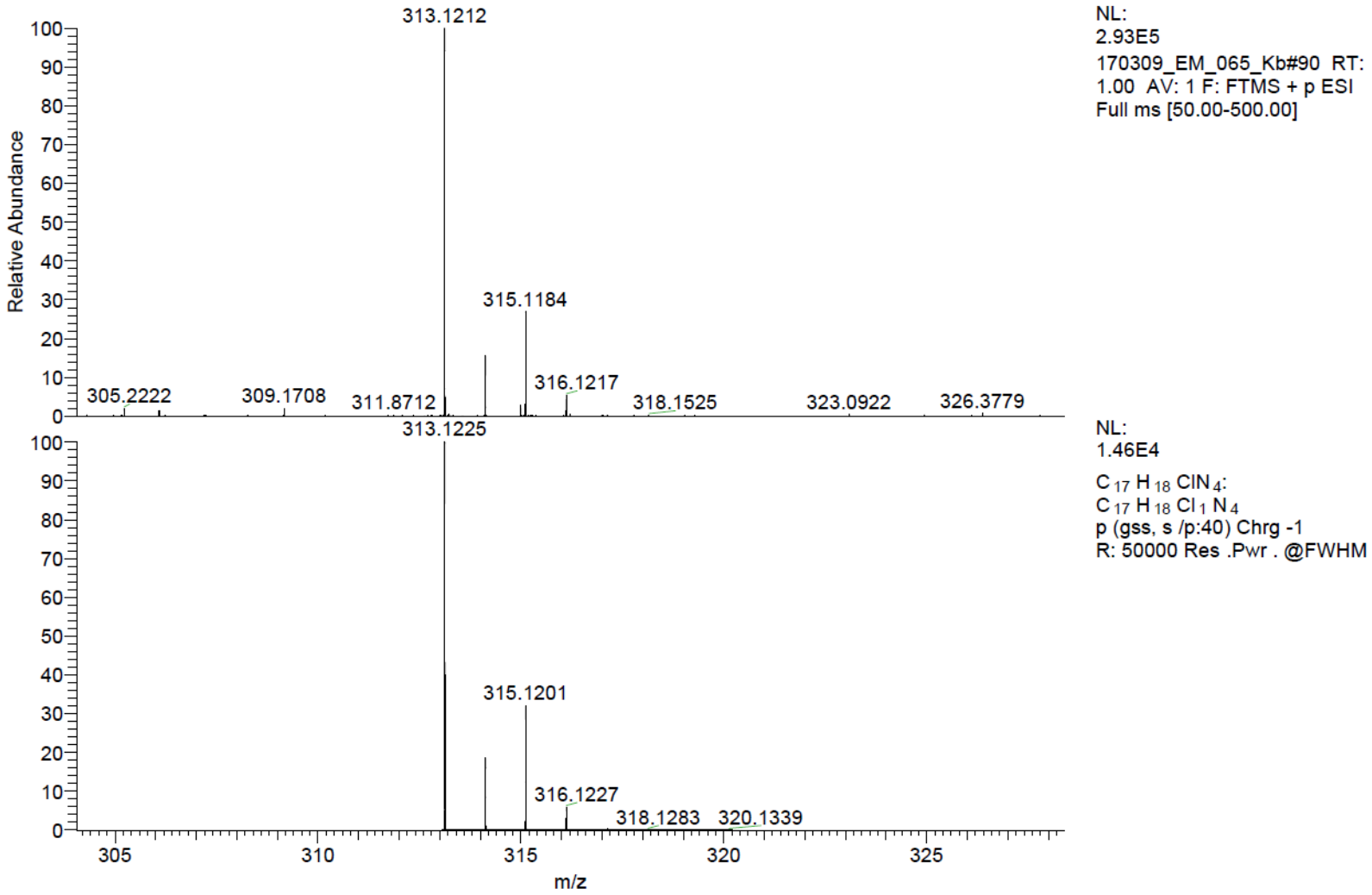

^{1}H NMR (400 MHz, DMSO-*d*$_6$)4-({[2-(6-hydroxy-2-methylpyrimidin-4-yl)ethyl]amino}methyl)-1-methyl-1*H*-pyrrole-2-carbonitrile (red_A05B13)

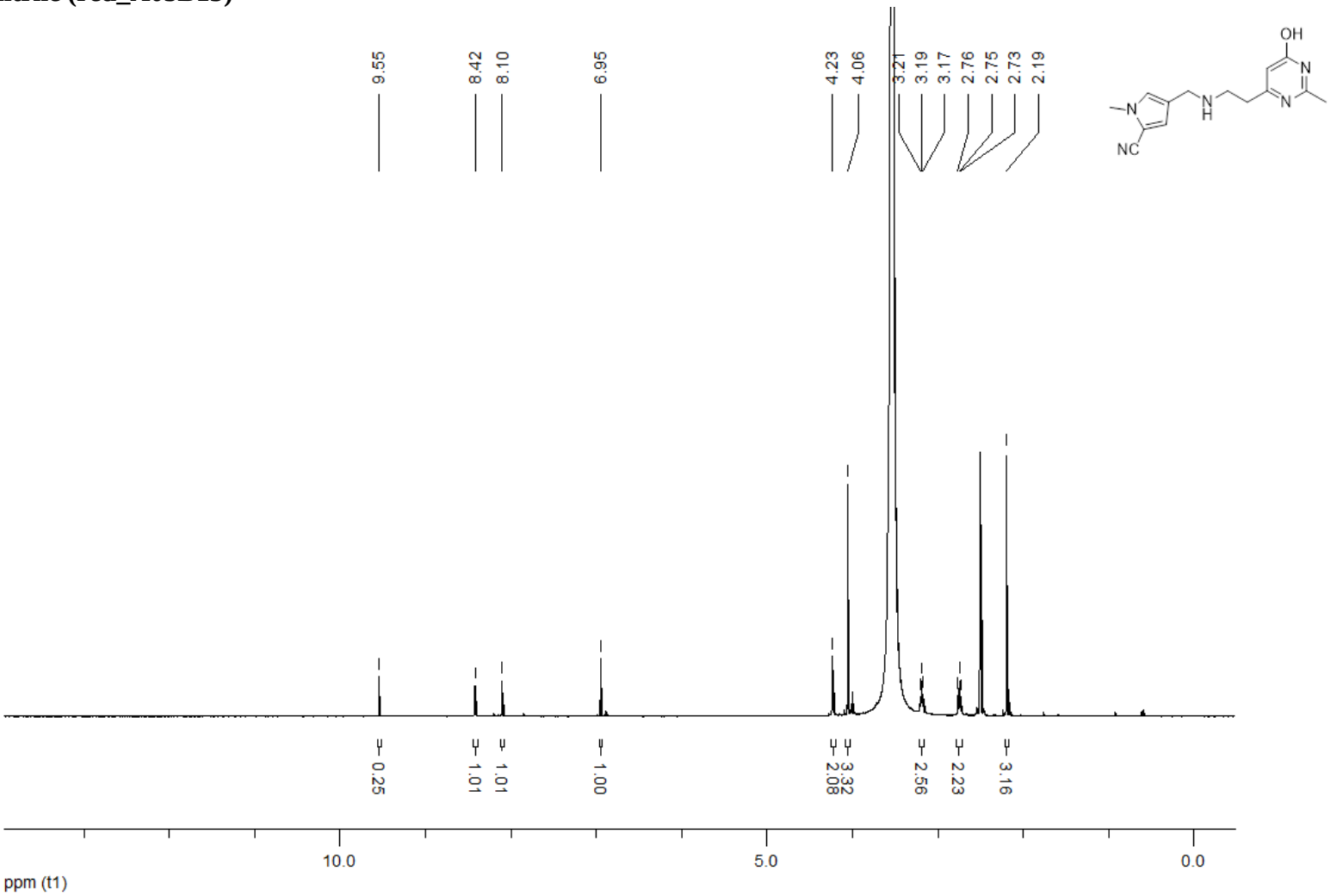

^{13}C NMR (100 MHz, DMSO-*d*$_6$)4-({[2-(6-hydroxy-2-methylpyrimidin-4-yl)ethyl]amino}methyl)-1-methyl-1*H*-pyrrole-2-carbonitrile (red_A05B13)

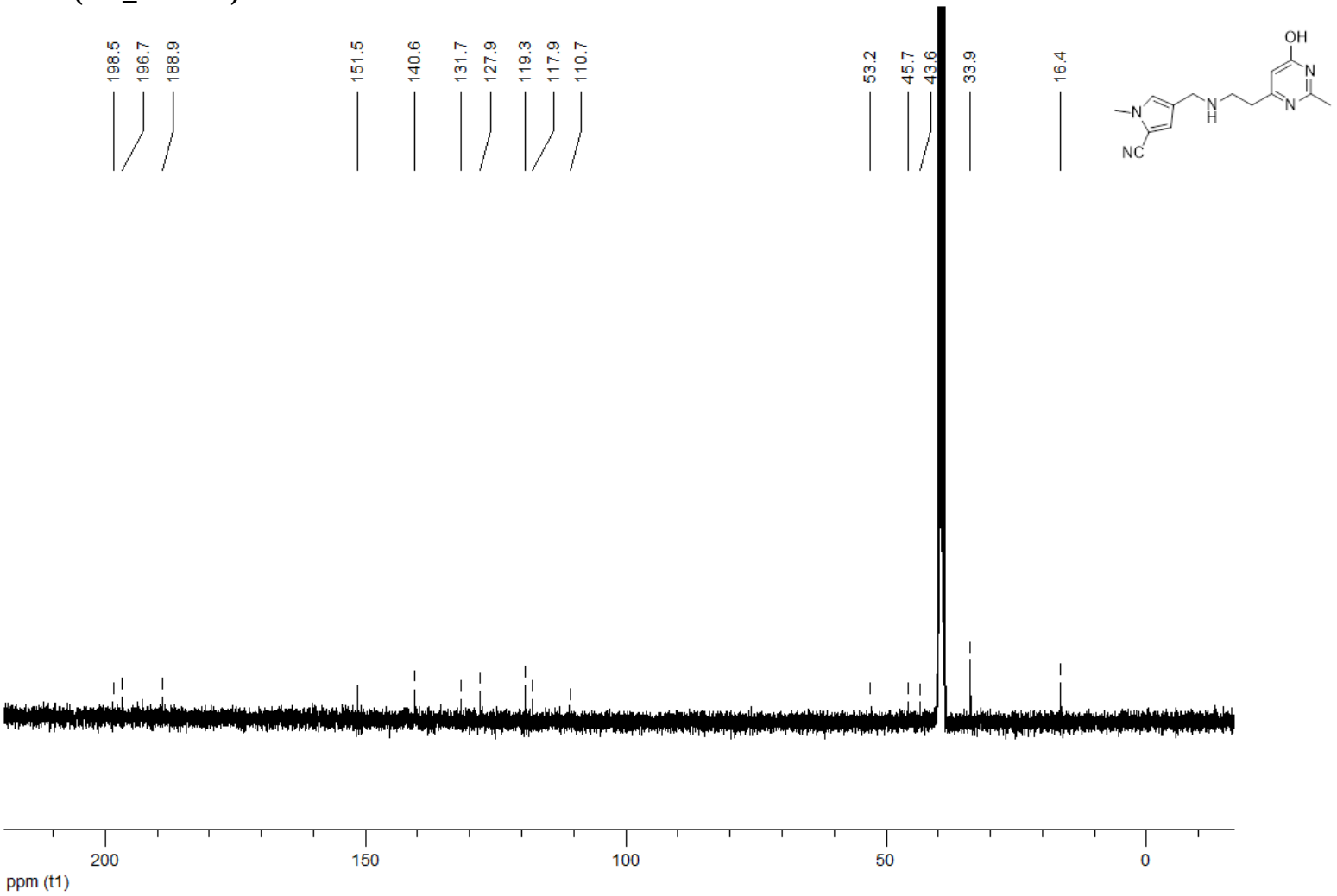

HRMS (ESI-MS)4-({[2-(6-hydroxy-2-methylpyrimidin-4-yl)ethyl]amino}methyl)-1-methyl-1*H*-pyrrole-2-carbonitrile (red_A05B13)

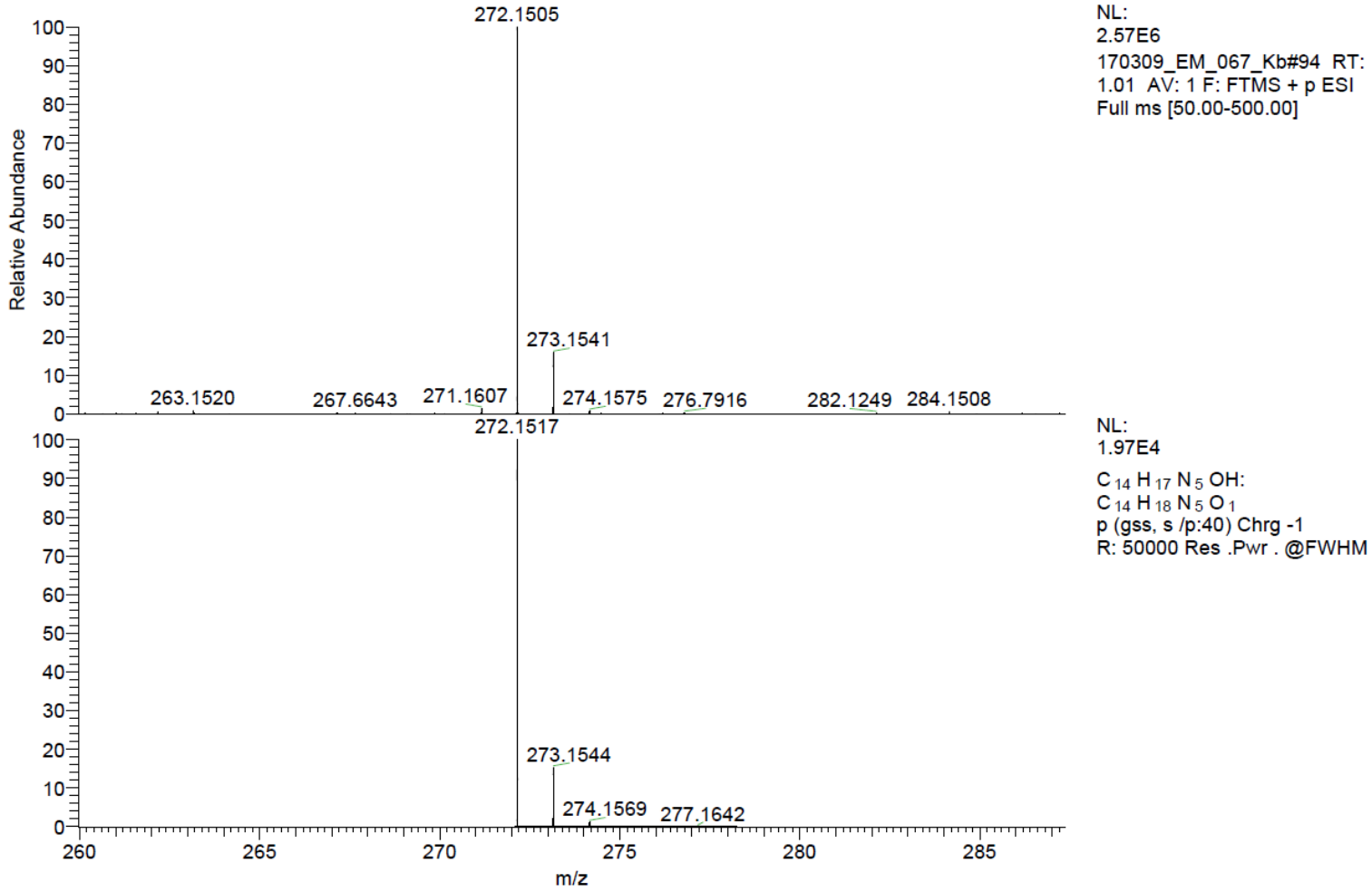

^{1}H, ^{13}C NMR, HRMS of some representative amidification products

^{1}H NMR (400 MHz, DMSO-*d*$_6$)2-(1,3-thiazinane-4-carbonyl)-1,2,3,4-tetrahydroisoquinolin-7-ol(amd_A06B37)

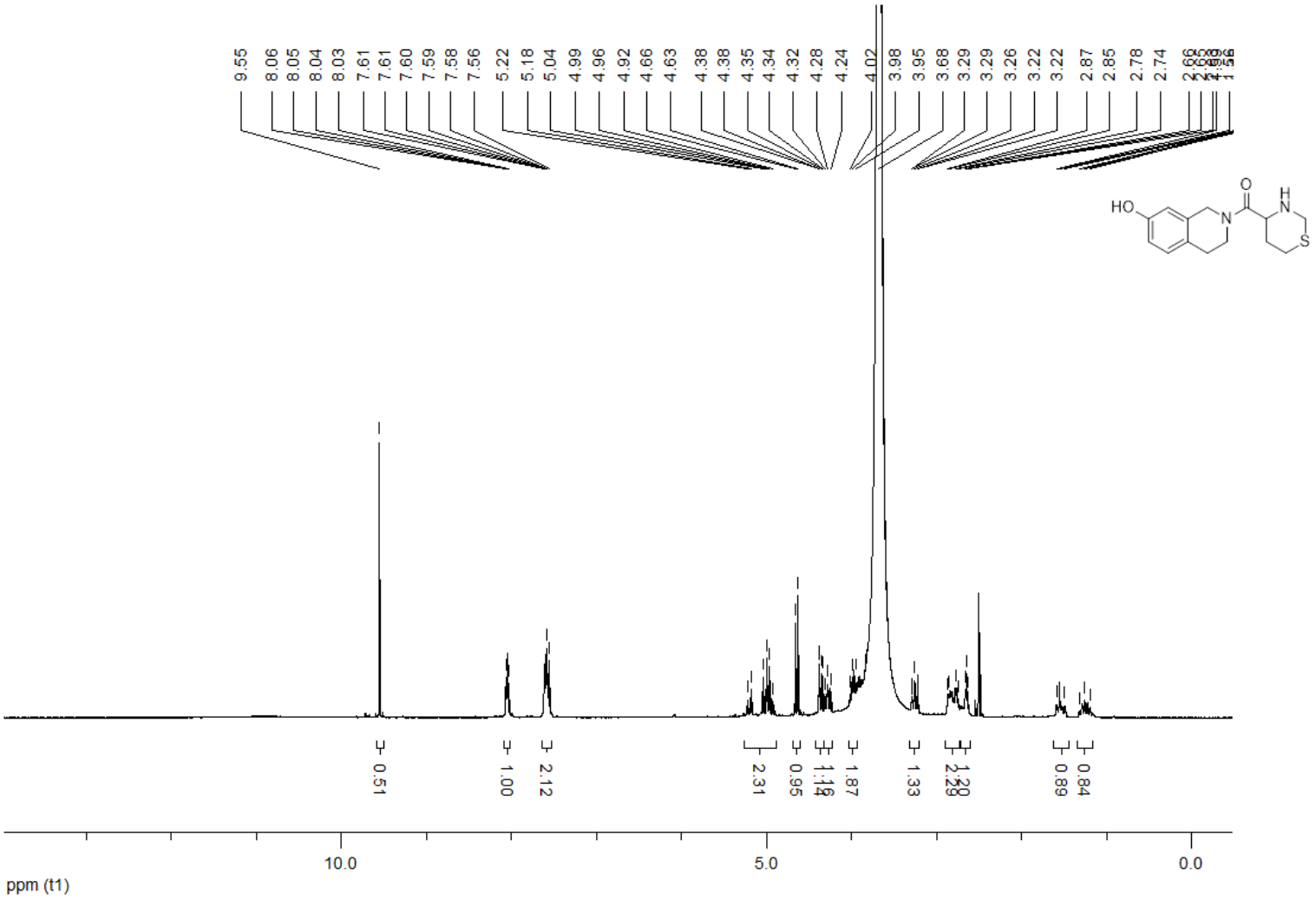

^{13}C NMR (100 MHz, DMSO-*d*$_6$)2-(1,3-thiazinane-4-carbonyl)-1,2,3,4-tetrahydroisoquinolin-7-ol(amd_A06B37)

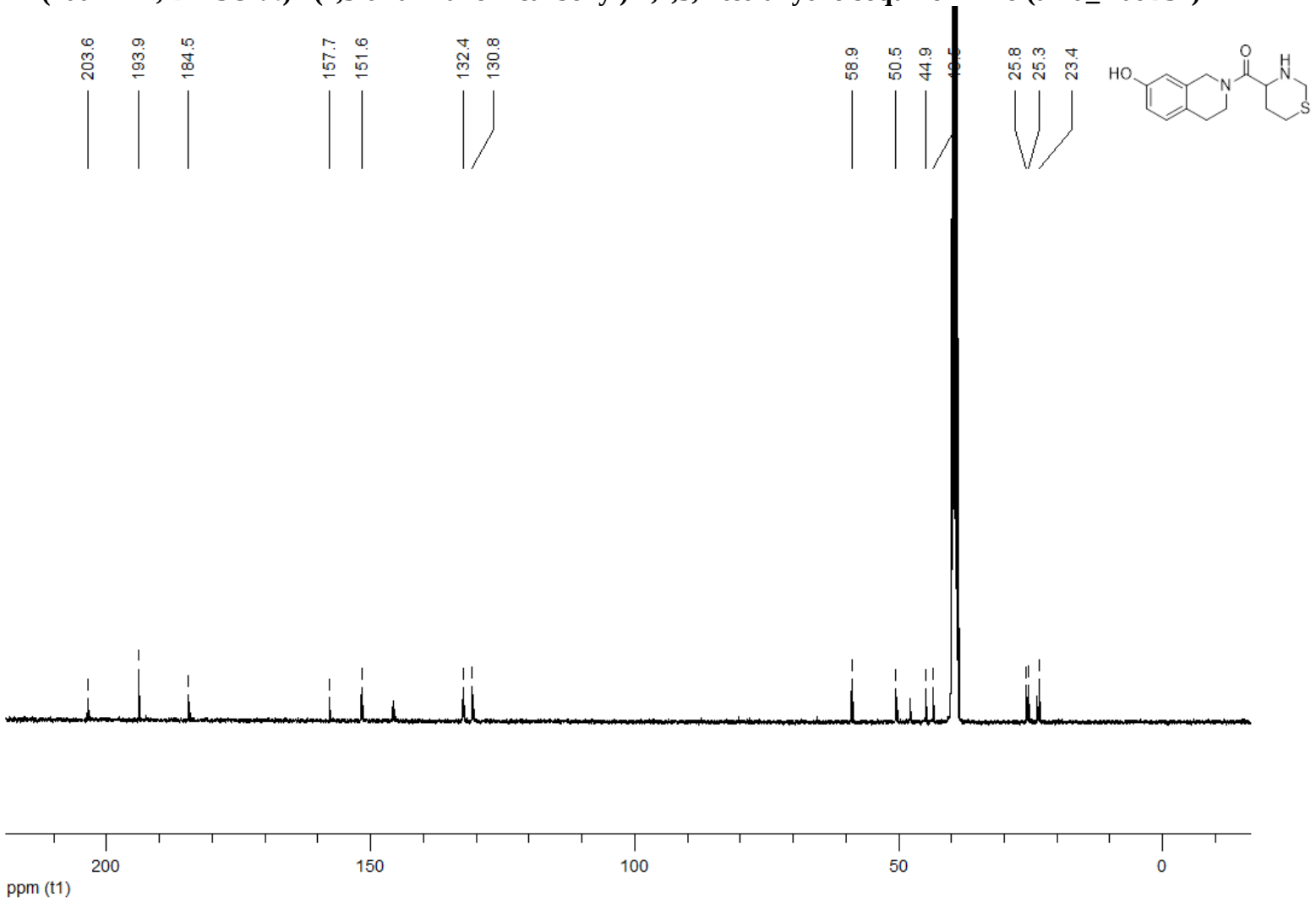

HRMS (ESI-MS)2-(1,3-thiazinane-4-carbonyl)-1,2,3,4-tetrahydroisoquinolin-7-ol(amd_A06B37)

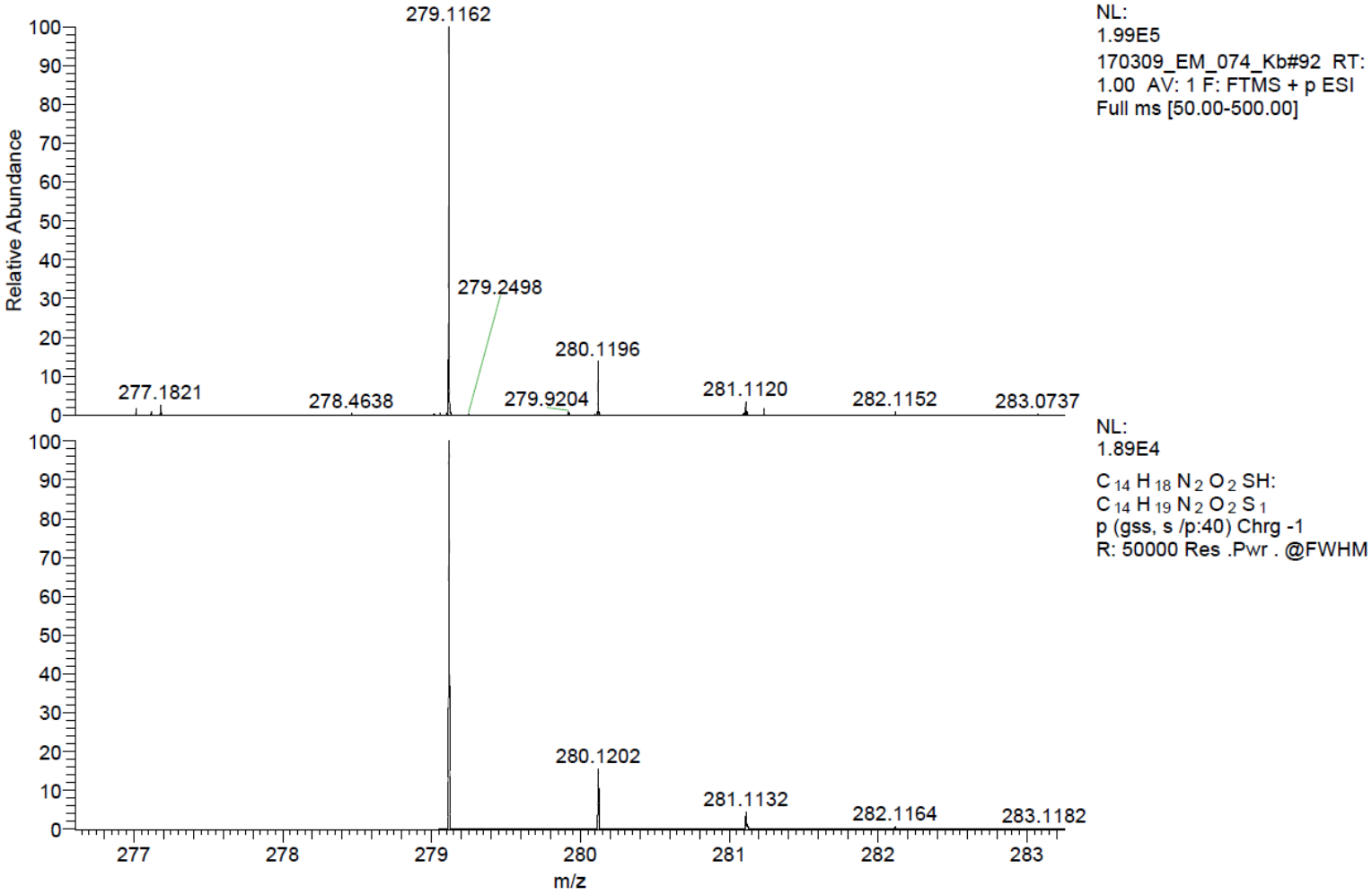

^{1}H NMR (400 MHz, DMSO-*d*$_6$) 2-(3-{[1,2,4]triazolo[4,3-a]pyridin-3-yl}piperidine-1-carbonyl)azepane (amd_A07B34)

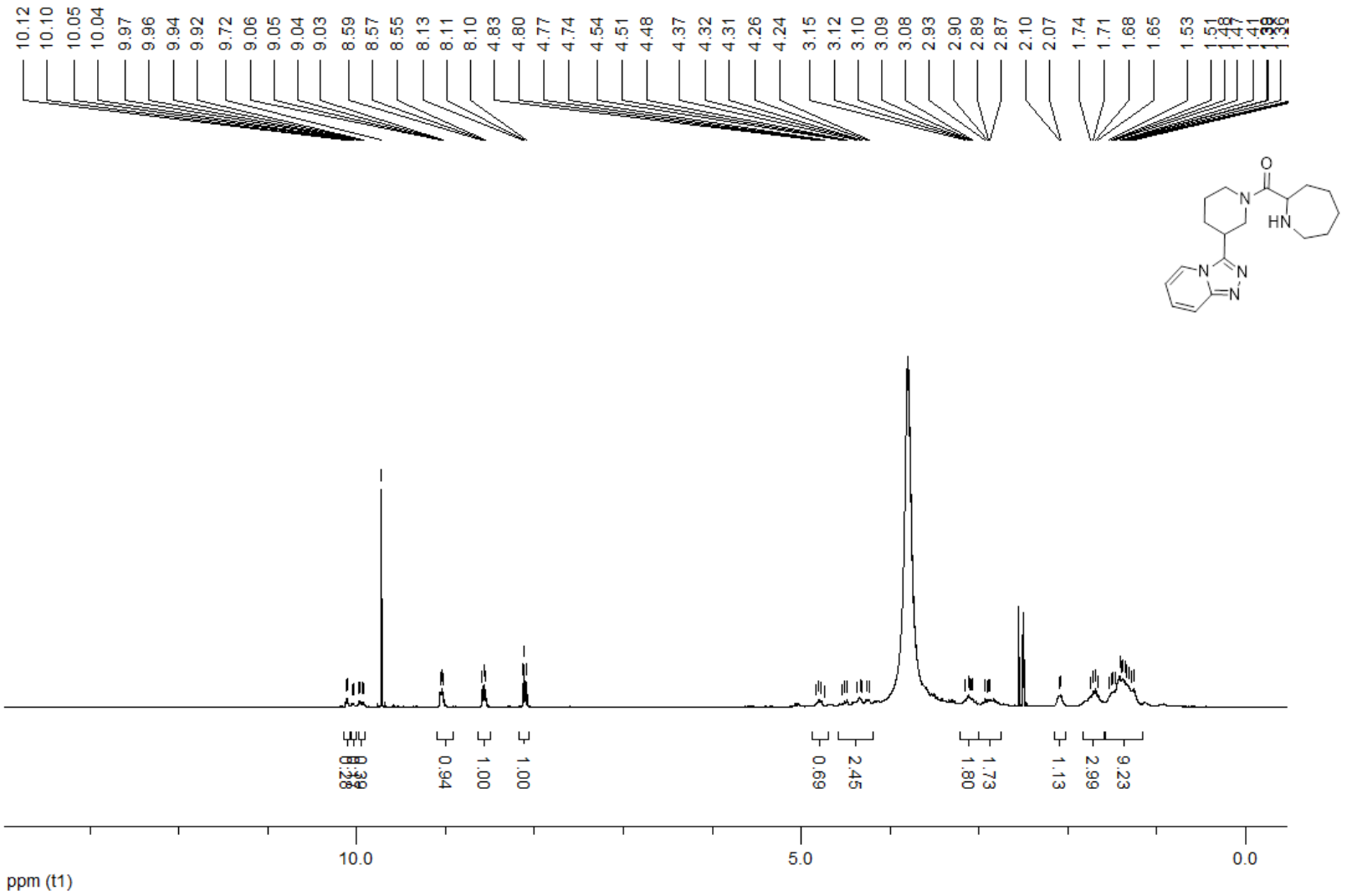

^{13}C NMR (100 MHz, DMSO-*d*$_6$) 2-(3-{[1,2,4]triazolo[4,3-a]pyridin-3-yl}piperidine-1-carbonyl)azepane (amd_A07B34)

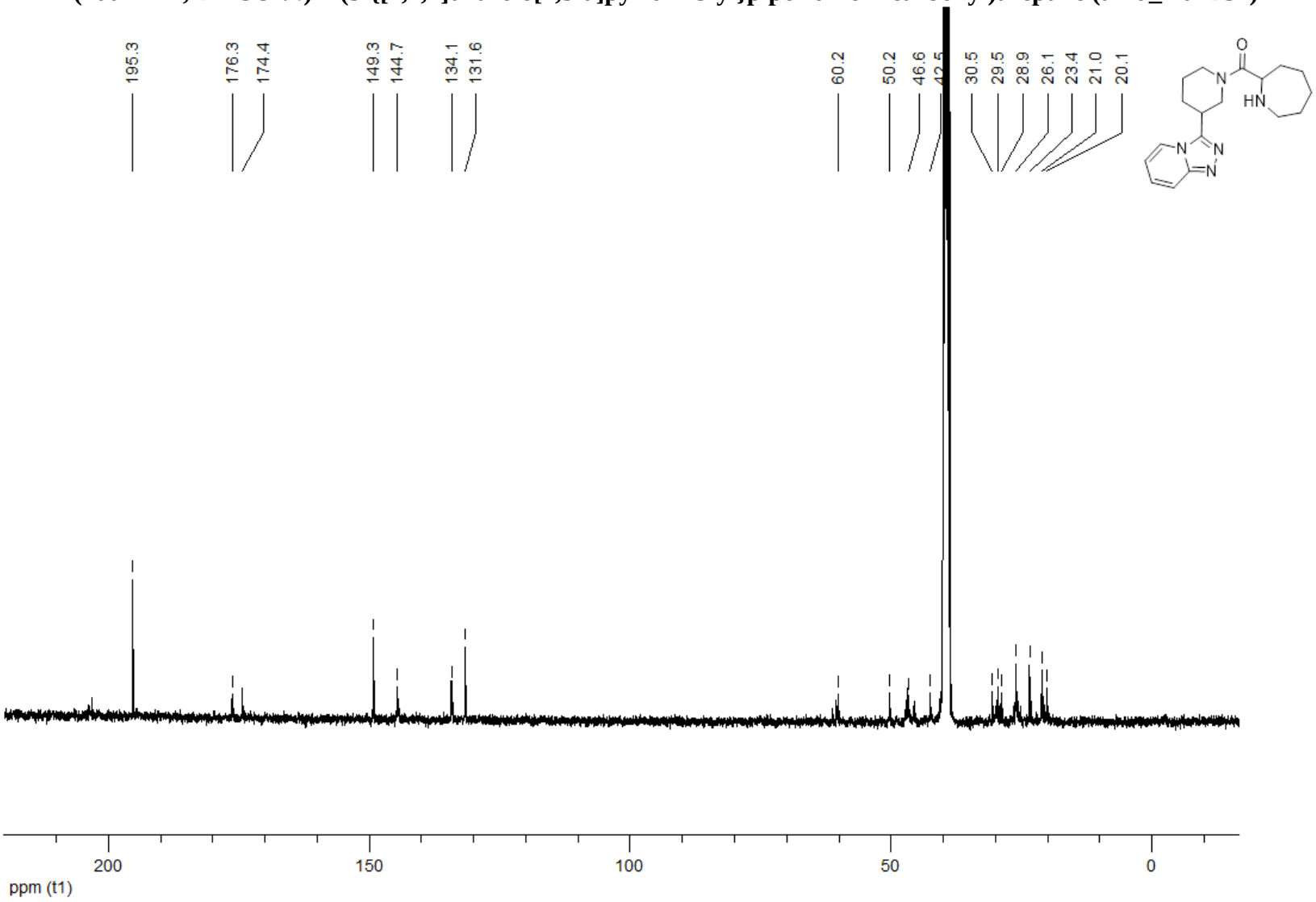

HRMS (ESI-MS)2-(3-{[1,2,4]triazolo[4,3-a]pyridin-3-yl}piperidine-1-carbonyl)azepane (amd_A07B34)

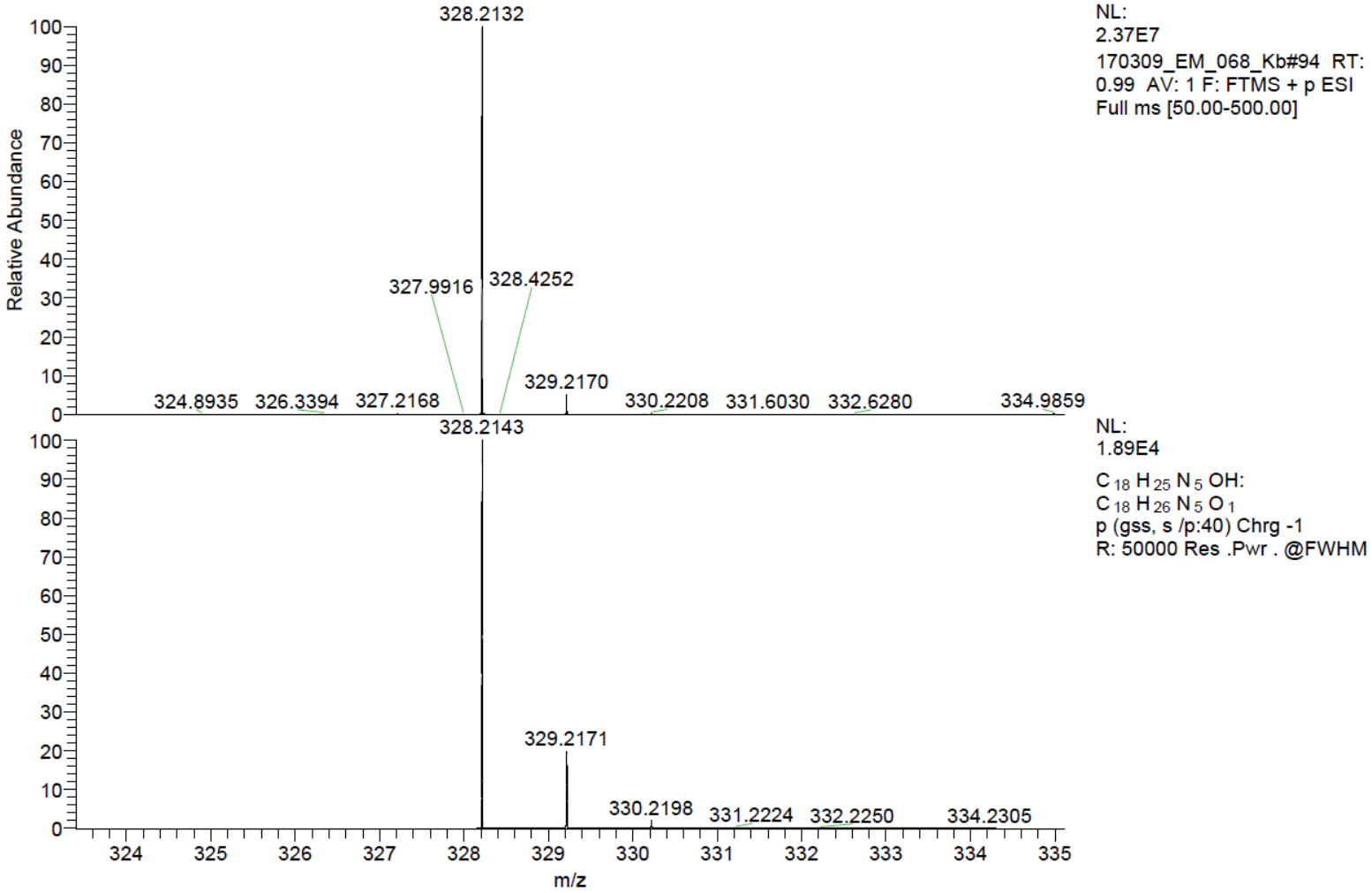

^{1}H NMR (400 MHz, DMSO-*d*$_6$) 9-(azepane-2-carbonyl)-2-methyl-2,9-diazaspiro[5.5]undecan-3-one (amd_A07B40)

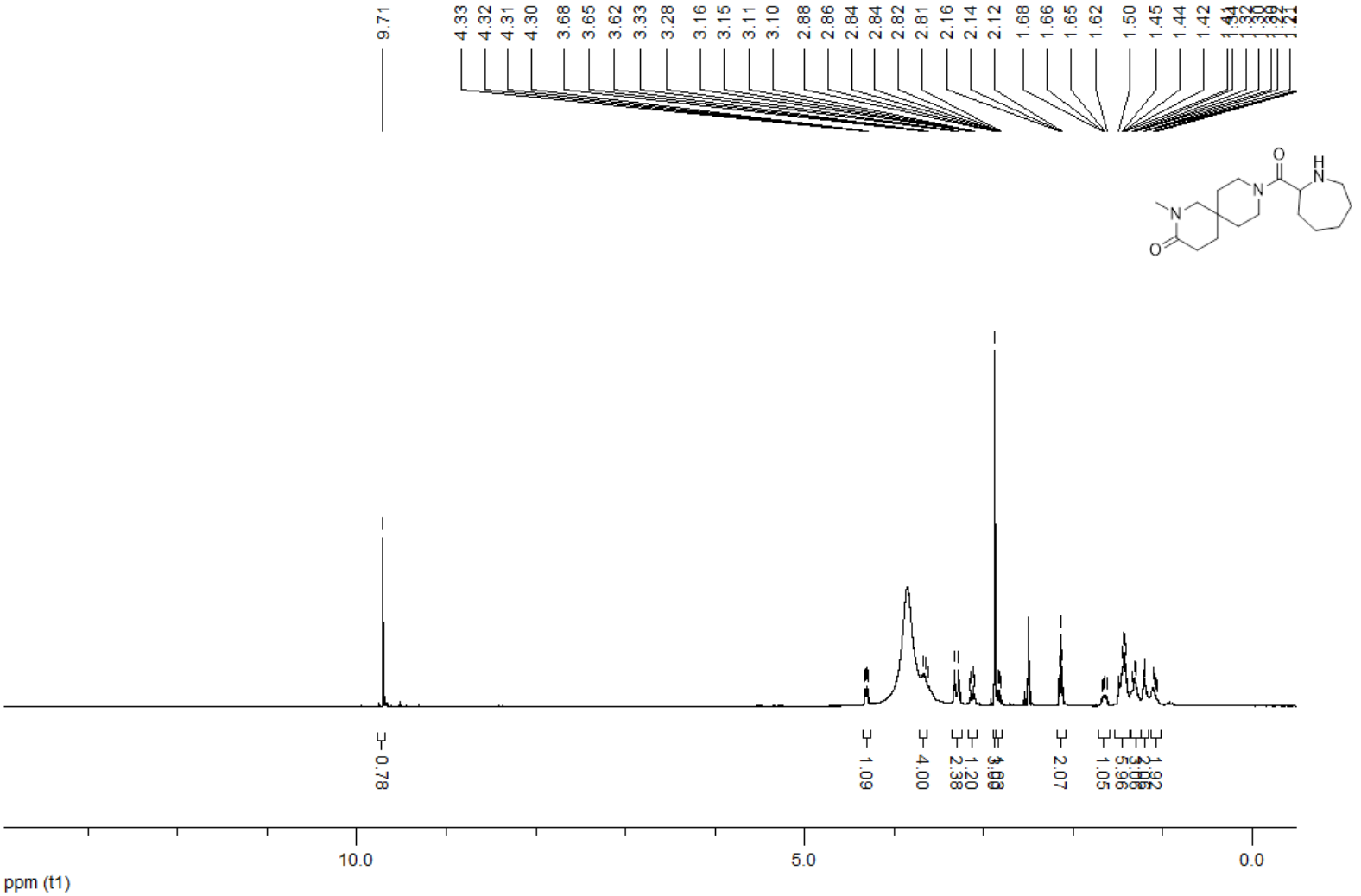

^{13}C NMR (100 MHz, DMSO-*d*$_6$) 9-(azepane-2-carbonyl)-2-methyl-2,9-diazaspiro[5.5]undecan-3-one(amd_A07B40)

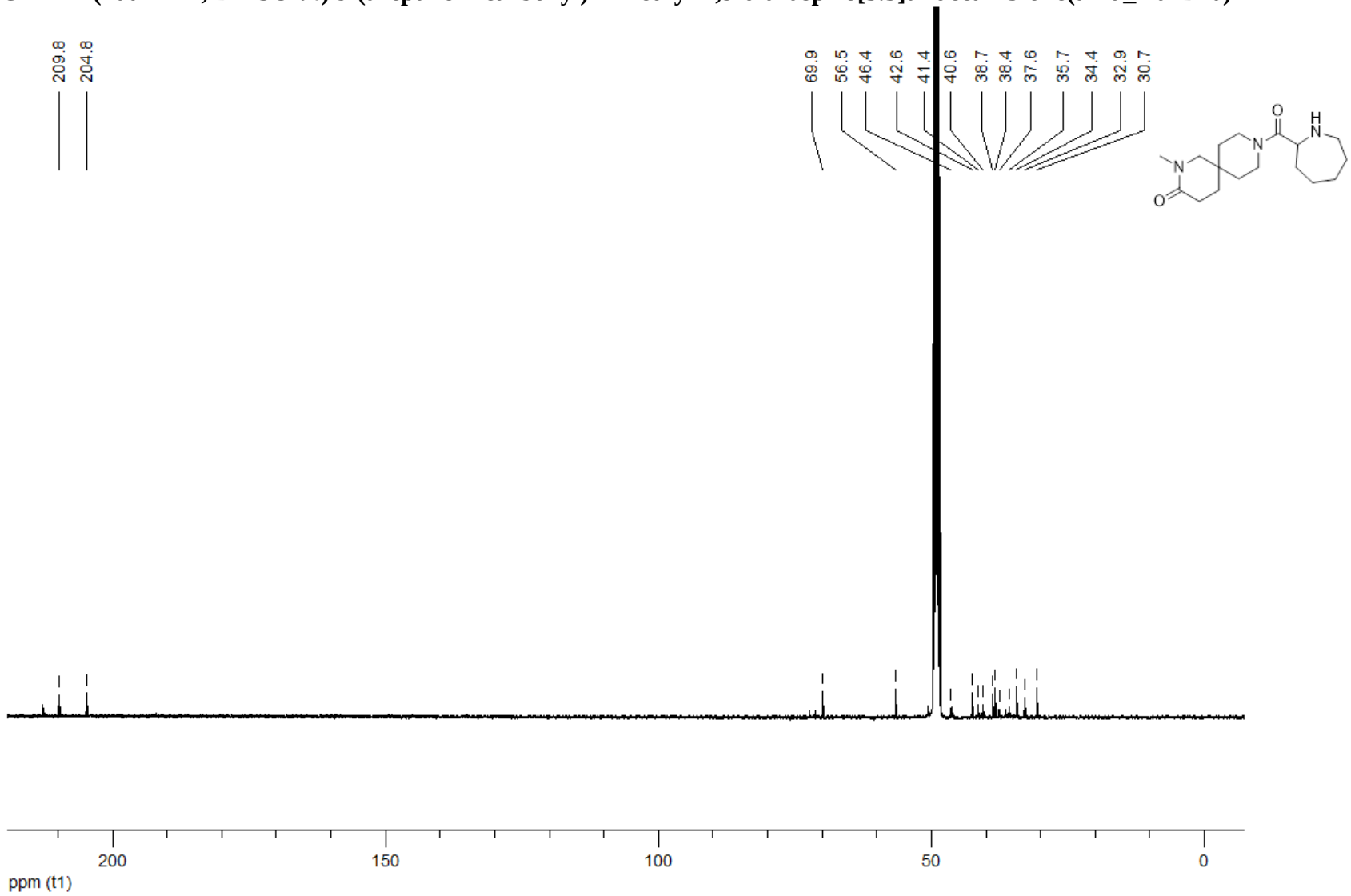

HRMS (ESI-MS)9-(azepane-2-carbonyl)-2-methyl-2,9-diazaspiro[5.5]undecan-3-one (amd_A07B40)

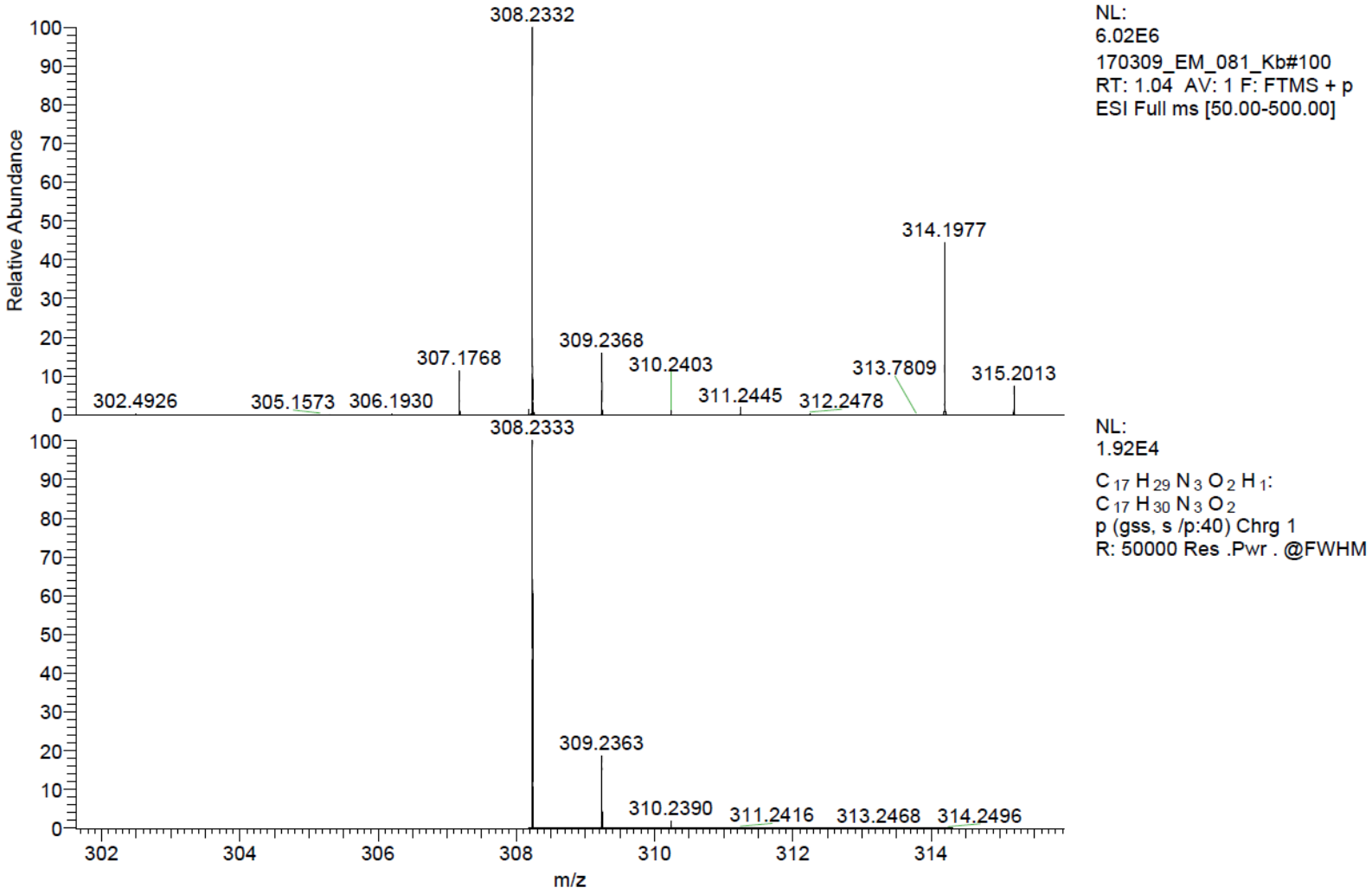

^{1}H NMR (400 MHz, DMSO-*d*$_6$) Methyl 5-[2-(pyrrolidin-2-yl)acetyl]-1*H*,4*H*,5*H*,6*H*,7*H*-pyrazolo[4,3-c]pyridine-3-carboxylate (amd_A08B42)

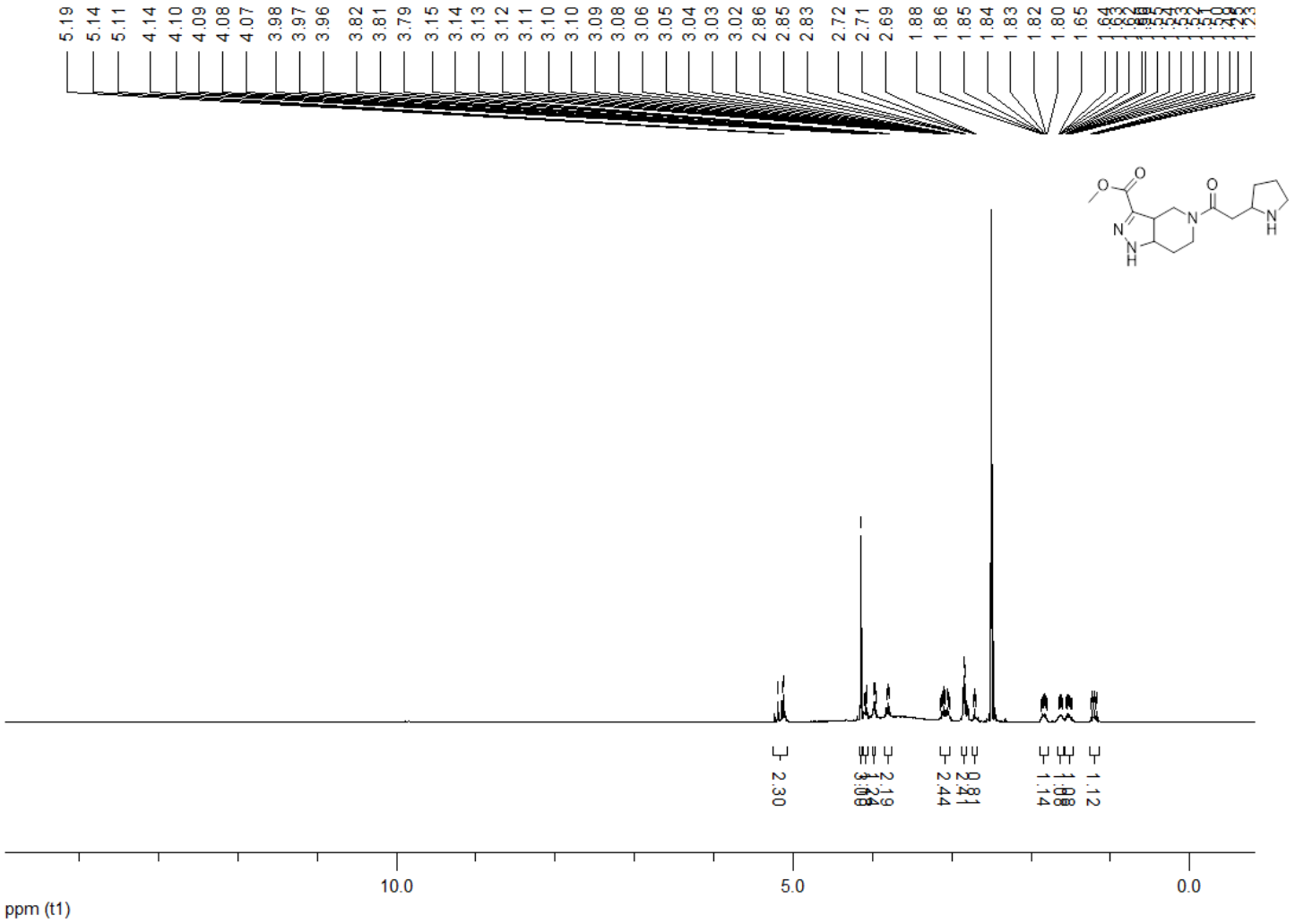

^{13}C NMR (100 MHz, DMSO-*d*$_6$) Methyl 5-[2-(pyrrolidin-2-yl)acetyl]-1*H*,4*H*,5*H*,6*H*,7*H*-pyrazolo[4,3-c]pyridine-3-carboxylate (amd_A08B42)

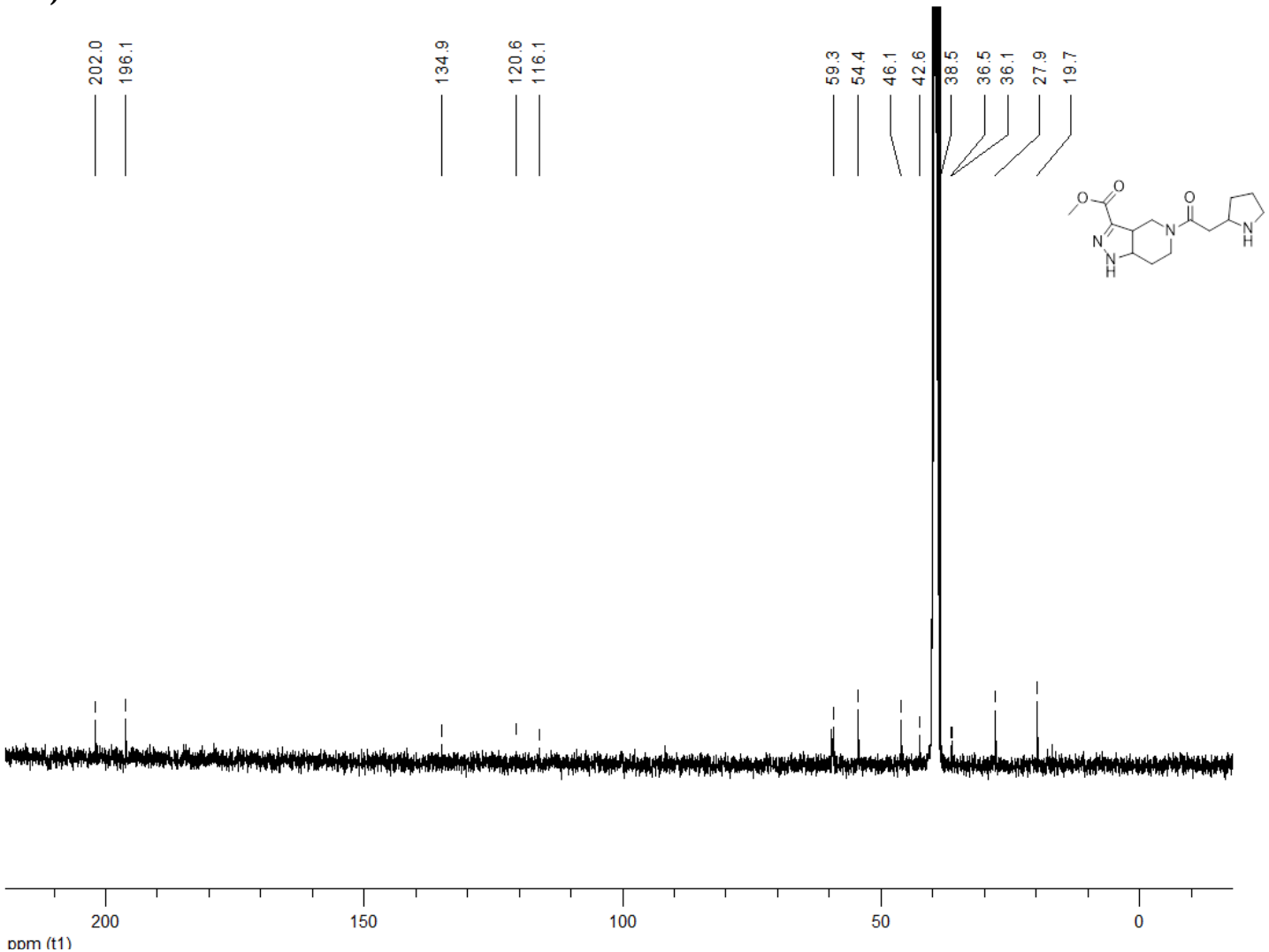

HRMS (ESI-MS)Methyl 5-[2-(pyrrolidin-2-yl)acetyl]-1*H*,4*H*,5*H*,6*H*,7*H*-pyrazolo[4,3-c]pyridine-3-carboxylate (amd_A08B42)

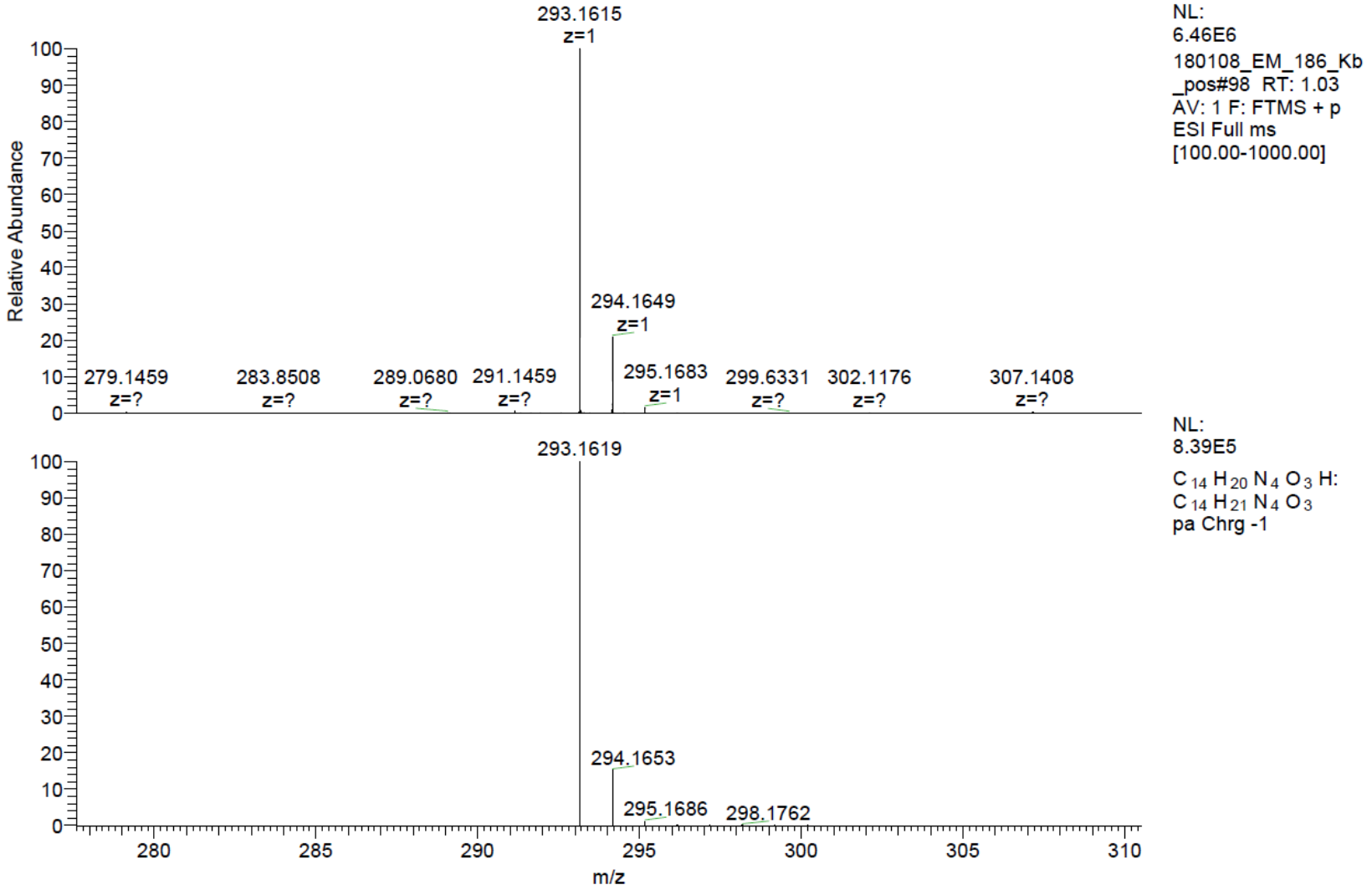

^{1}H NMR (400 MHz, DMSO-*d*$_6$) 1-methyl-5-[2-(pyrrolidin-2-yl)acetyl]-1*H*,4*H*,5*H*,6*H*,7*H*-pyrazolo[4,3-c]pyridine-3-carboxylate(amd_A08B45)

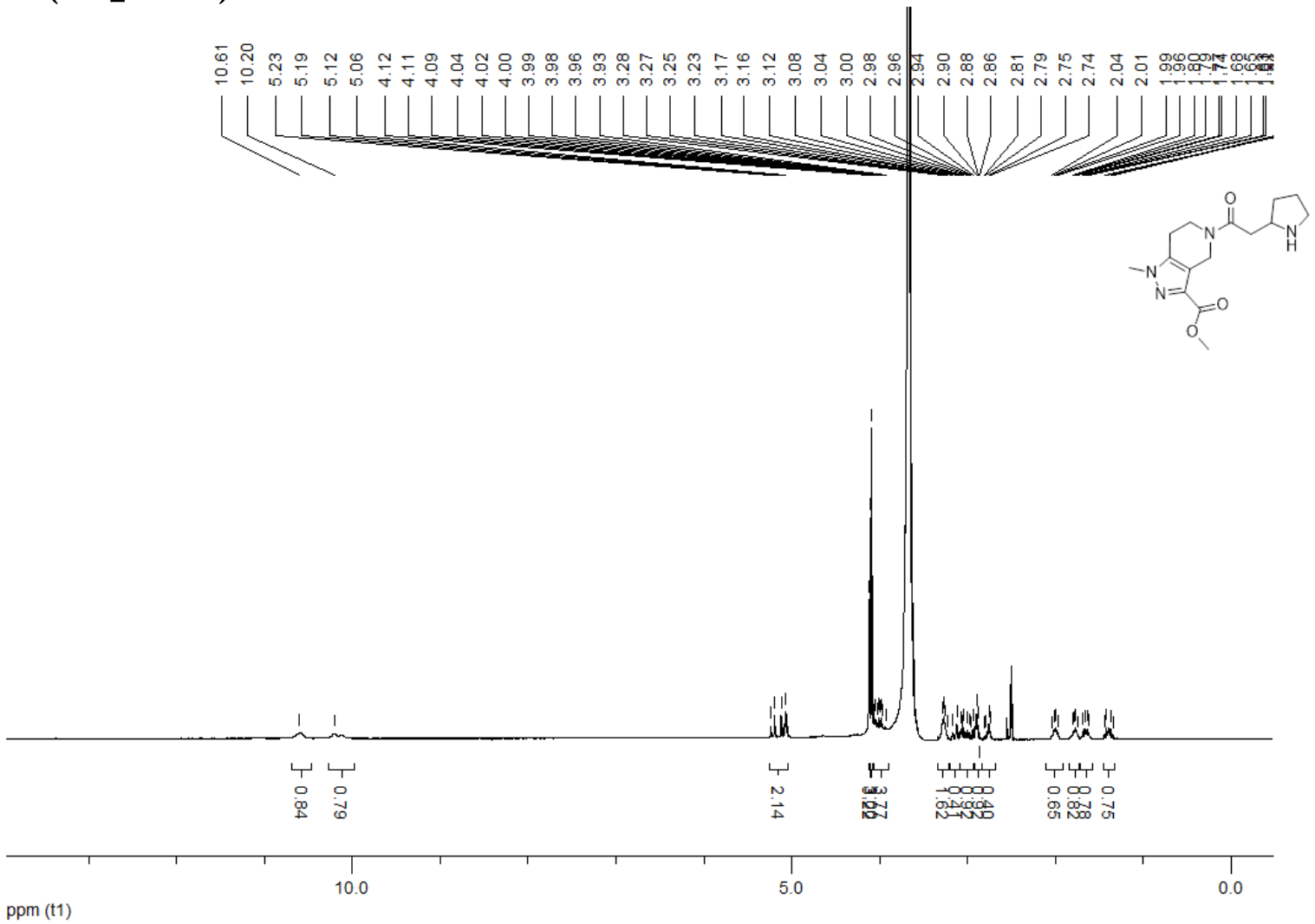

^{13}C NMR (100 MHz, DMSO-*d*$_6$) 1-methyl-5-[2-(pyrrolidin-2-yl)acetyl]-1*H*,4*H*,5*H*,6*H*,7*H*-pyrazolo[4,3-c]pyridine-3-carboxylate(amd_A08B45)

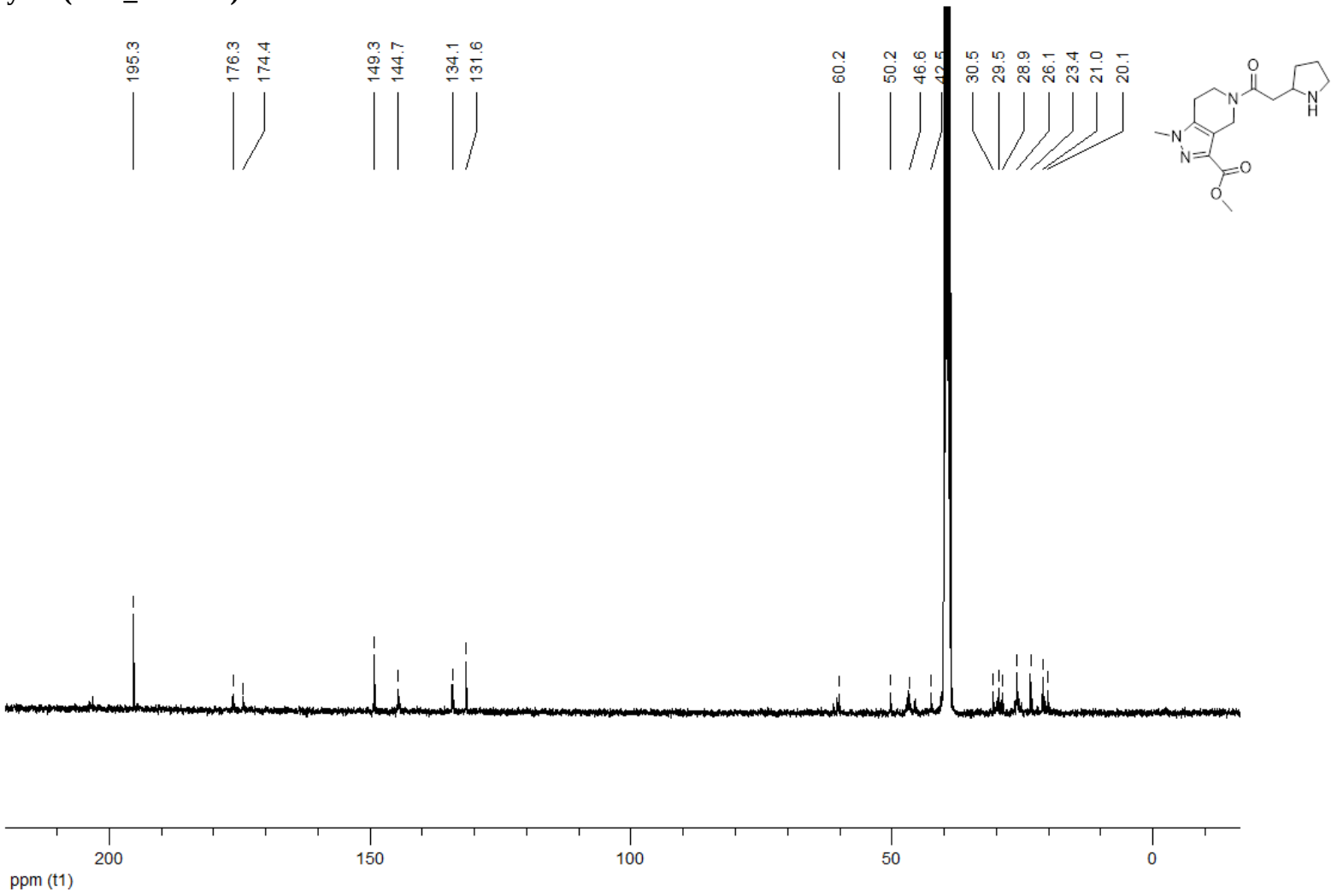

HRMS (ESI-MS)1-methyl-5-[2-(pyrrolidin-2-yl)acetyl]-1*H*,4*H*,5*H*,6*H*,7*H*-pyrazolo[4,3-c]pyridine-3-carboxylate(amd_A08B45)

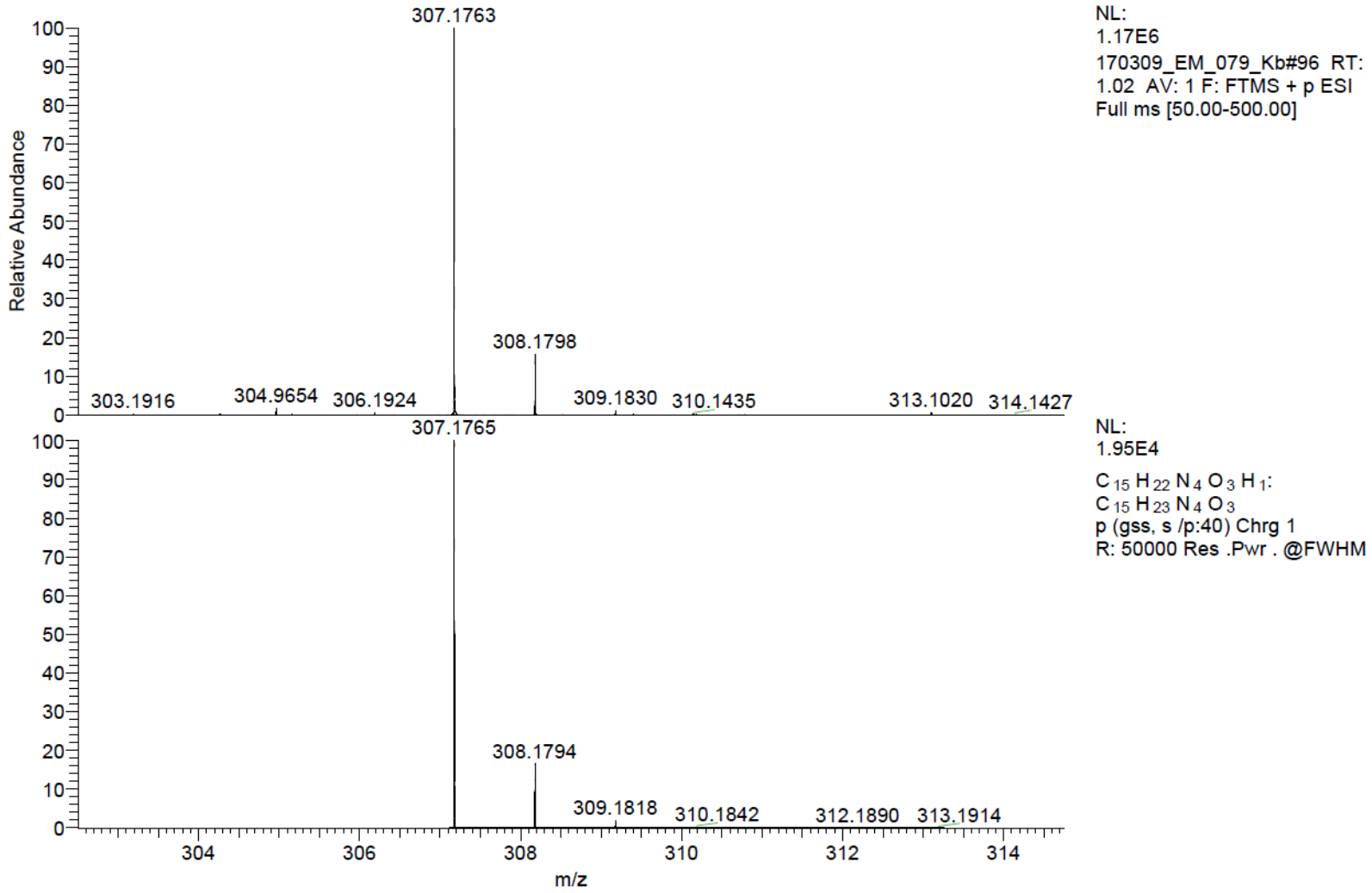

^{1}H NMR (400 MHz, DMSO-d_6) 2-(piperidin-2-yl)-1-(3-{[1,2,4]triazolo[4,3-a]pyridin-3-yl}piperidin-1-yl)ethan-1-one (amd_A09B34)

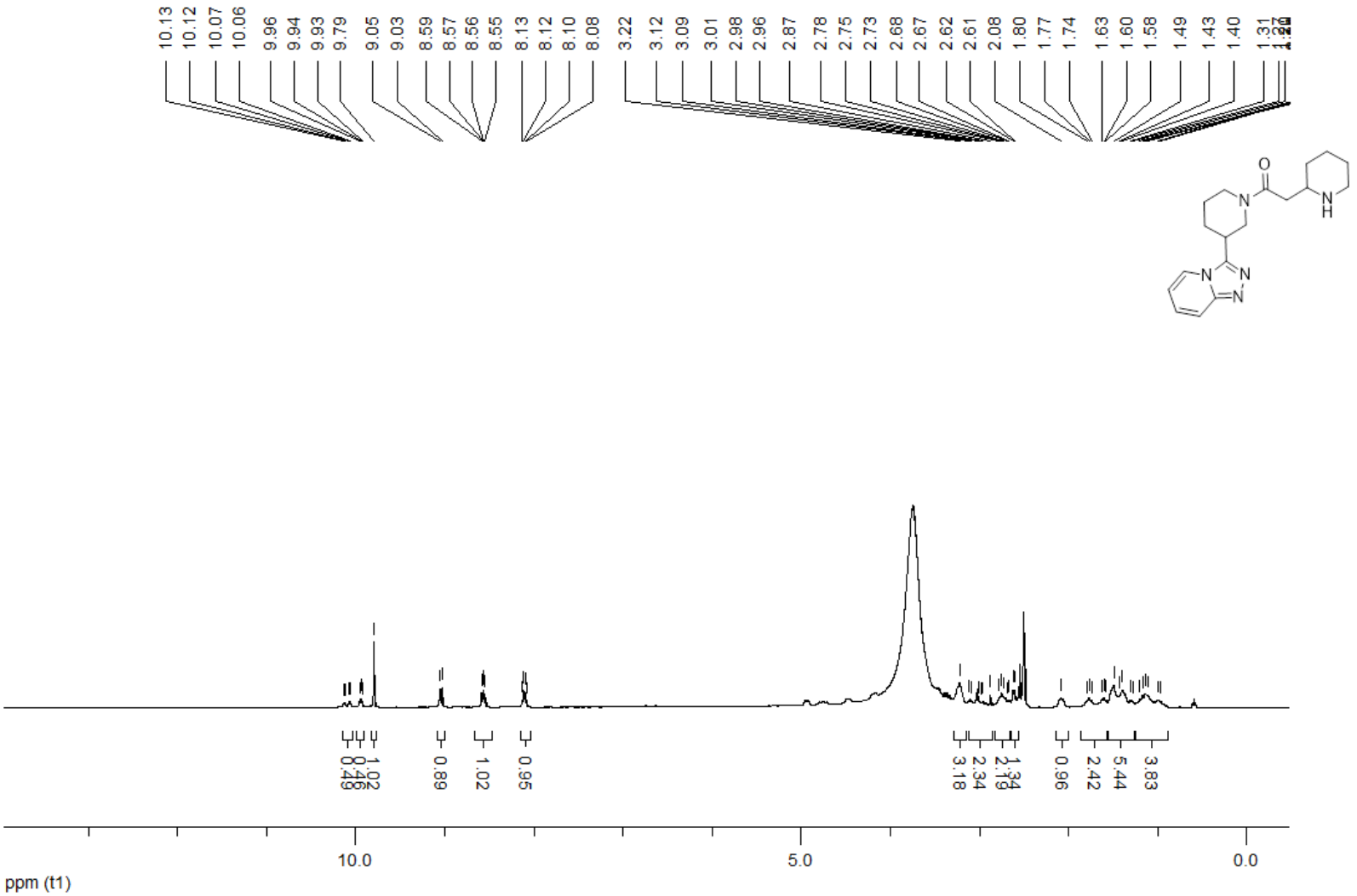
10.13
10.12
10.07
10.06
9.96
9.94
9.93
9.79
9.05
9.03
8.59
8.57
8.56
8.55
8.13
8.12
8.10
8.08
3.22
3.12
3.09
3.01
2.98
2.96
2.87
2.78
2.75
2.73
2.68
2.67
2.62
2.61
2.08
1.80
1.77
1.74
1.63
1.60
1.58
1.49
1.43
1.40
1.31
O
N
NH
N
N
N
0.49
0.48
1.02
0.89
1.02
0.95
3.18
2.34
2.19
1.34
0.96
2.42
5.44
3.83
10.0
5.0
0.0
ppm (t1)

^{13}C NMR (100 MHz, DMSO-*d*$_6$) 2-(piperidin-2-yl)-1-(3-{[1,2,4]triazolo[4,3-a]pyridin-3-yl}piperidin-1-yl)ethan-1-one (amd_A09B34)

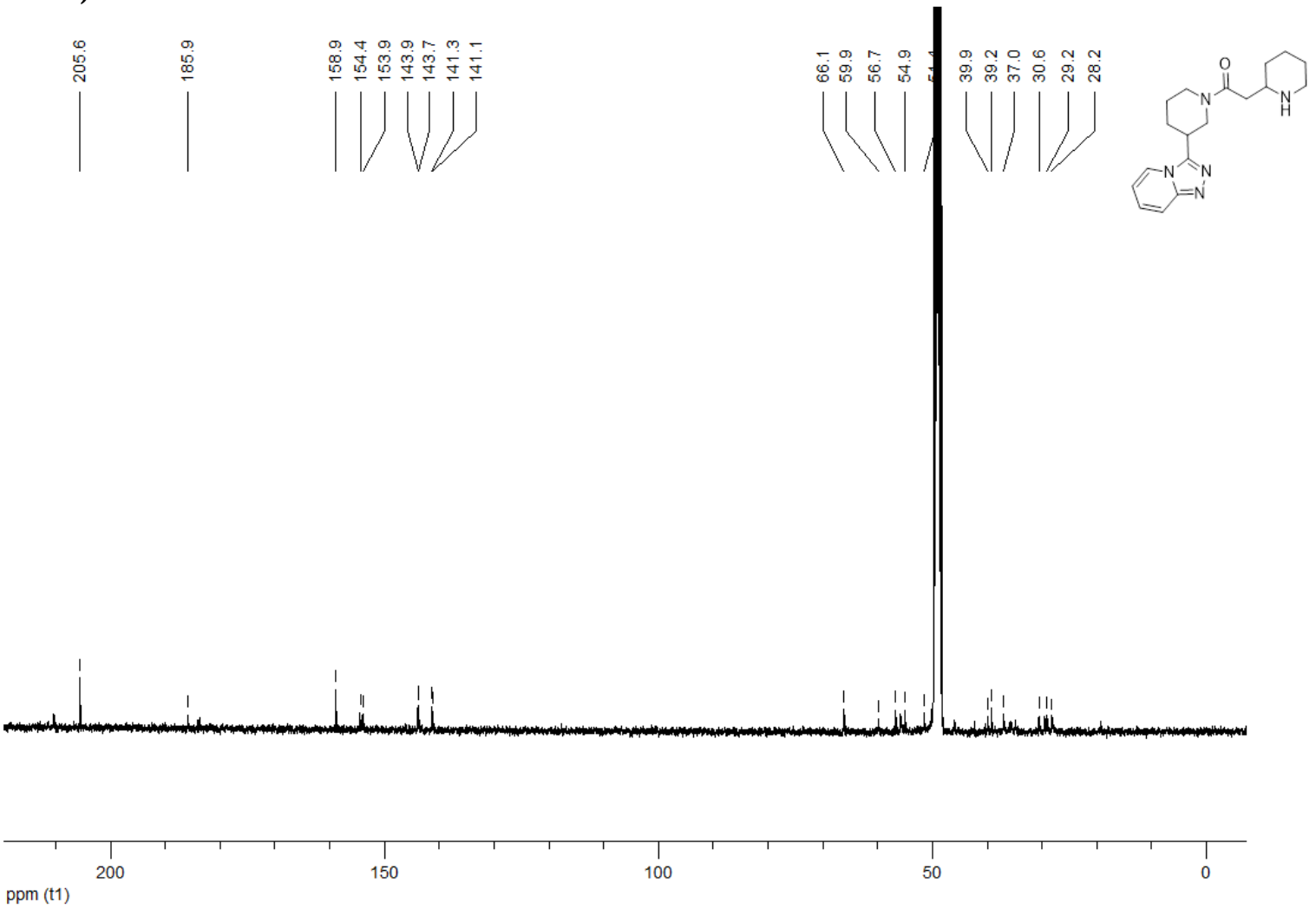

HRMS (ESI-MS)2-(piperidin-2-yl)-1-(3-{[1,2,4]triazolo[4,3-a]pyridin-3-yl}piperidin-1-yl)ethan-1-one (amd_A09B34)

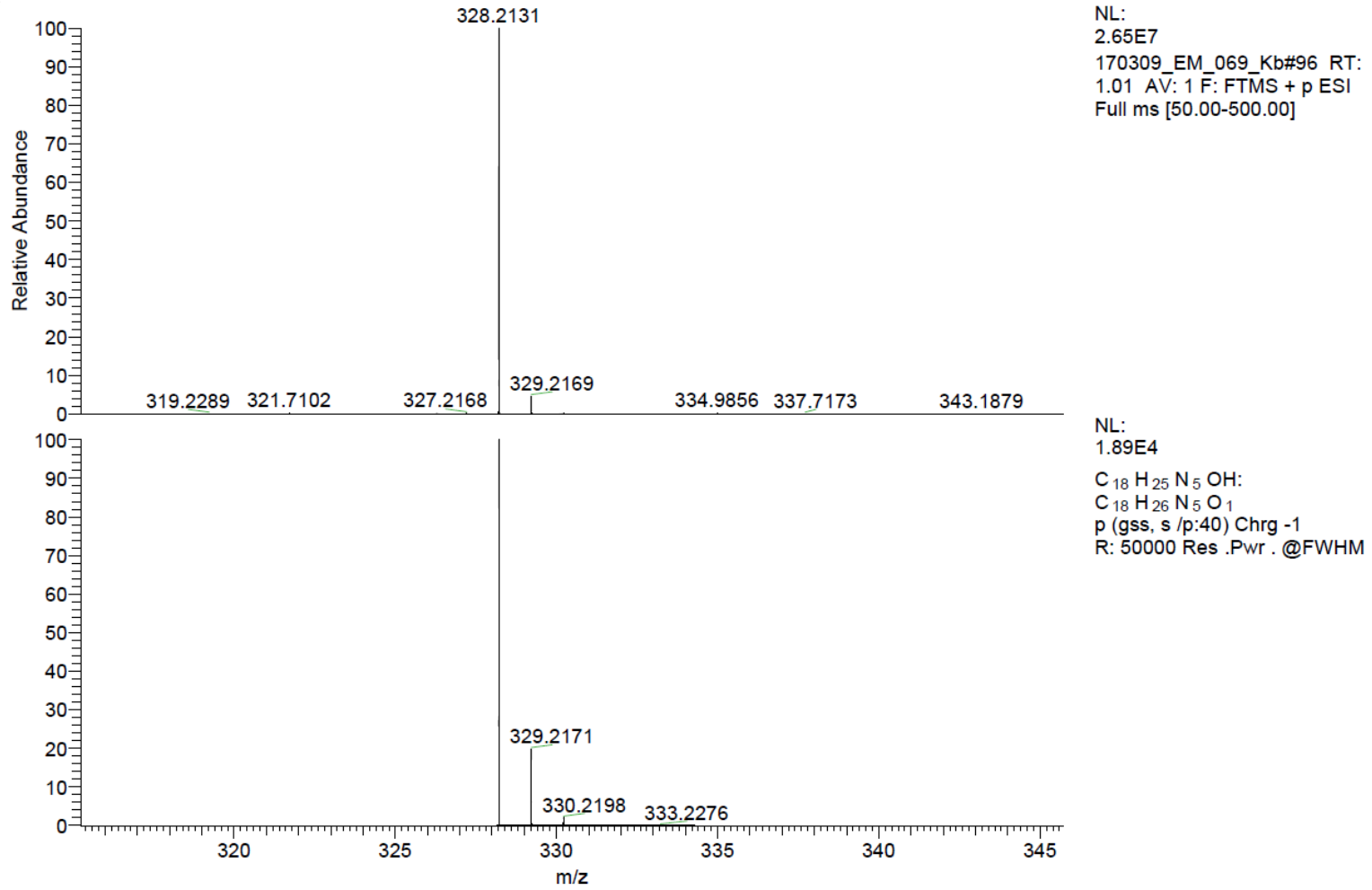

^{1}H NMR (400 MHz, DMSO-*d*$_6$) 1-(7-hydroxy-1,2,3,4-tetrahydroisoquinolin-2-yl)-2-(piperidin-2-yl)ethan-1-one (amd_A09B37)

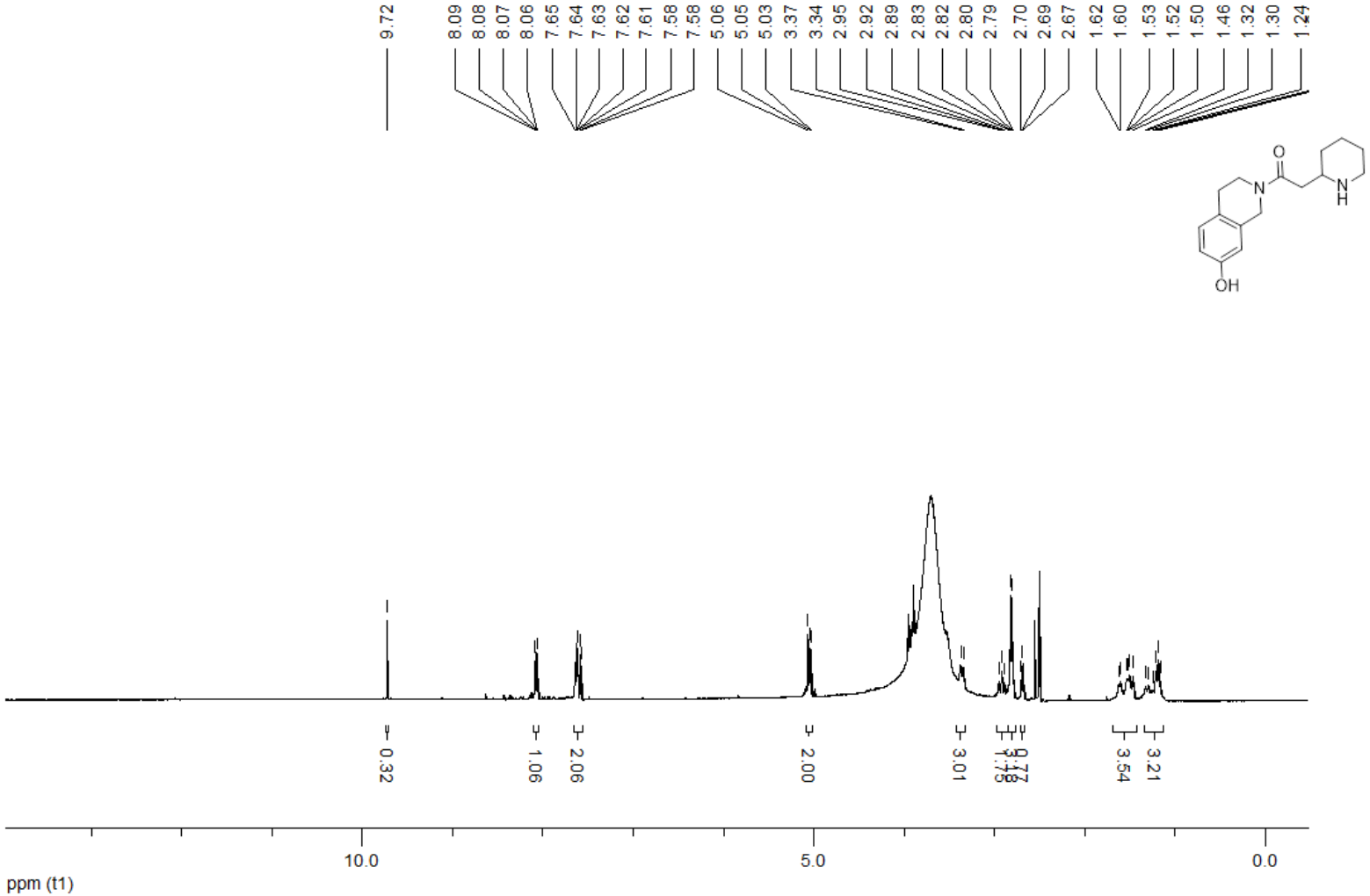

^{13}C NMR (100 MHz, DMSO-*d*$_6$) 1-(7-hydroxy-1,2,3,4-tetrahydroisoquinolin-2-yl)-2-(piperidin-2-yl)ethan-1-one (amd_A09B37)

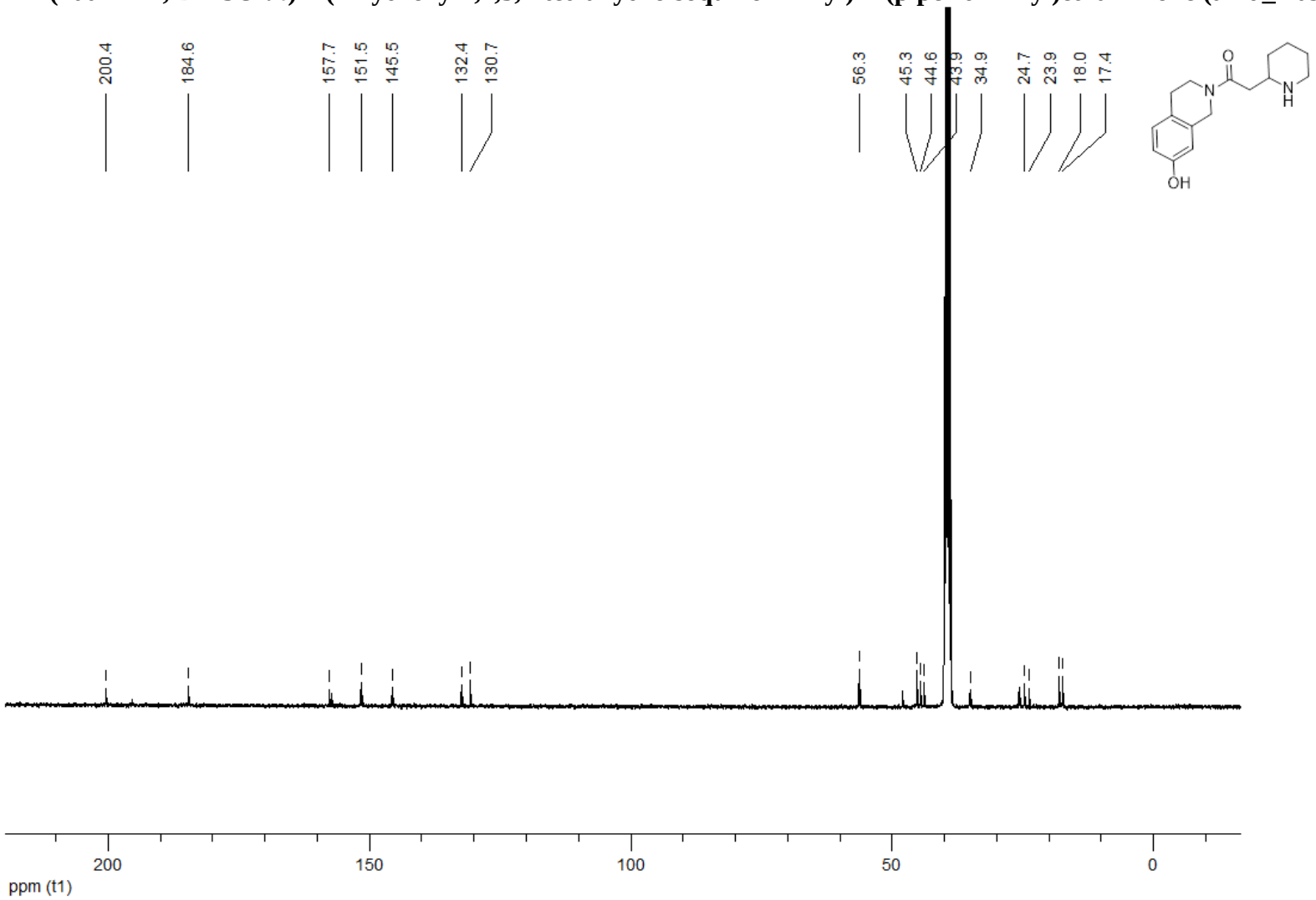

HRMS (ESI-MS)1-(7-hydroxy-1,2,3,4-tetrahydroisoquinolin-2-yl)-2-(piperidin-2-yl)ethan-1-one (amd_A09B37)

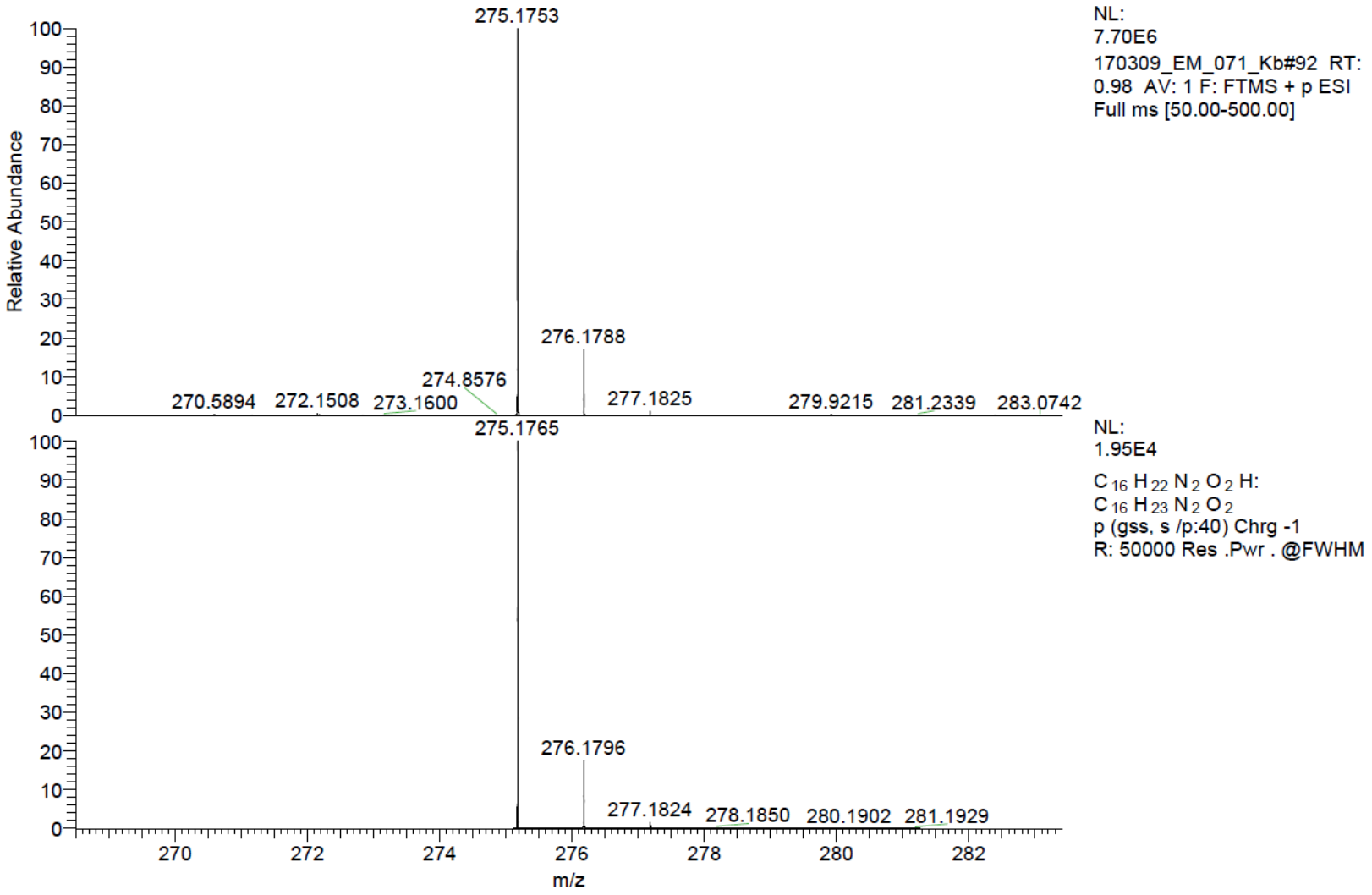

^{1}H NMR (400 MHz, DMSO-*d*$_6$) 2-methyl-9-[2-(piperidin-2-yl)acetyl]-2,9-diazaspiro[5.5]undecan-3-one (amd_A09B40)

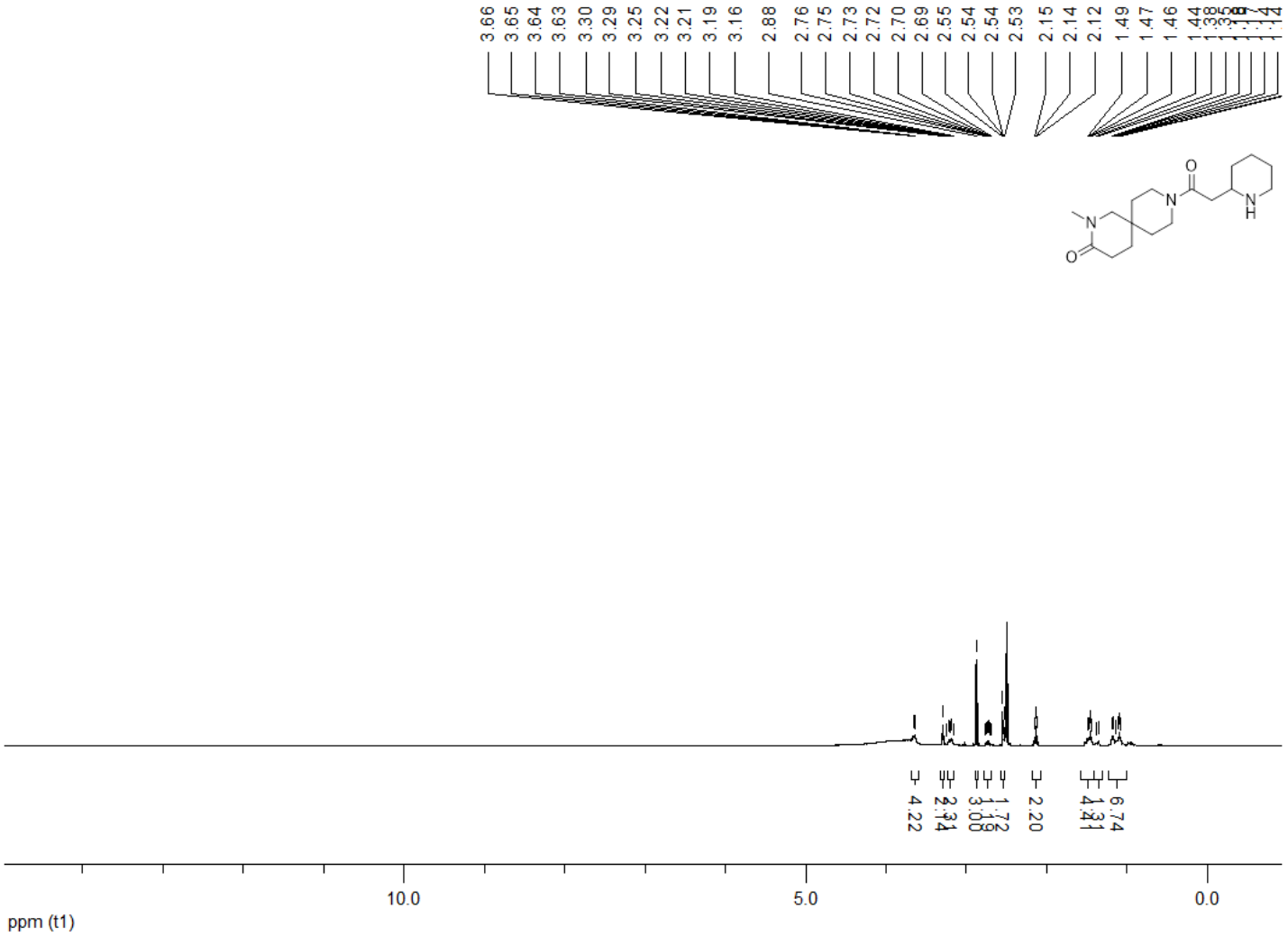

^{13}C NMR (100 MHz, DMSO-*d*$_6$) 2-methyl-9-[2-(piperidin-2-yl)acetyl]-2,9-diazaspiro[5.5]undecan-3-one (amd_A09B40)

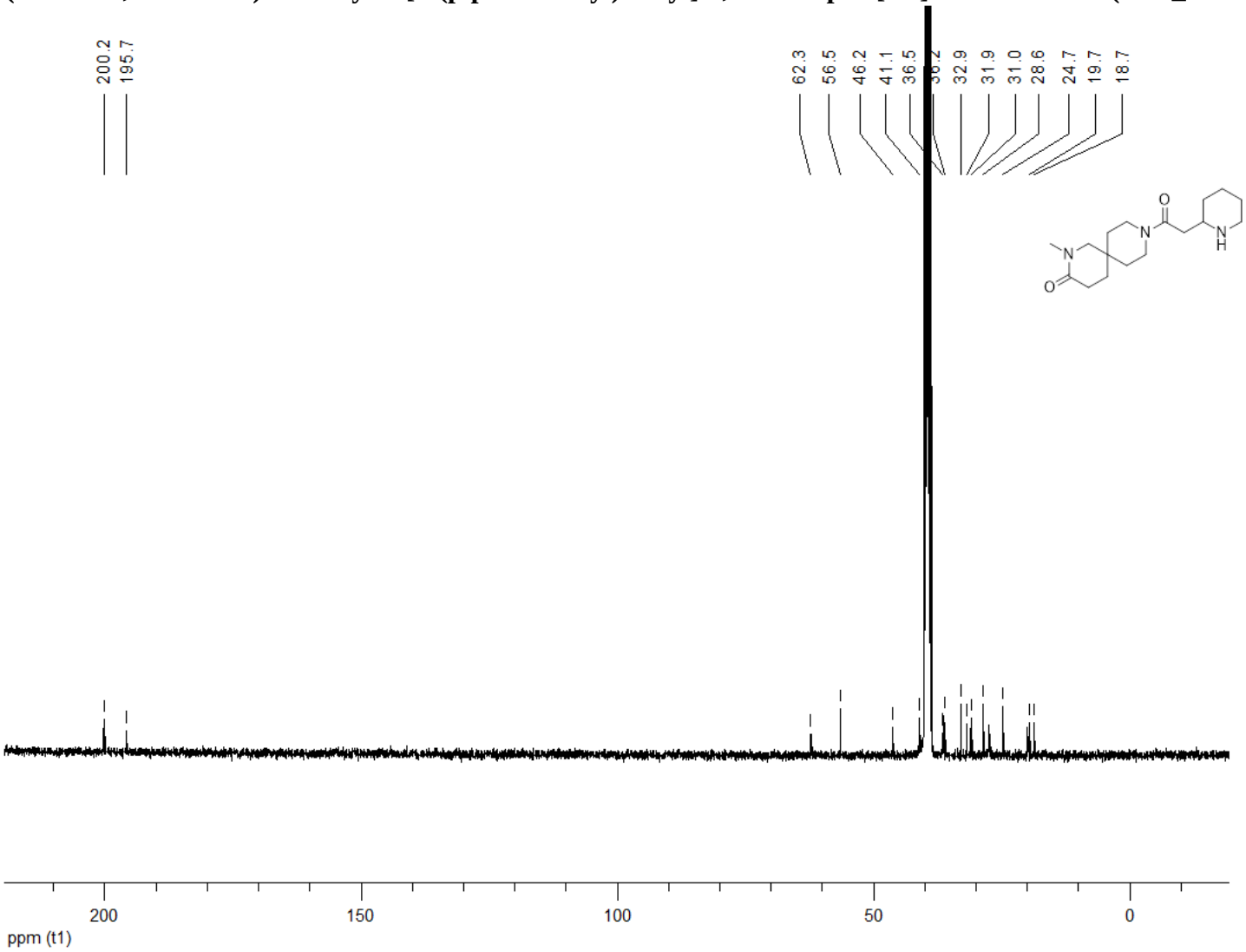

HRMS (ESI-MS)2-methyl-9-[2-(piperidin-2-yl)acetyl]-2,9-diazaspiro[5.5]undecan-3-one (amd_A09B40)

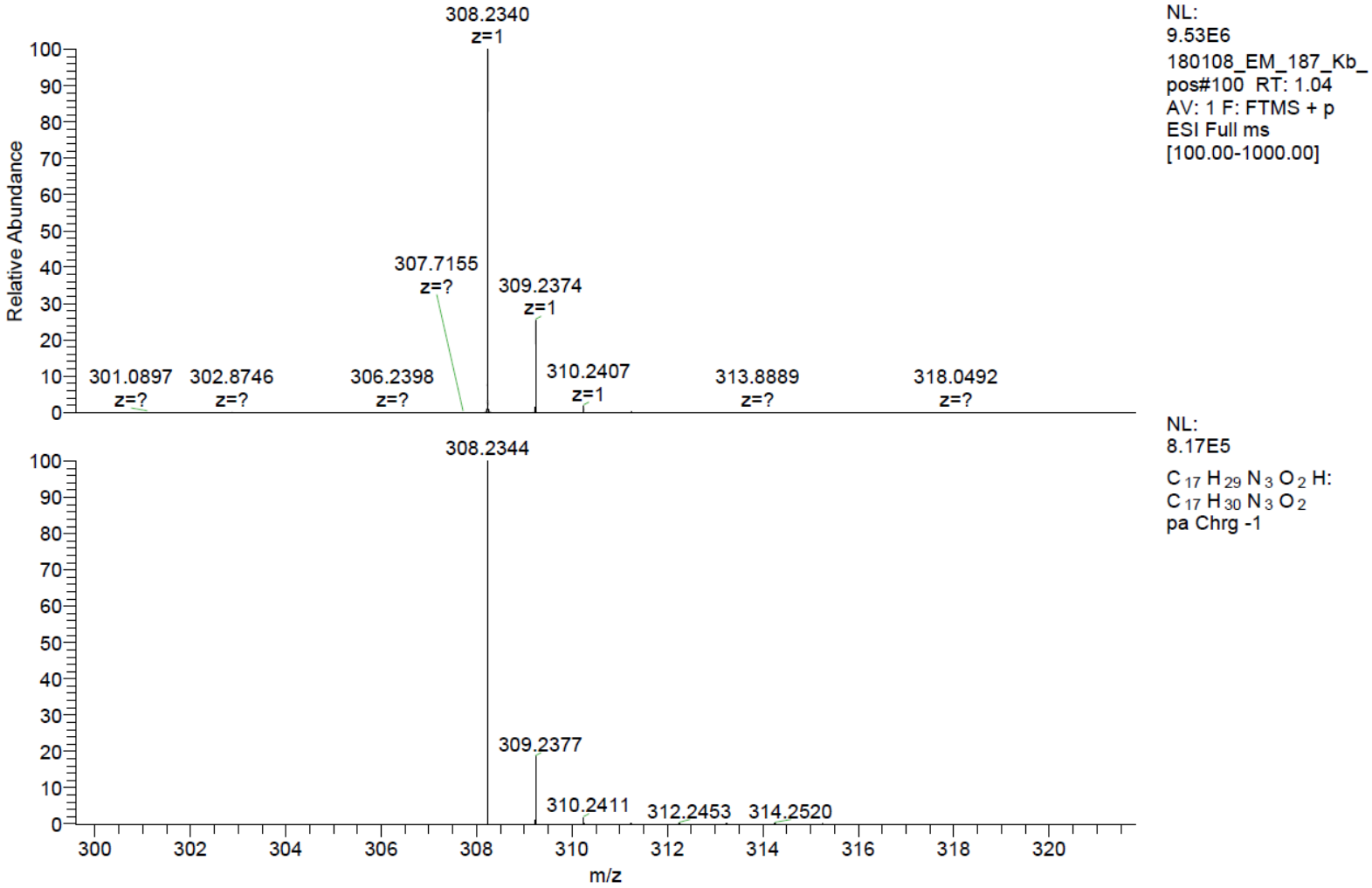

^{1}H NMR (400 MHz, DMSO-*d*$_6$) 2-{1-[2-(piperidin-2-yl)acetyl]piperidin-3-yl}acetonitrile (amd_A09B46)

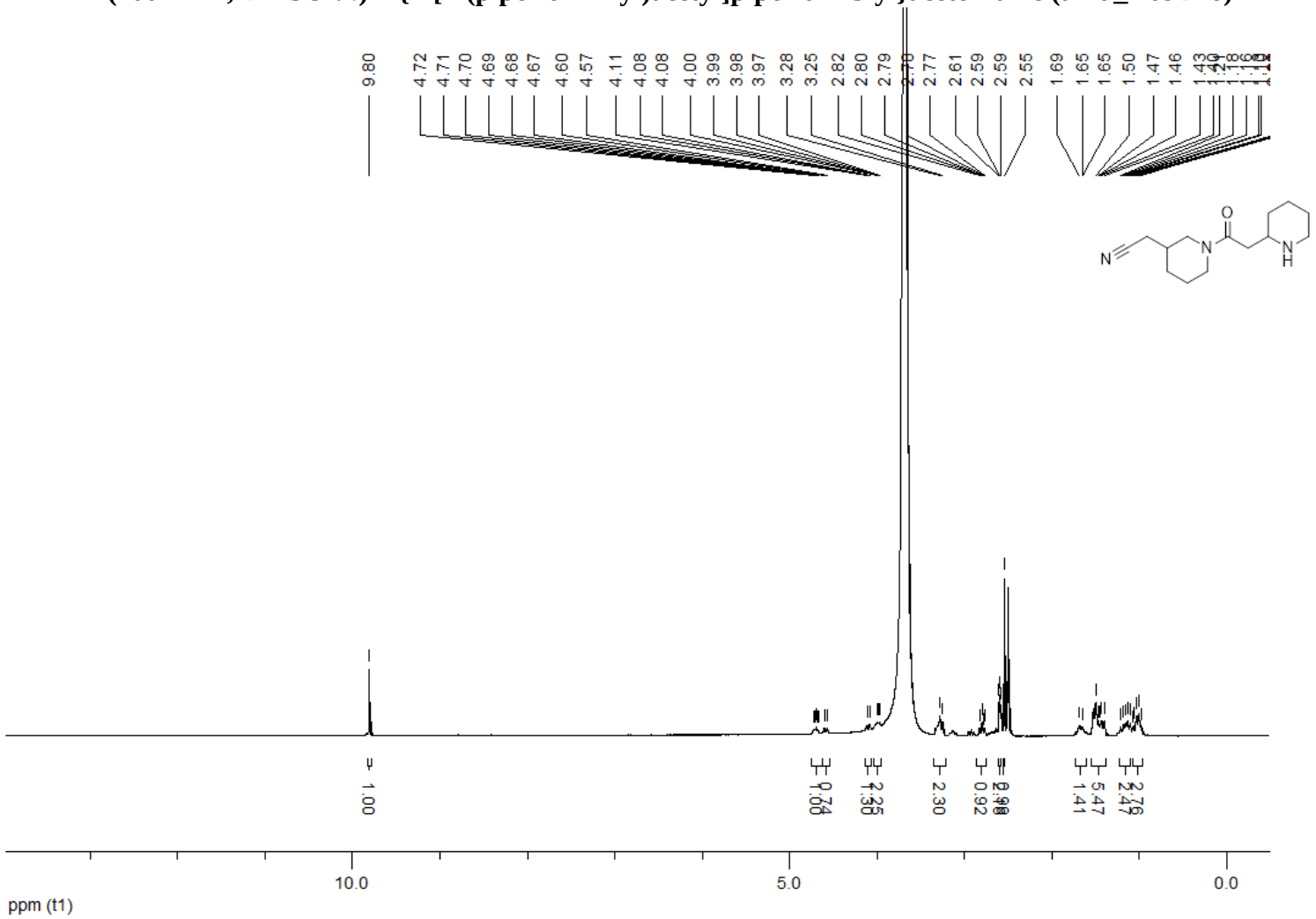

^{13}C NMR (100 MHz, DMSO-*d*$_6$) 2-{1-[2-(piperidin-2-yl)acetyl]piperidin-3-yl}acetonitrile (amd_A09B46)

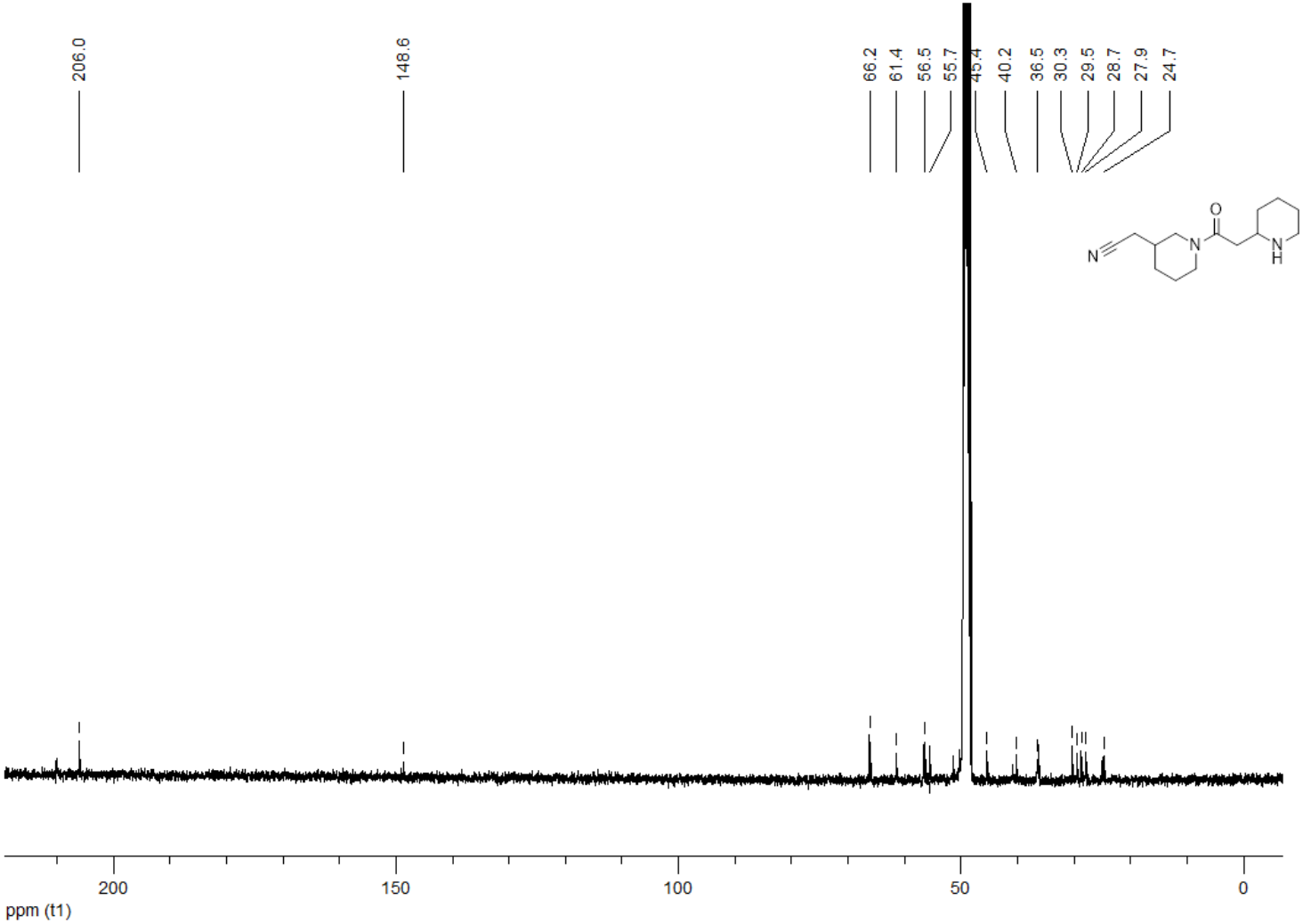

HRMS (ESI-MS)2-{1-[2-(piperidin-2-yl)acetyl]piperidin-3-yl}acetonitrile (amd_A09B46)

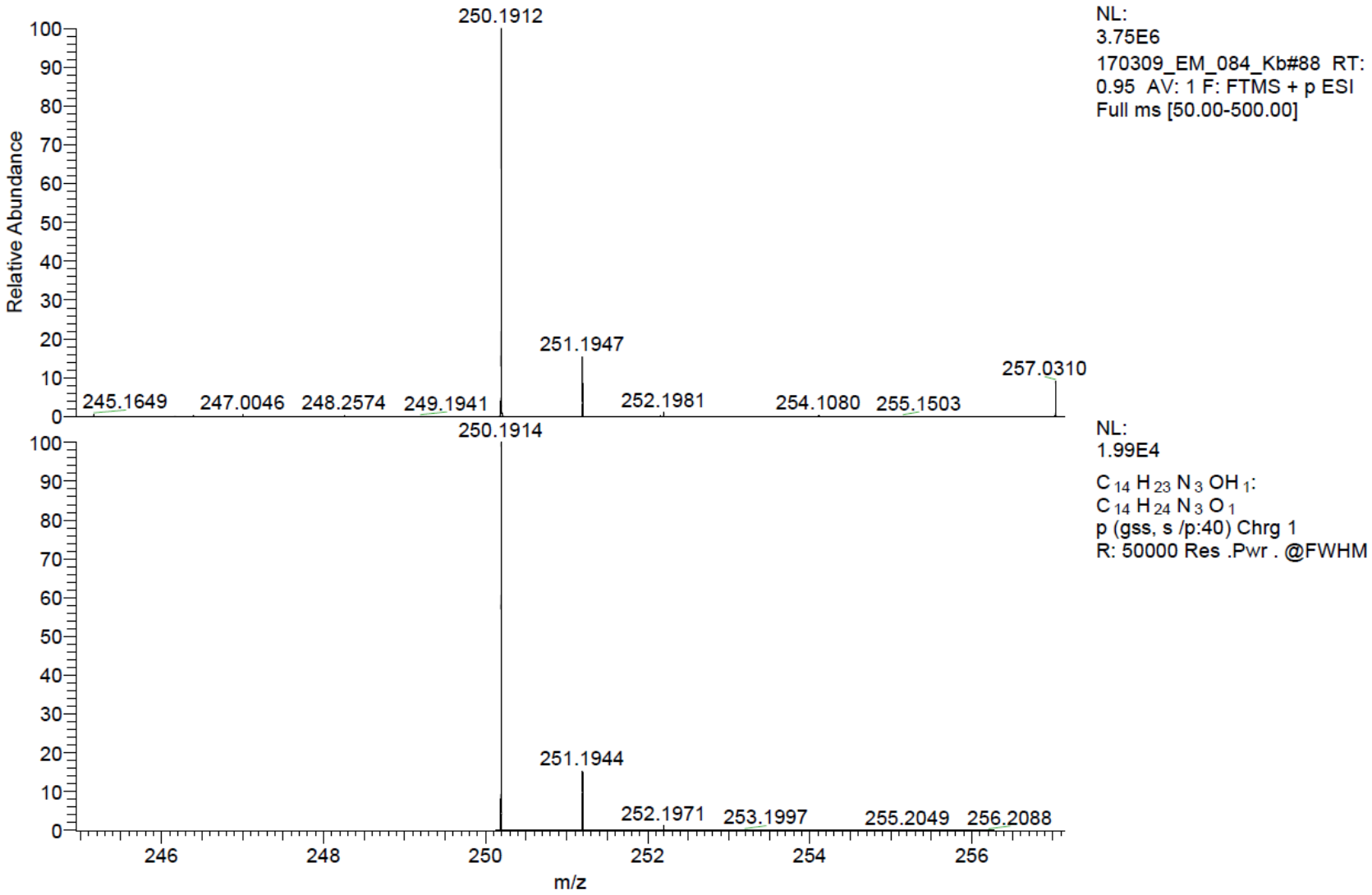

^{1}H NMR (400 MHz, DMSO-*d*$_6$) 2-methyl-9-(2-methylpyrrolidine-2-carbonyl)-2,9-diazaspiro[5.5]undecan-3-one (A10B40)

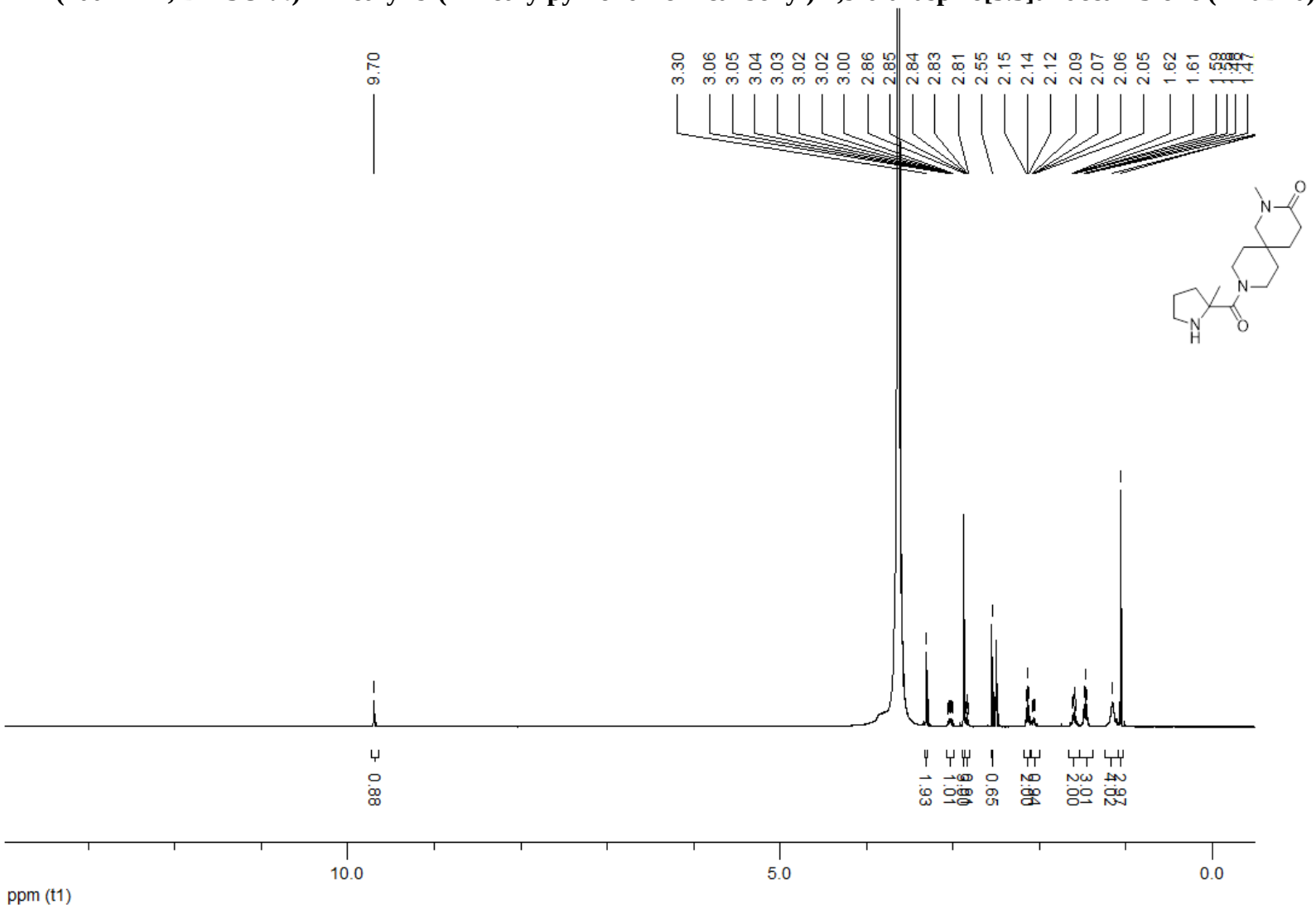

^{13}C NMR (100 MHz, DMSO-*d*$_6$) 2-methyl-9-(2-methylpyrrolidine-2-carbonyl)-2,9-diazaspiro[5.5]undecan-3-one (A10B40)

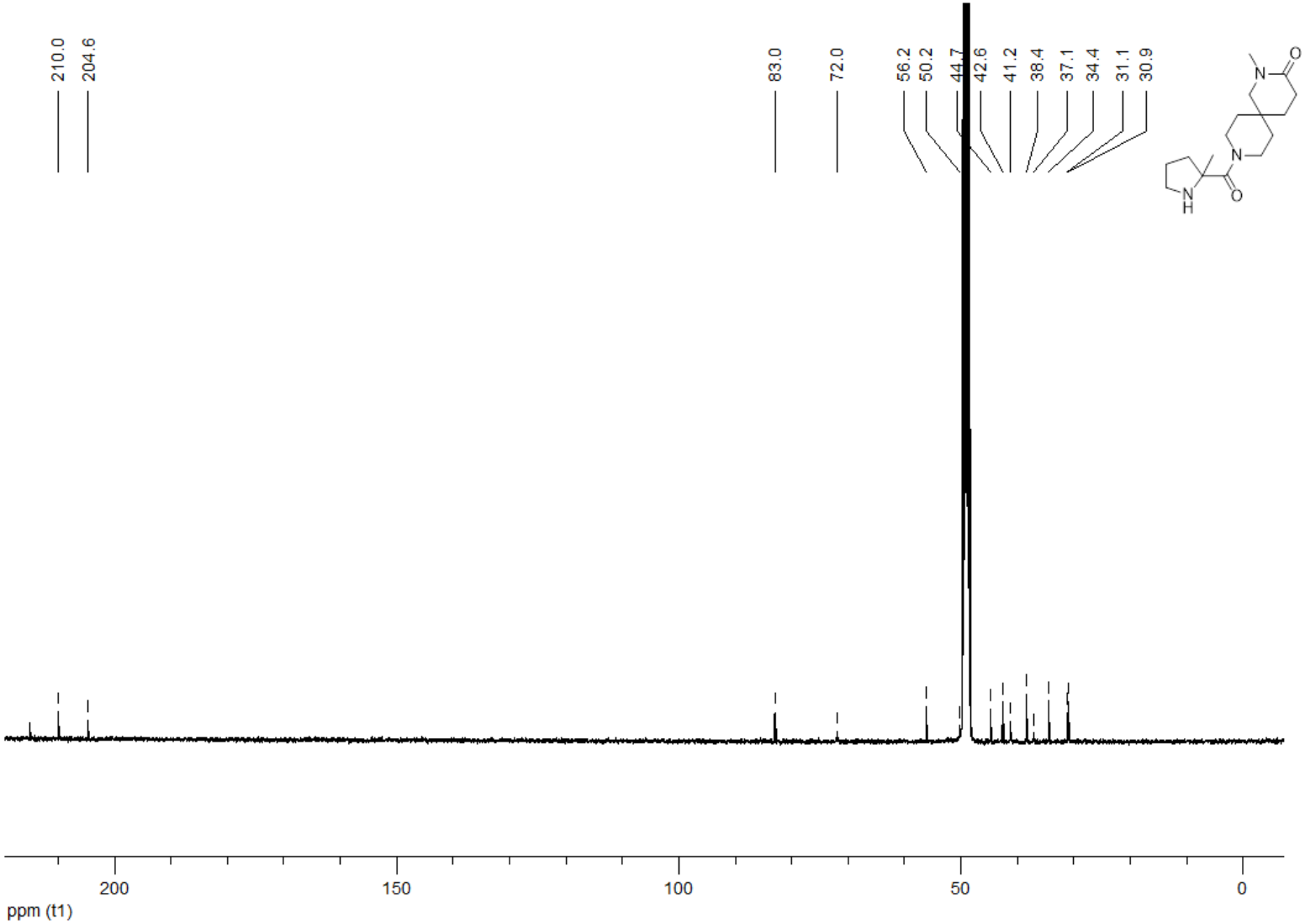

HRMS (ESI-MS)2-methyl-9-(2-methylpyrrolidine-2-carbonyl)-2,9-diazaspiro[5.5]undecan-3-one (A10B40)

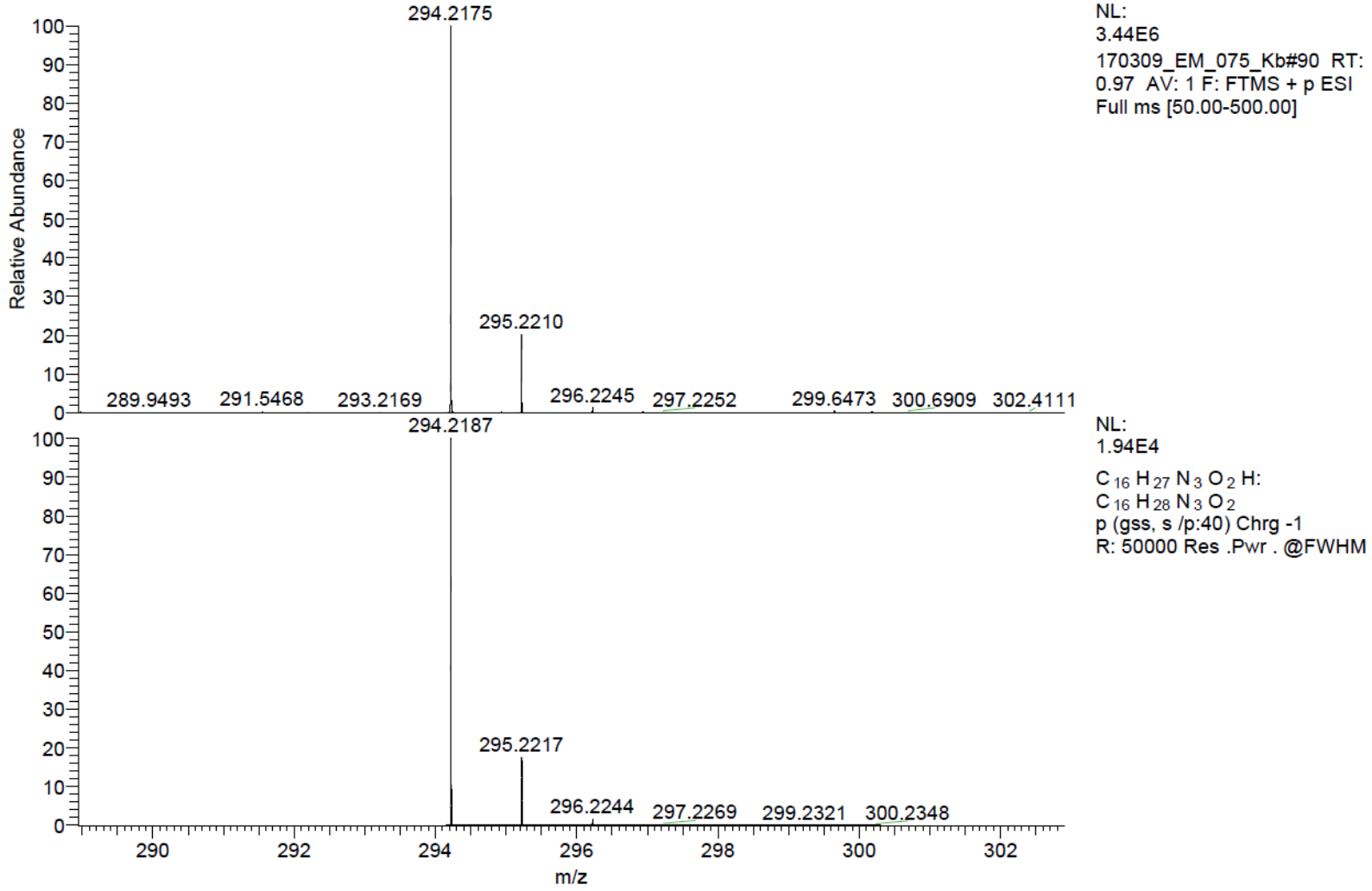

Experimental assays: Dose-response curves of the best tested compounds

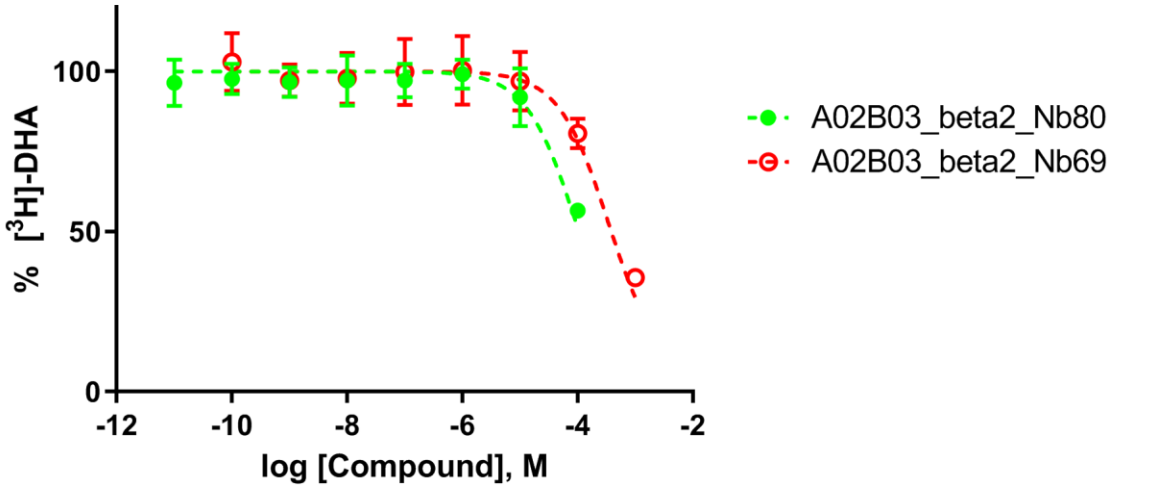
100
50
0
% [3H]-DHA
-12
-10
-8
-6
-4
-2
log [Compound], M
A02B03_beta2_Nb80
A02B03_beta2_Nb69

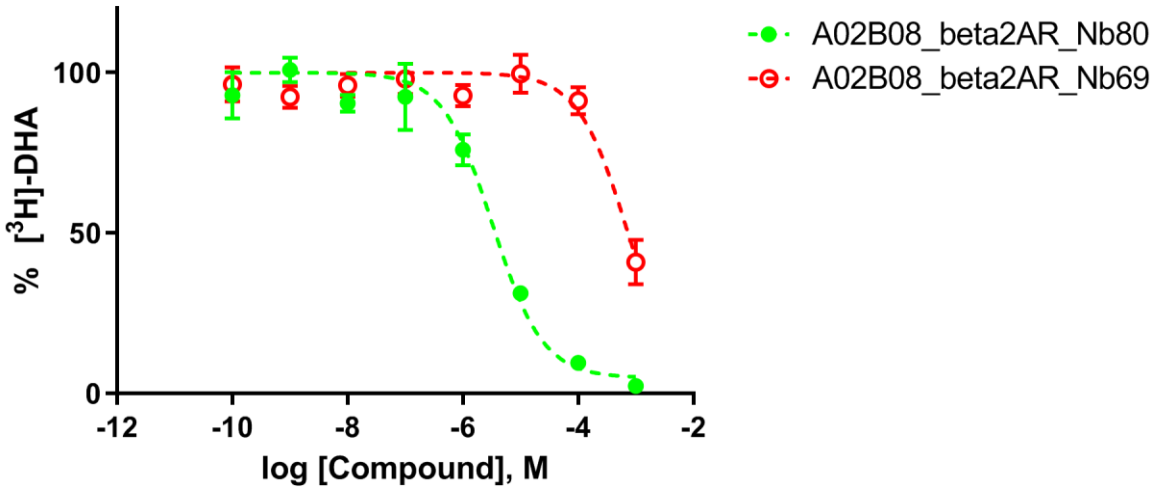
100
50
0
% [3H]-DHA
-12
-10
-8
-6
-4
-2
log [Compound], M
A02B08_beta2AR_Nb80
A02B08_beta2AR_Nb69

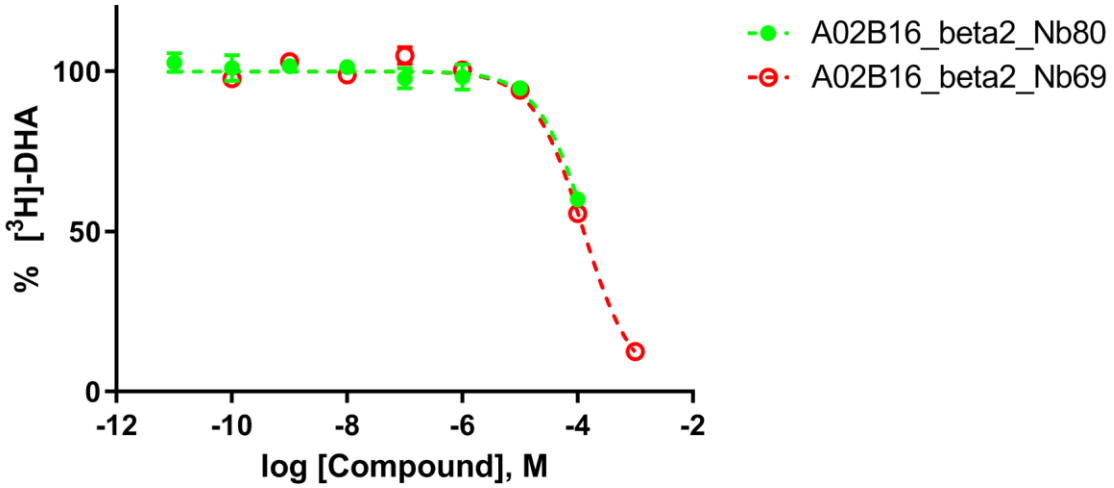
A02B16_beta2_Nb80
A02B16_beta2_Nb69
% [3H]-DHA
100
50
0
-12
-10
-8
-6
-4
-2
log [Compound], M

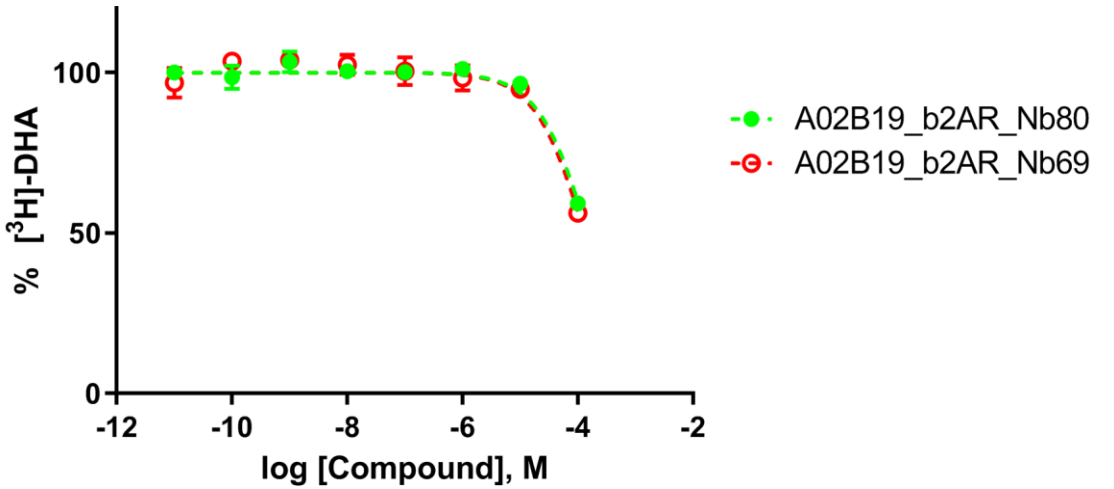
A02B19_b2AR_Nb80
A02B19_b2AR_Nb69
% [3H]-DHA
100
50
0
-12
-10
-8
-6
-4
-2
log [Compound], M

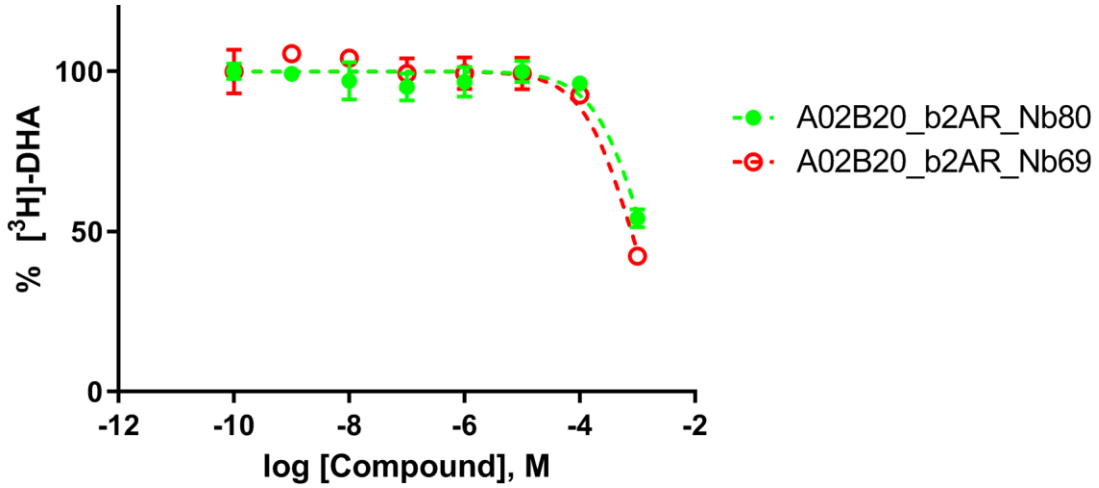
% [3H]-DHA
100
50
0
-12
-10
-8
-6
-4
-2
log [Compound], M
A02B20_b2AR_Nb80
A02B20_b2AR_Nb69

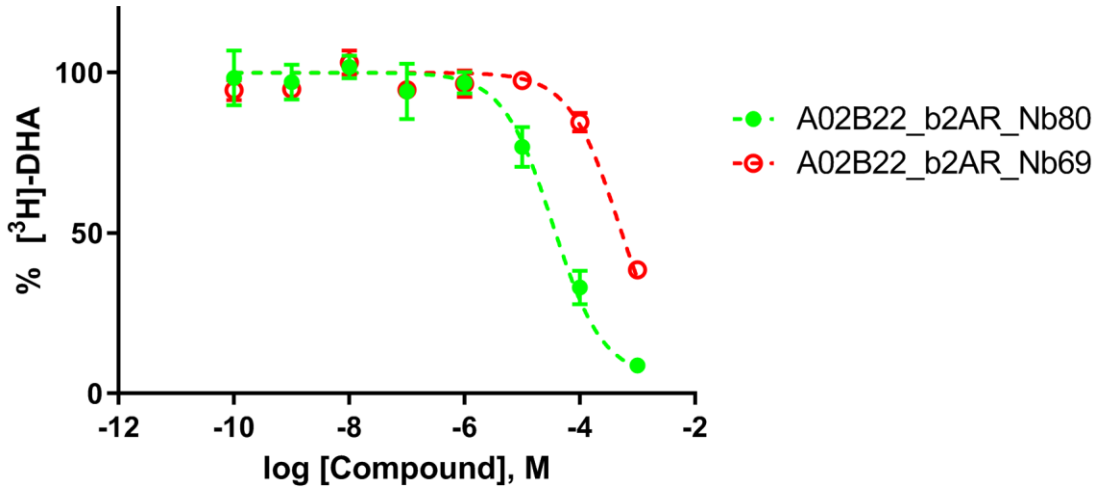
% [3H]-DHA
100
50
0
-12
-10
-8
-6
-4
-2
log [Compound], M
A02B22_b2AR_Nb80
A02B22_b2AR_Nb69

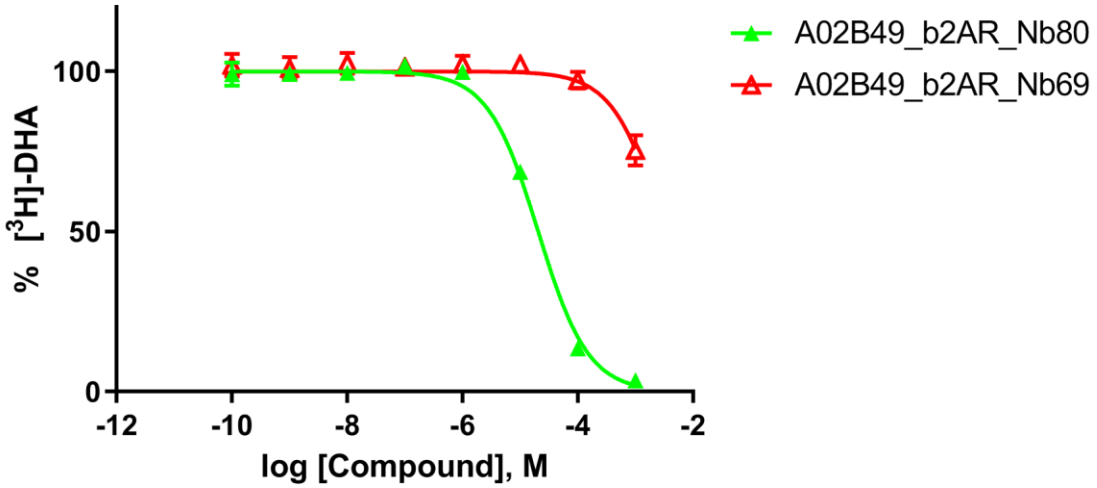
A02B49_b2AR_Nb80
A02B49_b2AR_Nb69
% [3H]-DHA
100
50
0
-12
-10
-8
-6
-4
-2
log [Compound], M

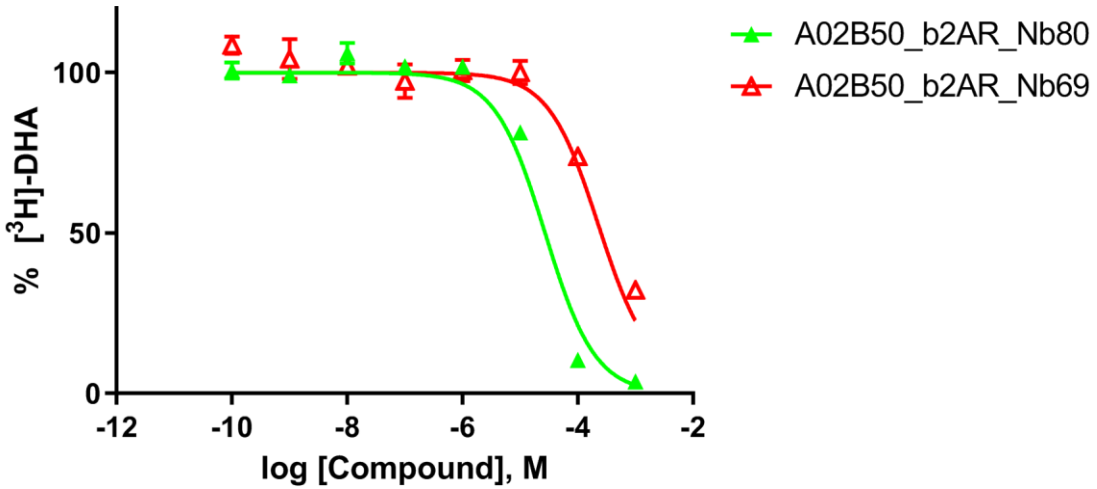
A02B50_b2AR_Nb80
A02B50_b2AR_Nb69
% [3H]-DHA
100
50
0
-12
-10
-8
-6
-4
-2
log [Compound], M

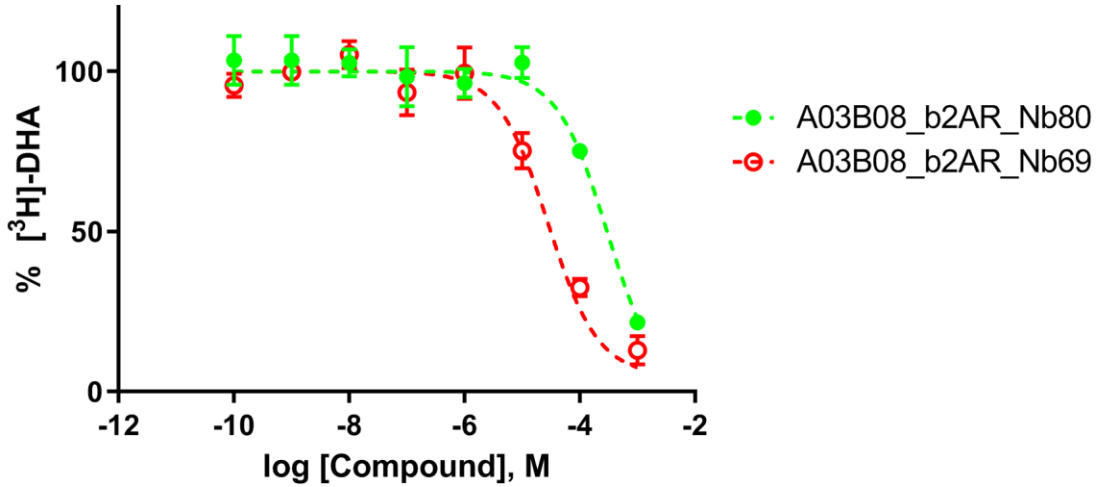
% [3H]-DHA
100
50
0
-12
-10
-8
-6
-4
-2
log [Compound], M
A03B08_b2AR_Nb80
A03B08_b2AR_Nb69

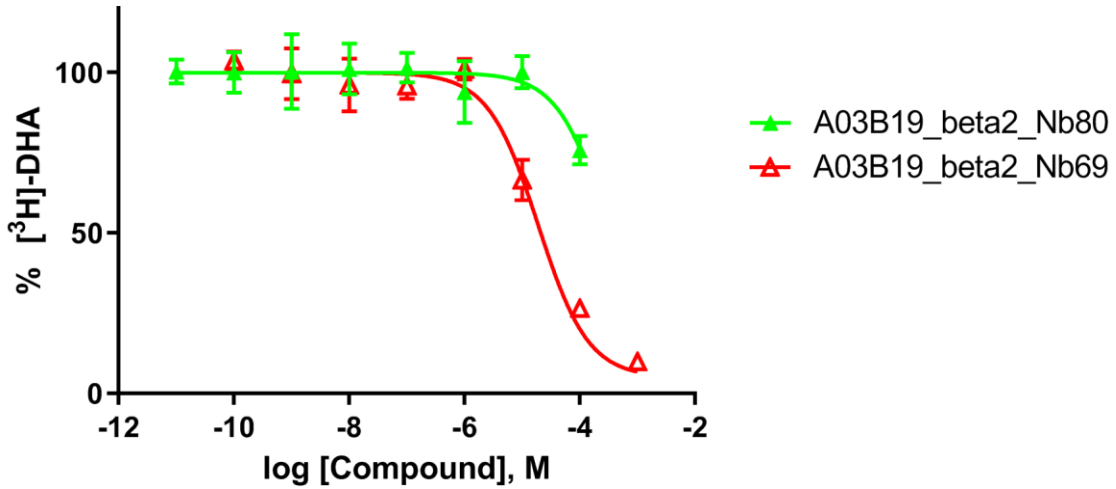
% [3H]-DHA
100
50
0
-12
-10
-8
-6
-4
-2
log [Compound], M
A03B19_beta2_Nb80
A03B19_beta2_Nb69

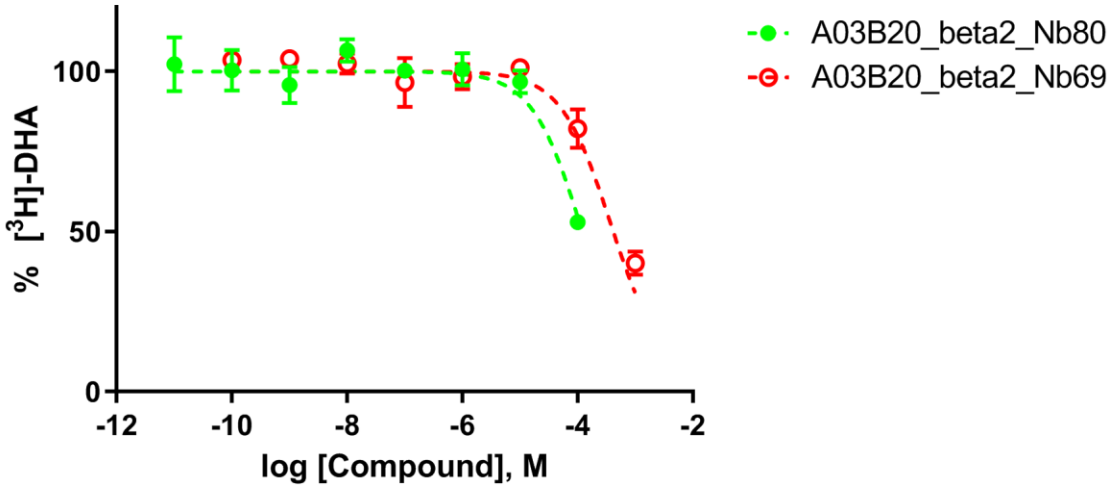
A03B20_beta2_Nb80
A03B20_beta2_Nb69
% [3H]-DHA
100
50
0
-12
-10
-8
-6
-4
-2
log [Compound], M

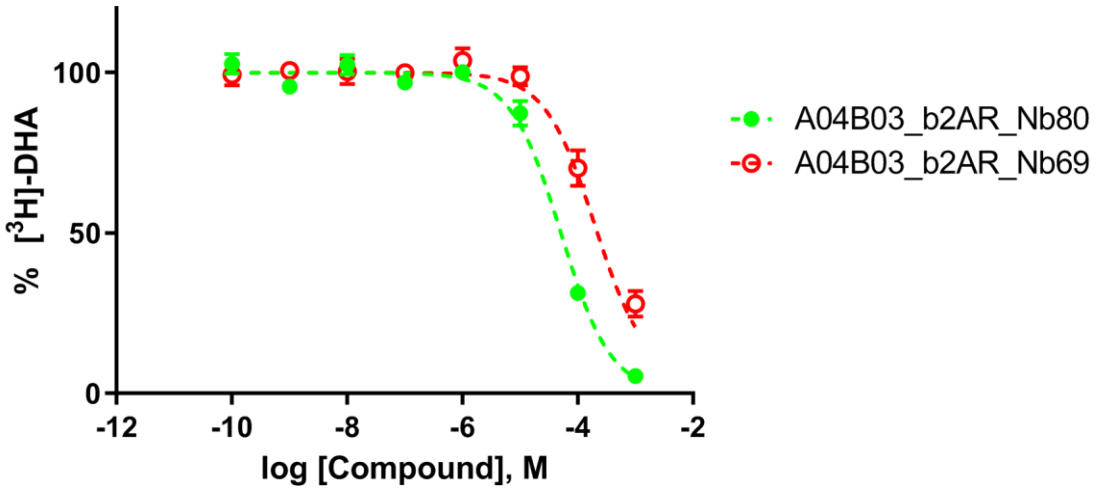
A04B03_b2AR_Nb80
A04B03_b2AR_Nb69
% [3H]-DHA
100
50
0
-12
-10
-8
-6
-4
-2
log [Compound], M

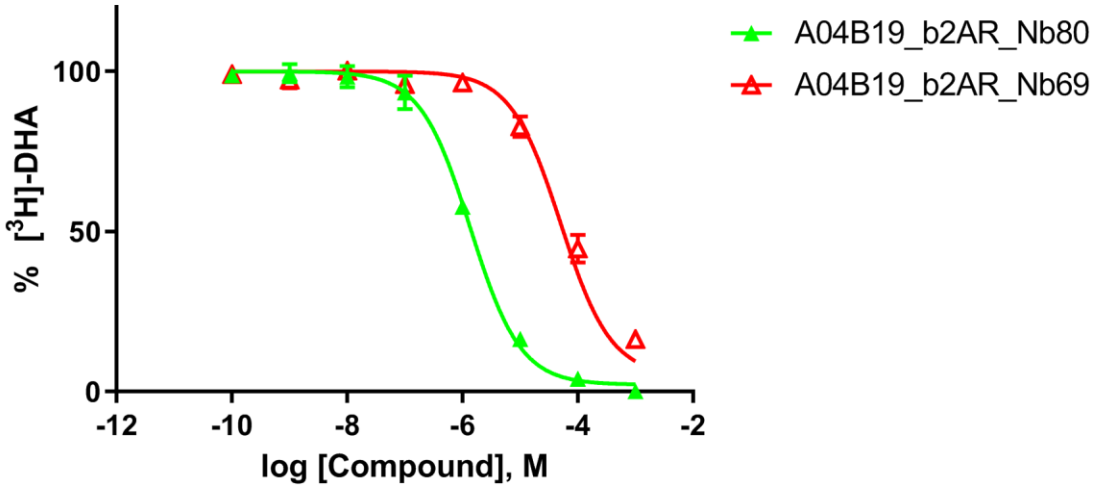
A04B19_b2AR_Nb80
A04B19_b2AR_Nb69
% [3H]-DHA
100
50
0
-12
-10
-8
-6
-4
-2
log [Compound], M

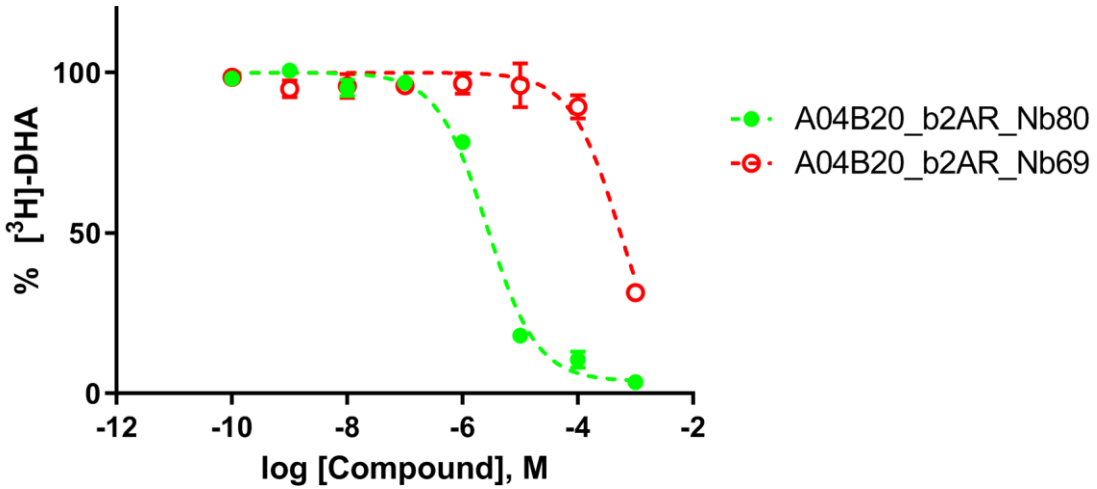
A04B20_b2AR_Nb80
A04B20_b2AR_Nb69
% [3H]-DHA
100
50
0
-12
-10
-8
-6
-4
-2
log [Compound], M

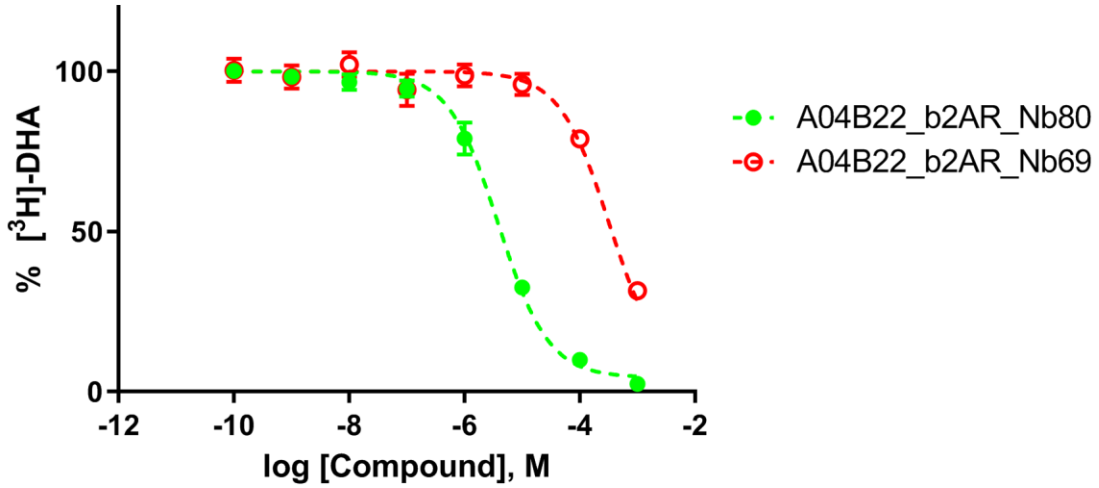
100
50
0
% [3H]-DHA
-12
-10
-8
-6
-4
-2
log [Compound], M
A04B22_b2AR_Nb80
A04B22_b2AR_Nb69

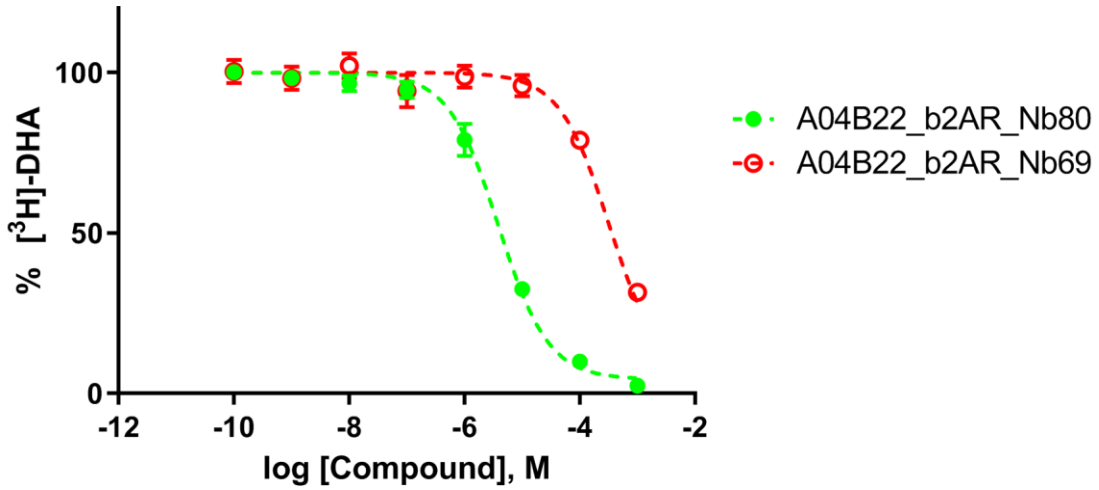
100
50
0
% [3H]-DHA
-12
-10
-8
-6
-4
-2
log [Compound], M
A04B22_b2AR_Nb80
A04B22_b2AR_Nb69

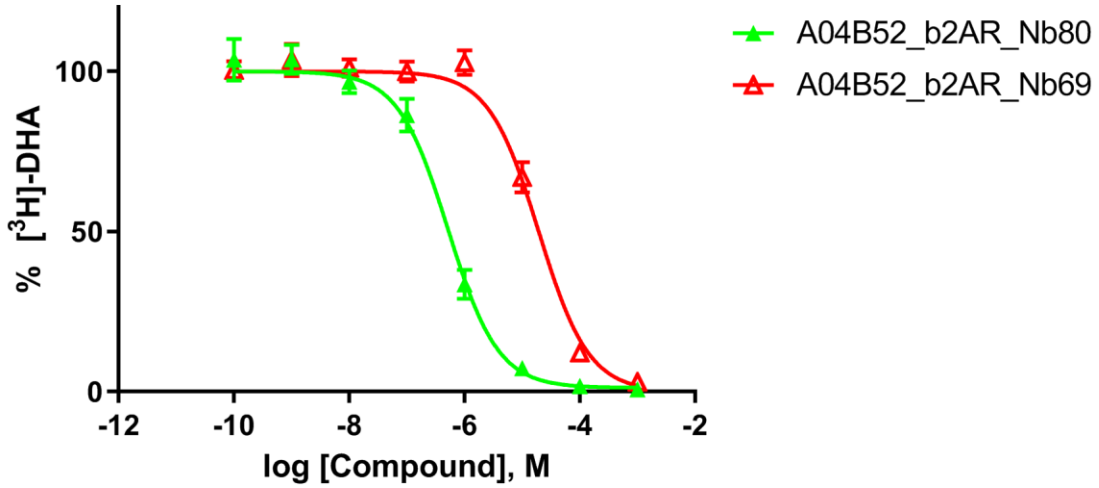
A04B52_b2AR_Nb80
A04B52_b2AR_Nb69
% [3H]-DHA
100
50
0
-12
-10
-8
-6
-4
-2
log [Compound], M

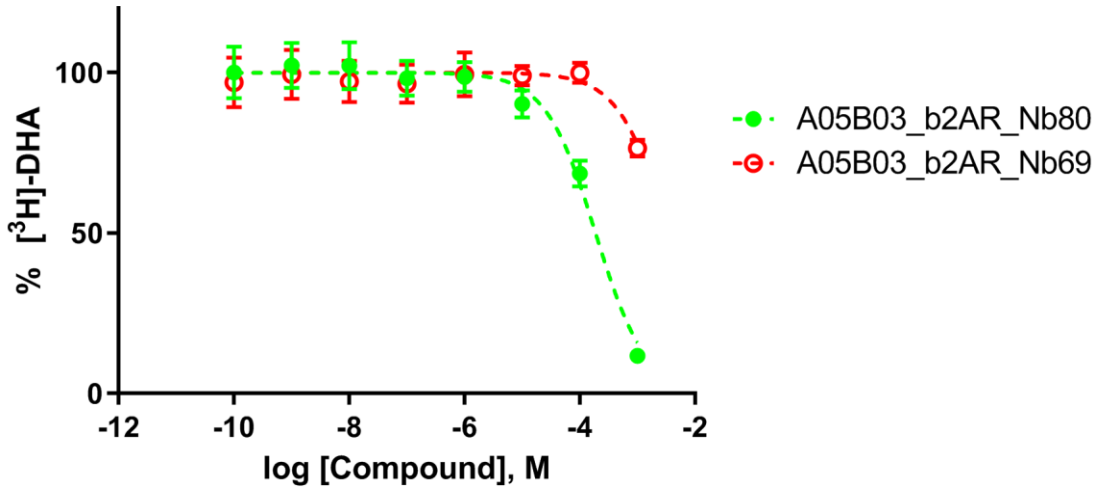
A05B03_b2AR_Nb80
A05B03_b2AR_Nb69
% [3H]-DHA
100
50
0
-12
-10
-8
-6
-4
-2
log [Compound], M

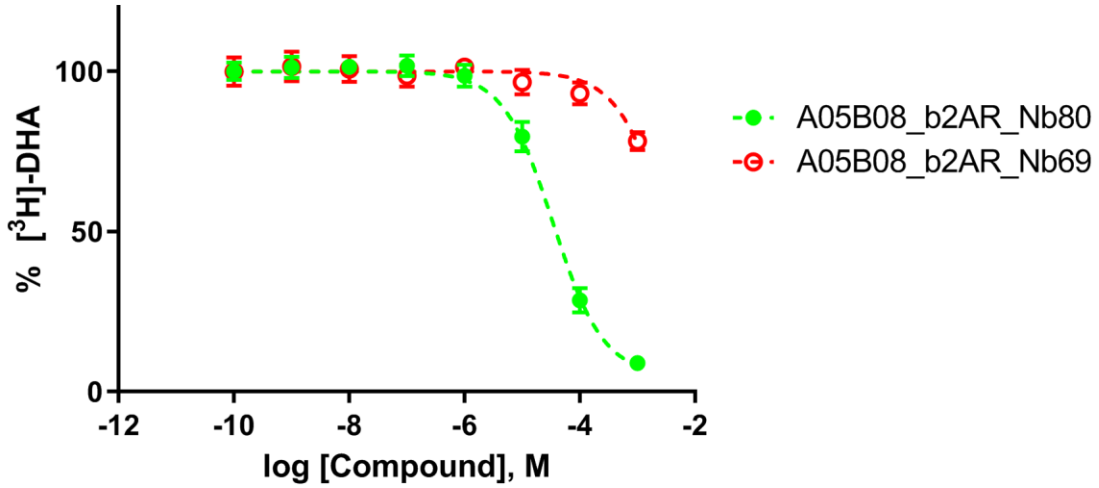
100
50
0
% [3H]-DHA
-12
-10
-8
-6
-4
-2
log [Compound], M
A05B08_b2AR_Nb80
A05B08_b2AR_Nb69

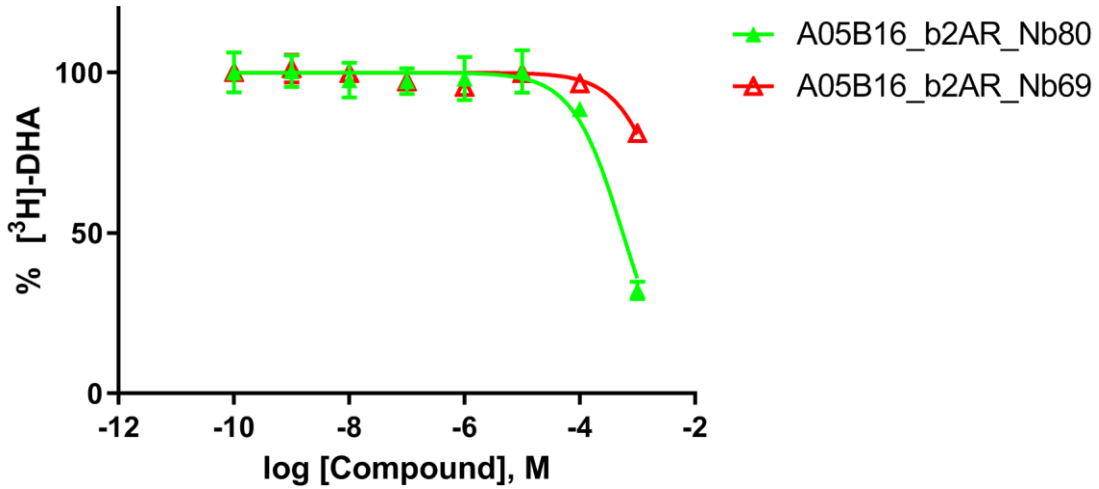
100
50
0
% [3H]-DHA
-12
-10
-8
-6
-4
-2
log [Compound], M
A05B16_b2AR_Nb80
A05B16_b2AR_Nb69

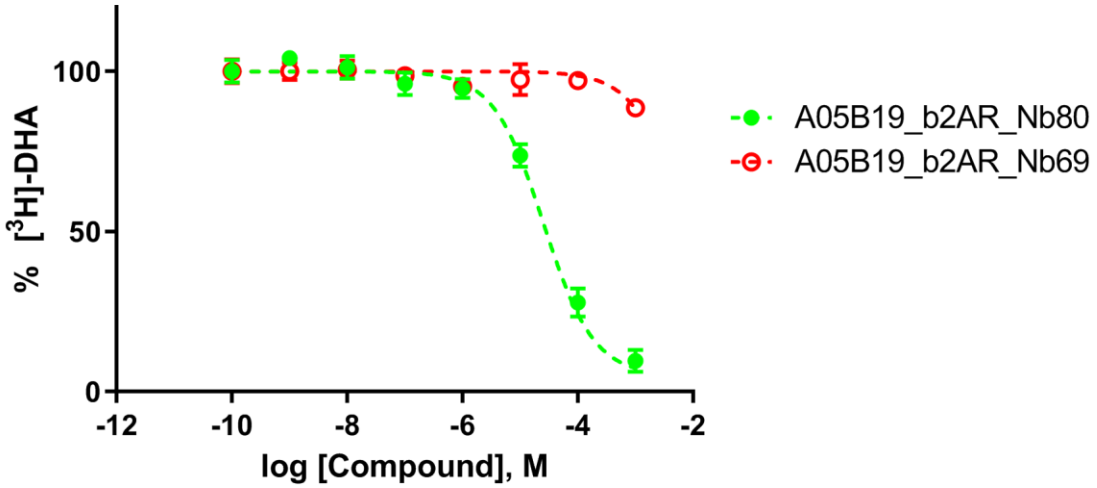
100
50
0
% [3H]-DHA
-12
-10
-8
-6
-4
-2
log [Compound], M
A05B19_b2AR_Nb80
A05B19_b2AR_Nb69

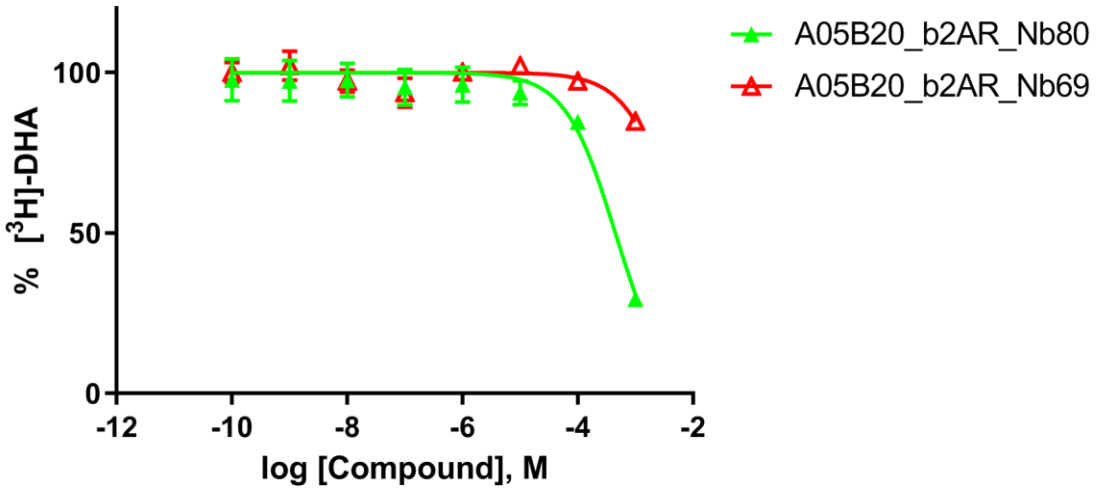
100
50
0
% [3H]-DHA
-12
-10
-8
-6
-4
-2
log [Compound], M
A05B20_b2AR_Nb80
A05B20_b2AR_Nb69

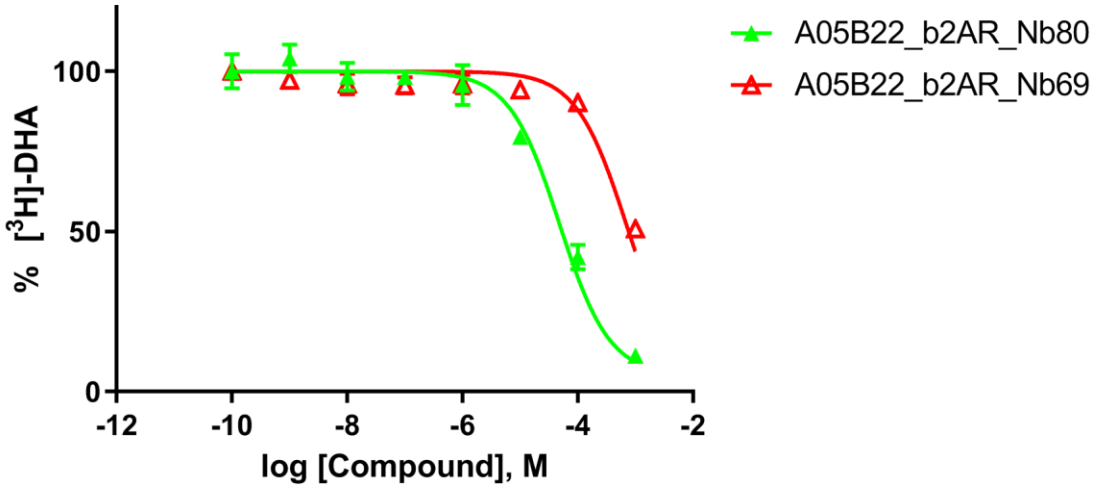
A05B22_b2AR_Nb80
A05B22_b2AR_Nb69
% [3H]-DHA
100
50
0
-12
-10
-8
-6
-4
-2
log [Compound], M

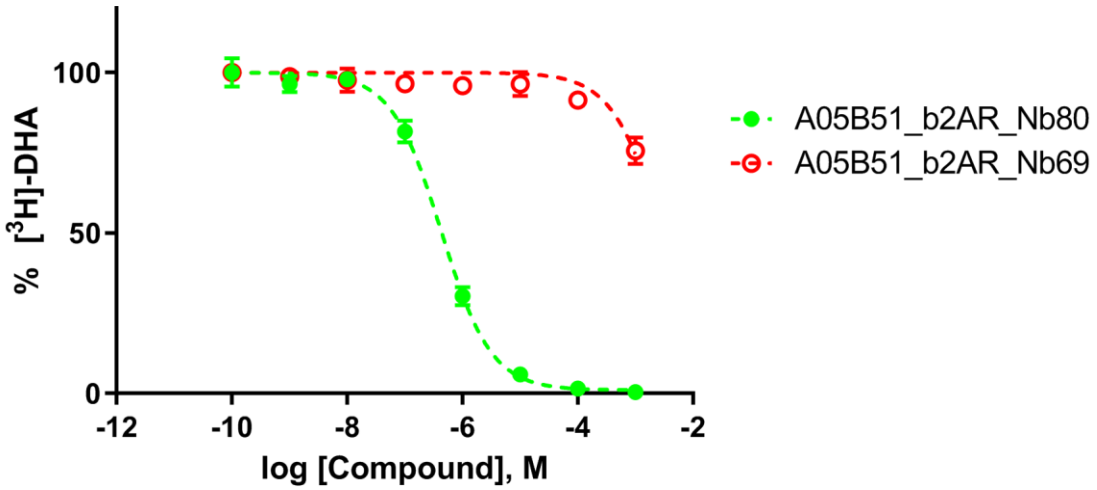
A05B51_b2AR_Nb80
A05B51_b2AR_Nb69
% [3H]-DHA
100
50
0
-12
-10
-8
-6
-4
-2
log [Compound], M

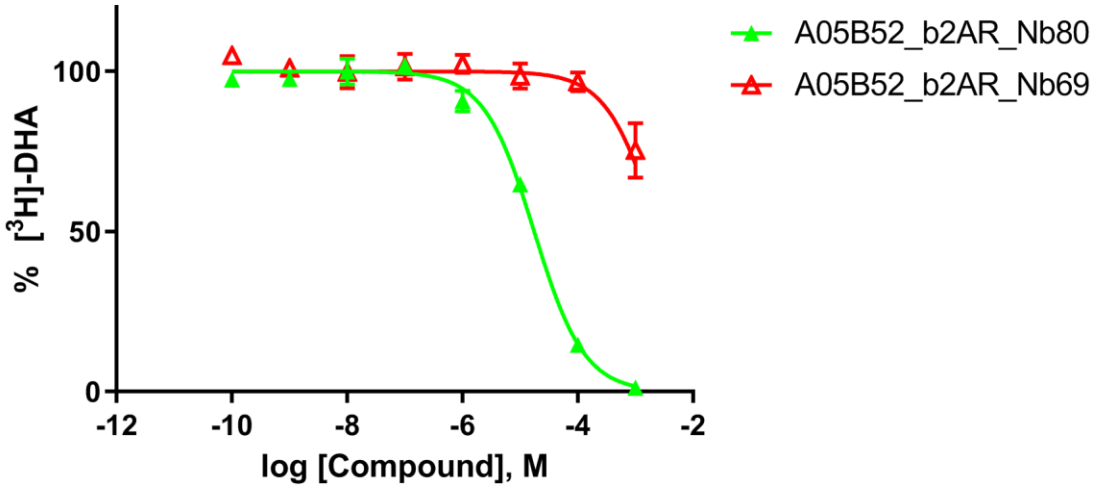
A05B52_b2AR_Nb80
A05B52_b2AR_Nb69
% [3H]-DHA
100
50
0
-12
-10
-8
-6
-4
-2
log [Compound], M

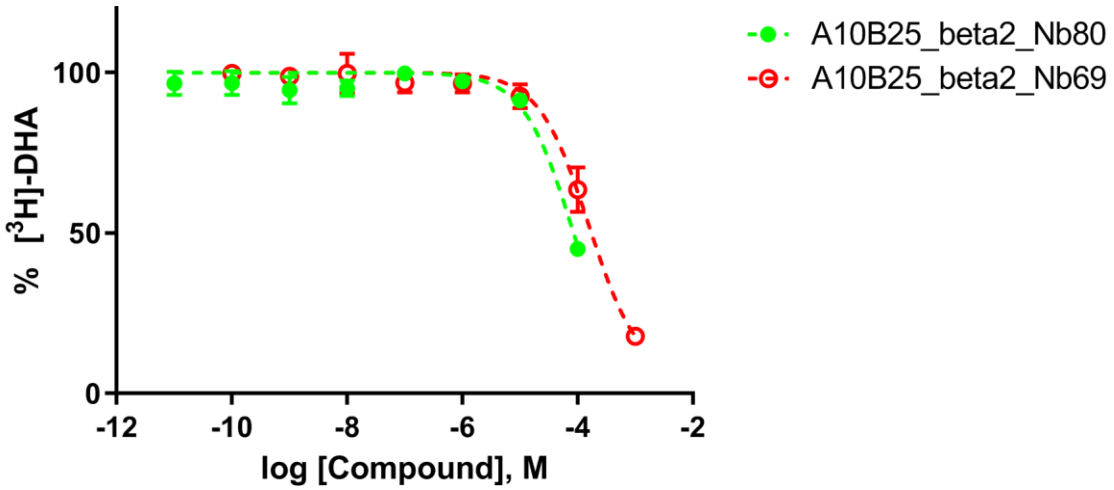
A10B25_beta2_Nb80
A10B25_beta2_Nb69
% [3H]-DHA
100
50
0
-12
-10
-8
-6
-4
-2
log [Compound], M

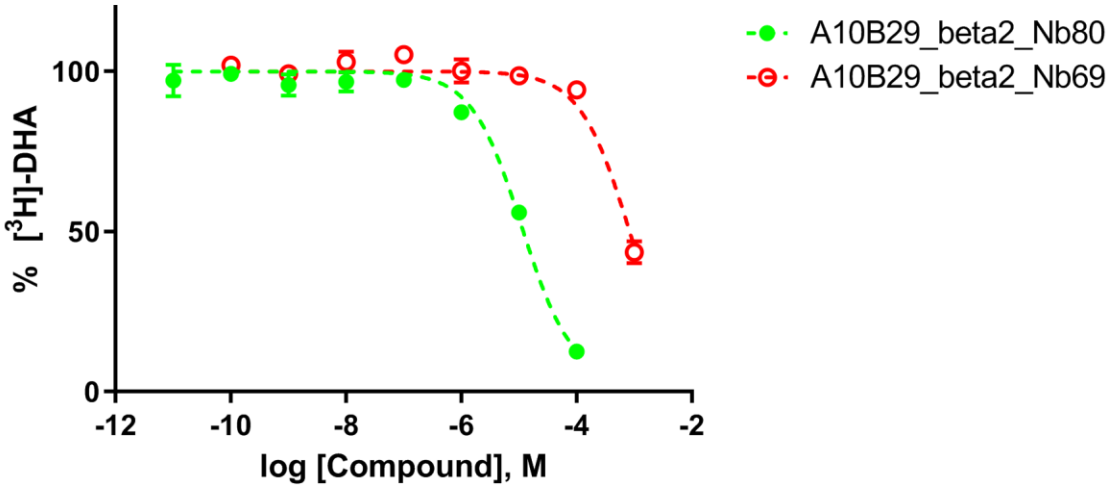
A10B29_beta2_Nb80
A10B29_beta2_Nb69
% [3H]-DHA
100
50
0
-12
-10
-8
-6
-4
-2
log [Compound], M

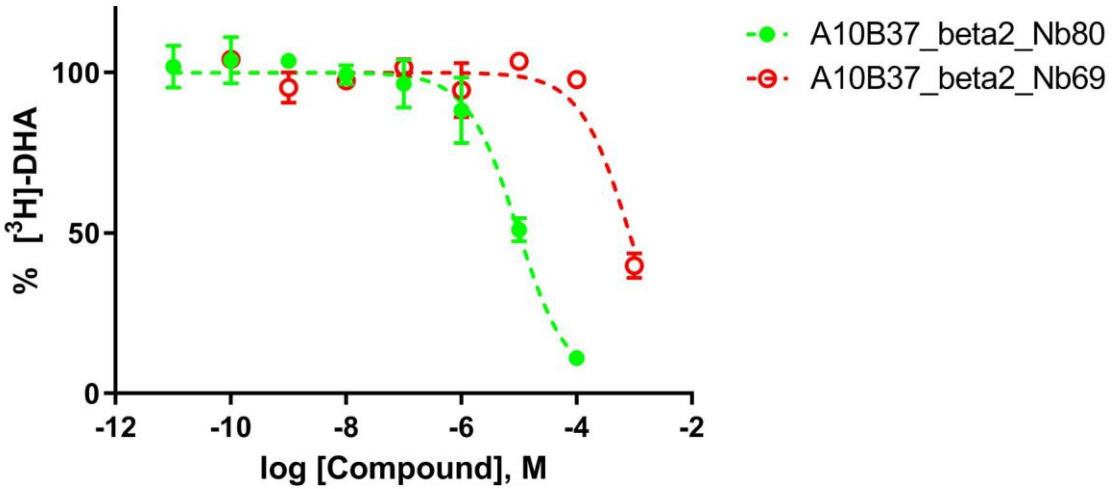
A10B37_beta2_Nb80
A10B37_beta2_Nb69
% [3H]-DHA
100
50
0
-12
-10
-8
-6
-4
-2
log [Compound], M

Bibliography

1. Cherezov V, et al. (2007) High-resolution crystal structure of an engineered human β_2-adrenergic G protein-coupled receptor. *Science* 318(5854):1258-1265.

2. Rosenbaum DM, et al. (2007) {GPCR engineering yields high-resolution structural insights into β_2-adrenergic receptor function}. *Science* 318(5854):1266-1273.

3. Ring AM, et al. (2013) Adrenaline-activated structure of β_2-adrenoceptor stabilized by an engineered nanobody. *Nature* 502(7472):575-579.

4. Mcgann M (2011) FRED pose prediction and virtual screening accuracy. *J. Chem. Inf. Model.* 51:578-596.

5. McGann MR, Almond HR, Nicholls A, Grant JA, Brown FK (2003) Gaussian docking functions. *Biopolymers* 68(1):76-90.

6. McGann M (2012) Fred and hybrid docking performance on standardized datasets. *J. Comput. Aided Mol. Des.* 26(8):897-906.

7. McGaughey GB, et al. (2007) Comparison of topological, shape, and docking methods in virtual screening. *J. Chem. Inf. Model.* 47(4):1504-1519.

8. Brooks BR, et al. (1983) CHARMM: A program for macromolecular energy, minimization, and dynamics calculations. *J. Comput. Chem.* 4:187-217.

9. Momany FA, Rone R (1992) Validation of the general purpose QUANTA 3.2/CHARMm force field. *J. Comput. Chem.* 13(7):888-900.

10. No K, Grant J, Scheraga H (1990) Determination of net atomic charges using a modified partial equalization of orbital electronegativity method. 1. Application to neutral molecules as models for polypeptides. *J. Phys. Chem.* 94:4732-4739.

11. No K, Grant J, Jhon M, Scheraga H (1990) Determination of net atomic charges using a modified partial equalization of orbital electronegativity method. 2. Application to ionic and aromatic molecules as models for polypeptides. *J. Phys. Chem.* 94:4740-4746.

12. Hawkins PCD, Skillman AG, Warren GL, Ellingson BA, Stahl MT (2010) Conformer generation with {OMEGA}: Algorithm and validation using high quality structures from the protein databank and cambridge structural database. *J. Chem. Inf. Model.* 50(4):572-584.

13. OpenEye Scientific Software, Santa Fe N QUACPAC 1.6.3.1. (accessed Nov 15, 2014).

14. Gatica EA, Cavasotto CN (2011) Ligand and decoy sets for docking to G protein-coupled receptors. *J. Chem. Inf. Model.* 52(1):1-6.

15. Landrum G RDKit: Open-source chemoinformatics. (accessed Nov 15, 2014).

16. Rogers D, Hahn M (2010) Extended-connectivity fingerprints. *J. Chem. Inf. Model.* 50(5):742-754.

17. GraphPad~Software, La Jolla U Graphpad prism version 7.00 for windows. (accessed Nov 17, 2014).

18. Cheng Y, Prusoff WH (1973) Relationship between the inhibition constant (ki) and the concentration of inhibitor which causes 50 per cent inhibition (i50) of an enzymatic reaction. *Biochem. Pharm.* 22(23):3099-3108.